Experimental characterization and in situ measurements of chemical processes in the martian surface environment

Quinn, R.C.

Experimental characterization and in situ measurements of chemical processes in the martian surface environment

Proefschrift

ter verkrijging van de graad van Doctor aan de Universiteit Leiden
op gezag van de Rector Magnificus Dr. D. D. Breimer,
hoogleraar in de faculteit der Wiskunde en
Natuurwetenschappen en die der Geneeskunde,
volgens besluit van het College voor Promoties
te verdedigen op woensdag 18 Mei 2005
te klokke 15:15 uur

door

Richard Charles Quinn
geboren te New York, USA

Promotiecommissie

Promotor:	Prof. Dr. P. Ehrenfreund
Referent:	Prof. Dr. C. Chyba (Stanford University, USA)
Overige leden:	Prof. Dr. J. Fraaije Prof. Dr. R. A. Mathies (University of California, Berkeley, USA) Dr. F. J. Grunthaner (JPL, California Institute of Technology, USA) Dr. C. P. McKay (NASA Ames Research Center, USA) Dr. A. P. Zent (NASA Ames Research Center, USA) Dr. O. Botta (ISSI, Switzerland)

Cover: Photo of the Atacama Desert, which is located along the northern Chilean pacific coast from 30° S to 20° S latitude. This image was taken near the Mars Oxidant Instrument deployment site which is located at 24°4'10" S, 69°51'59" W.

Contents

Chapter 1

Introduction

The question of whether life is currently present on Mars or was present in the past is of great interest to both planetary scientists and the general public. Studies of life in extreme environments on Earth indicate that it is possible that habitable zones may exist on the surface of Mars. Mars exploration strategies have generally focused on habitability and in particular the search for two key requirements for the existence of life as we know it, the presence of liquid water and complex organic molecules.

Remotely obtained images of Mars have provided evidence of a history of liquid water on the planet's surface. For example, the images collected by the Mars Global Surveyor which indicate the presence of gullies, may be explained by ground water seepage and surface runoff (Malin and Edgett, 2000). However, it should be noted that other explanations for these features have been proposed, including ice pack build up during obliquity oscillations (Costard et al., 2002). More recently, the NASA Mars Exploration Rovers were sent to regions which based on remote imaging, appeared to have been altered by the presence of liquid water (Squyres et al., 2004a). The Spirit rover landed at Gusev Crater, possibly a former lake. It appears that Gusev, a Noachian aged crater, at one point filled with water and sediment from Ma'adim Vallis which breaches the crater on its southern rim. However, evidence of only minor aqueous alteration at the site was observed by Spirit and it is hypothesized that if lacustrine sediments exist at the site, they have been buried by impact altered lavas (Squyres et al., 2005a). The Opportunity rover landed at Meridiani Planum, which was selected as a landing site on the basis of Thermal Emission Spectrometer (TES) data returned by Mars Global Surveyor. The TES data indicated that the surface at Meridiani Planum contains course grained hematite (15 to 20%) which may have formed in liquid water (Christensen et al., 2000). Data returned from the Opportunity payload confirmed a history of aqueous processes at the site including, sulfur-rich sedimentary rocks thought to have deposited in shallow surface water and hematite rich spherules thought to be concretions formed in liquid water (Squyres et al., 2005b).

The search for organic compounds on the surface of Mars has proven to be a difficult task. Recently, methane appears to have been detected in the atmosphere of Mars at a mixing ratio of 10 ± 5 parts per billion by volume (ppbv) by the Planetary Infrared Fourier

Spectrometer on the European Space Agency Mars Express spacecraft (Formisano et al., 2004). Aside from possible trace amounts of atmospheric methane, no other organic chemicals have been detected on the surface or in the atmosphere of Mars. The Viking landers performed an in situ search on the surface of Mars for both life and organic compounds. The Viking experiments indicate that the surface material was most likely not biologically active, but chemically reactive and depleted of organic compounds. The general conclusion, based on these results, is that the martian surface material contains a number of oxidizing species. There are currently competing hypotheses to explain identity of the oxidants, oxidant formation on Mars, and the roles of oxidants in both the Viking biology experiments and the decomposition of organics on the planet's surface. It is likely that, in fact, the processes described by a number of these hypotheses are occurring on Mars to some extent. There is undoubtedly a large number of complex, photochemically driven oxidative processes on Mars involving interrelated atmospheric, aerosol, dust, soil, and organic chemical interactions. To a large extent, the role of these photochemical processes in altering carbon compounds on Mars is unknown.

The purpose of this thesis is to characterize reactive chemical processes occurring on the surface of Mars and their relationships to planetary carbon chemistry and the potential for the existence of habitable environments. In the following sections, background information on the reactive nature of martian surface chemistry is presented, along with an overview of proposed measurement techniques for the in situ characterization of chemical surface processes.

1.1 Results from the Viking Mars missions

The Viking biology experiments were designed to test martian surface samples for the presence of life by measuring metabolic activity and distinguishing it from physical or chemical activity. In the Labeled Release (LR) experiment, an aqueous medium containing several organic compounds labeled with ^{14}C was introduced to a martian surface sample that had been placed in a sealed chamber. Briefly, the major results of the LR experiment were: upon contact of the aqueous medium with the surface material, ^{14}C labeled CO_2 was rapidly released into the cell headspace; the reaction slowed down after only a fraction of the organic medium decomposed; and preheating the sample to 160°C for three hours (followed by cooling to approximately 10°C) completely inhibited the response seen in the samples that were not heated (Levin and Straat, 1977). The Gas Exchange experiment attempted to identify microbial activity by using gas chromatography to measure changes in the headspace gas composition upon introduction of an aqueous nutrient medium designed to promote microbial growth. The major results of the Viking GEx experiment were: the rapid release of O_2 gas into the headspace upon contact of the soil with water vapor and a slow log linear release of CO_2 gas into the headspace upon contact with the organic nutrient medium (Oyama and Berdahl, 1977). Heating the samples to 145°C

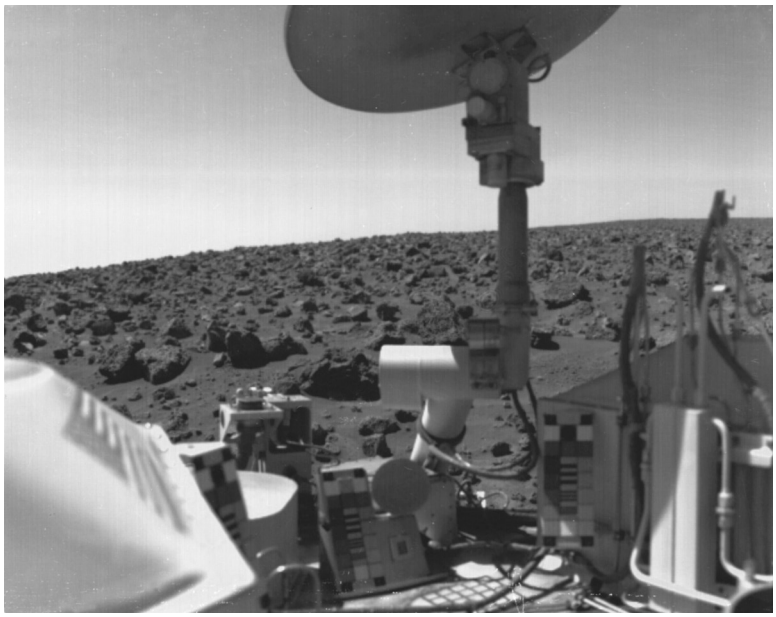

Figure 1. Image taken from the NASA Viking 2 Lander. Viking 2 landed on Utopia Planitia (47.97°N, 225.7° W). Photo: NASA/JPL Caltech

(followed by cooling to approximately 10°C) prior to wetting may have diminished, but did not eliminate the release of oxygen. In both the GEx and the LR, positive responses were seen in all samples that were not heat treated, including samples collected from surface environments shielded from direct UV radiation (samples collected at 10-20 cm below the surface and from under Notched Rock). Additionally, the Viking gas chromatograph/mass spectrometer (GCMS) did not detect organic compounds in amounts above the instrument's detection limits, which were in the parts-per-million level for light hydrocarbons and in the parts-per-billion levels for heavy hydrocarbons (Toulmin et al., 1977). While it is possible that the Viking GCMS may have failed to detect certain types of organic material (Benner et al., 2000 Glavin et al., 2001), at the time of the Viking mission, these results were surprising since models of atmospheric photochemistry and meteoritic influx to the planet's surface predicted that hydrocarbons would be present in amounts above these detection limits (Biemann et al., 1977; Biemann and Lavoie, 1979). Even in the absence of in situ organic production, meteoritic infall would carry organics to Mars at a rate of 2.4 x 10^8 g yr^{-1}, or about 0.1 nm surface coverage per year (Zent, 1994; Flynn, 1996).

These results have lead to the conclusion that the surface material was most likely not biologically active, but was chemically reactive under the conditions of the Viking biol-

ogy experiments. Although the response observed in the LR experiment has been interpreted by some as a biological signature (Levin and Levin, 1998), the most widely accepted explanation for the results of the GEx and LR experiments is the presence of oxidants in the martian soil (Klein, 1978; Klein, 1979; Zent and McKay, 1994). Differences in stability of the active agents in the two experiments suggest that the GEx and LR oxidants are different species and that at least three different oxidizing species are needed to explain all of the experimental results (Klein, 1978). The combined results of the Viking GEx, LR, and GCMS led to the hypothesis that the GEx and LR oxidants are evidence for the oxidative decomposition of organic compounds (Klein, 1978; Klein, 1979) in the martian environment. Although, it has been suggested by some researchers (Zent and McKay, 1994) that the oxidant responsible for the GEx and LR results are also responsible for actively destroying incoming organics at the martian surface, there is no direct evidence that this is the case. It is quite possible that the oxidants present in the martian surface material are products of chemical processes that are independent (although most likely interrelated) to organic chemical degradation mechanisms. Additionally, no chemical model has been presented which can explain all the important details of both the GEx and LR results exactly and, although numerous hypotheses have been presented, the chemical nature, identity, and relationship between soil oxidants and organic compounds remains largely unknown.

1.2 Mars oxidant hypotheses

There are currently competing hypotheses to explain oxidant formation on Mars and the roles of oxidants in both the Viking biology experiments and the decomposition of organics on the planet's surface. The majority of these hypotheses fall into two broad categories:

1) Oxidants are photochemically produced in the atmosphere. Solar ultraviolet radiation photolysis of the atmosphere (and for some species, subsequent recombination) can generate “odd-hydrogen” and "odd oxygen" (e.g. H, OH, HO_2, H_2O_2, O, O_3). Some of these oxidizing species may deposit onto the surface and hence may be able to diffuse through the regolith to unknown depths, removing the early chemical record as it proceeds (e.g. Hunten, 1974; Barth et al., 1992). The total oxidant load detected by Viking could have been produced in as little as 2-10 years by this mechanism (Kong and McElroy, 1977). Photochemical oxidant production ceases at sunset, and it has been hypothesized that some oxidants, such as hydrogen peroxide, may deposit on the surface at an accelerated rate just after sunset (Barth et al., 1992). Encrenaz et al. (2004) has reported the detection of H_2O_2 in the martian atmosphere using ground based infrared spectroscopy. H_2O_2 is capable of degrading Mars analog organics (McDonald et al., 1998; Benner, 2000). Based on a coupled soil/atmosphere transport model for H_2O_2 on Mars, Bullock *et al.* (1994)

concluded that for H_2O_2 lifetimes up to 10^5 years, the extinction depth in the martian surface material was found to be less than three meters.

2) Oxidants are photochemically produced on soil surfaces. UV-surface interactions may lead to decomposition of organics due to superoxide radical formation on the surface of titanium oxides in the soil (Chun et al., 1978), or superoxide radicals may form directly in the soil silicate matrices (Yen et al., 1999), resulting in the generation of the Viking oxidants. The soil and dust surfaces would be strongly oxidizing, but the atmosphere itself need not be oxidizing. In this case, surface diffusion of superoxide radicals across grain boundaries, or regolith mixing combined with extremely long oxidant lifetimes, are required to explain the detection by Viking of oxidants in soil shielded from UV light (e.g. beneath Notched Rock).

There are other mechanisms that have been proposed to explain the formation of the Viking oxidants (for a review see Zent and McKay, 1994); in almost all cases UV light, atmospheric oxidants, or both are required. Each proposed mechanism for the degradation of organic compounds on Mars has a potentially different consequence for the stability of organics on the planet's surface. In case one, hydrogen peroxide would be expected to selectively oxidize organic compounds on Mars, resulting in the formation of species that may not have been detected by the Viking GCMS, such as mellitic acid salts (Benner, 2000). In case two, superoxide radicals, which are more strongly oxidizing than hydrogen peroxide, are generally responsible for "deep oxidation" of organics, resulting in more complete oxidation (Haber, 1996) and, possibly, the complete removal of organic material from the surface of Mars (Chun et al., 1978).

1.3 Results from the NASA Mars Exploration Rovers

There is ample evidence that acidic oxidizing surface environments exist on Mars. Observations returned from the Mars Exploration Rover Opportunity have revealed the presence of sulfur-rich sedimentary rocks (figure 2). Squyres et al. (2004b) have concluded the that the sediments observed with the Opportunity payload at the Meridiani Planum site formed in shallow surface water followed by evaporation and desiccation. Sulfur salts appear to be abundant in the sedimentary outcrops and jarosite has been identified using Opportunity's Mössbauer spectrometer (Klingelhöfer et al., 2004). The detection of jarosite is significant since it forms in strongly acidic-sulfate rich aqueous environments. From an astrobiological perspective, sedimentary rocks are an environment that may potentially act to preserve organic chemicals and signatures from a biotic period on the planet. Skelley et al. (2005) reported on field tests, performed in the California desert, using the Mars Organic Analyzer (MOA) in which amino acids were readily detected in jarosite samples. On the other hand, Sumner (2005) presented a theoretical model of

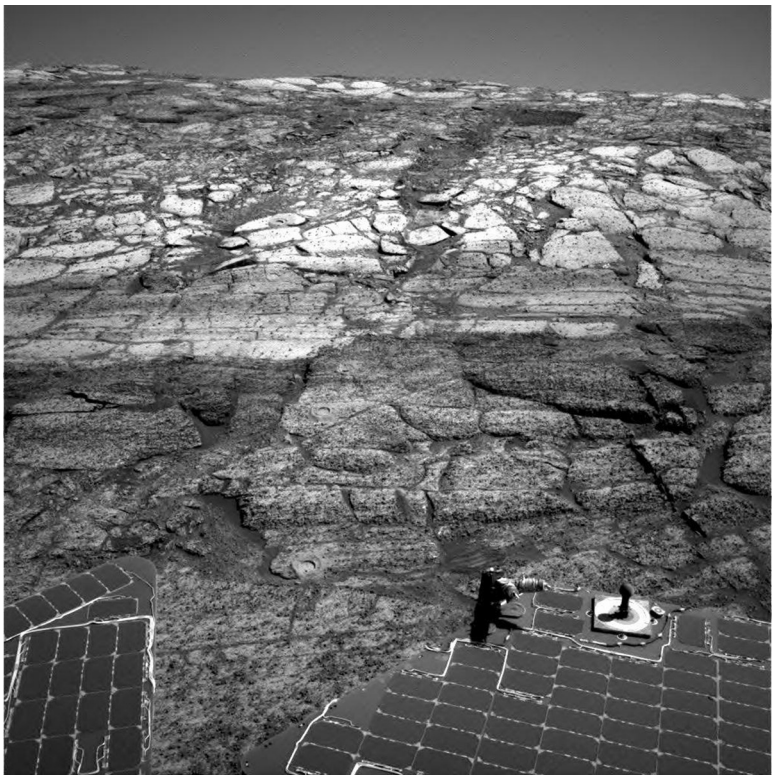

Figure 2. Layered sedimentary outcrops located in Endurance Crater The image was taken by the Opportunity Mars Exploration Rover. Photo: NASA Caltech.

organic stability under typical jarosite formation conditions and concludes that organics would be poorly preserved in such environments.

The discrepancy between the field measurements of Skelley et al. (2005) and the model by Sumner raises important questions about carbon chemistry on Mars. Extremely little is known about carbon sources and sinks in the martian environment. Clearly organics can be incorporated into minerals that form under acidic and oxidizing conditions, such as jarosite, even if from a thermodynamic perspective they are unstable. Questions that remain to be answered are, how organics are incorporated into these types of sedimentary deposits and, if unstable, what are the decomposition kinetics. Most models of Mars oxidant production focus on surface processes, and as a result, exploration strategies for the detection of organics on Mars often assume that organics will be incorporated into

and preserved in the interior of rocks. However, the extent to which this assumption is valid is unknown. The indigenous versus contaminant fraction of organics present in Mars meteorites is the subject of debate (McKay et al., 1996; Bada et al., 1998; Jull et al., 1998). Additionally, the sedimentary deposits observed on Mars by MER may have formed under oxidizing conditions inhospitable to the preservation of organics (Sumner, 2005). The in situ measurement strategies presented in this thesis focus on characterizing oxidation mechanisms and kinetics in the martian environment, including the chemistry of rock-core samples. The techniques allow the potential for preservation of organics in martian environments to be evaluated. These techniques, coupled with a highly sensitive organic detection instrument such as MOA (Skelley et al., 2005) will allow the relationship between reactive soil processes and the presence of organic compounds on Mars to be evaluated.

1.4 Acid-base soil chemistry on Mars

As mentioned in the section above, Mars soil pH is of interest because it plays a direct role in a number of processes that affect oxidative chemistry, organic chemistry, biological load and soil mineralogy. Soil parameters that are typically pH-dependant include the solubility of soil components (which determines the availability of plant nutrients and toxins); soil microorganism population diversity; and activity; and organic chemical degradation mechanisms. The recent discovery at the Mars Exploration Rover (MER) Opportunity site of jarosite (Klingelhöfer et al., 2004), which forms in strongly acidic-sulfate rich oxidizing environments, highlights the importance of pH on local chemical environments on Mars.

Although examined less than the data from the Viking experiments that indicates that the martian surface material is oxidizing, the first information on the acid-base chemistry of the martian surface material was also returned by the Viking biology experiments. Viking did not measure pH directly, but examination of CO_2 partitioning between the headspace and aqueous phases in the biology experiments has yielded limited insight into the acid-base chemistry of the surface material at the landing sites. Oyama et al. (1977) concluded that the surface material at the Viking site had a weak acidic nature. The experimental evidence that indicates the presence of this acidic component is the release of CO_2 from the soil prior to the wet mode in the GEx, an initial small CO_2 peak in the Pyrolytic Release Experiment (PR) (Horowitz et al., 1977), and the release of $^{14}CO_2$ from the heat-sterilized LR cycle 2 sample (injection 1). The observation of higher background counts in the LR experiment after the sterilization treatment led Oyama et al. (1977) to suggest that the acidic component may be $H_2SO_4 \cdot 2H_2O$, and that it is semi-volatile when heated during the sterilization sequence. The initial increase in headspace CO_2 levels seen in the Viking biology experiments has been attributed to an acidic soil component, however, the magnitude of CO_2 uptake subsequent to any initial CO_2 release during the GEX and LR

indicates that the acid component is neutralized upon wetting. Oyama et al. 1977 attributed this resorption of desorbed CO_2 to the generation of hydroxyl ions from the reaction of soil superoxides with water. Simulations of the GEx have indicated that after neutralization of the acidic components, the overall pH of the aqueous soil mixtures tested by Viking were slightly to moderately basic (Quinn and Orenberg, 1993). Although the Viking and MER do not represent identical chemical environments or past surface environments, it is interesting to note that jarosite would be expected to form in an aqueous acidic surface environment but not in an alkaline environment.

1.5 In situ measurement technologies

The Viking experiments were not designed to study the chemical reactivity of the martian surface material. It is not possible to deduce from the Viking results the exact identity, chemical behavior, and prevalence of oxidizing species in the martian environment. Additionally, these experiments provide no direct information on formation mechanisms, including whether oxidants are photochemically produced in the atmosphere or photochemically produced on soil surfaces. Even the relationship between the apparent absence of organics and the presence of oxidants in the surface material has not been experimentally established.

The first attempt to directly examine the chemical reactivity of the martian surface was planned as part of the Russian Mars ’96 mission. The Mars Oxidant Experiment (MOx), was contributed to the mission by NASA and was unfortunately lost with the mission shortly after launch (Grunthaner et al., 1995; McKay et al., 1998). MOx used a fiber-optic array operating in a micro-mirror sensing mode to monitor chemical changes in chemical thin-film reactants. MOx was designed as an in situ survey instrument capable of characterizing the chemical nature of the soil by using an array of chemical-thin films with different reactivities. The approach is derived from the classical “spot test” method of chemical identification where the identity of unknowns is elucidated through the reaction pattern of the sample with reference compounds.

Since MOx, improved designs for both soil and atmospheric oxidant sensors have been developed. The Thermo-Acoustic Oxidant Sensor (TAOS) extended the use of sensors for Mars applications to a thin-film resistance sensing mode (chemiresistors) and surface acoustic wave devices (Zent et al., 1998). Following TAOS, the Mars Oxidant Instrument (MOI), using a chemiresistor sensing approach, was developed to study soil oxidants. MOI added the capability of sealing the soil sample, and heating and humidifying the sample headspace. The Mars Atmospheric Oxidant Sensor (MAOS), expanded these technologies to investigate the effects of UV and dust interaction on oxidant formation (Figure 3).

A major technical challenge associated with the deployment of these sensors on Mars is the need to deliver unreacted and uncontaminated sensing films to the surface of the

planet. Because the films are highly reactive, exposure to air, water vapor, or other contaminants during instrument delivery, integration or during transport to Mars would seriously compromise experimental results. To accomplish the delivery of pristine films to Mars, they are encapsulated in a hermetically sealed enclosure using a micro-machined top seal cover that is bonded to the sensor substrate immediately following film deposition. Fabricated using bulk Si micro-machining, the seal cover consists of a thick frame with suspended, films of silicon nitride. The silicon nitride film is strong enough to withstand more than 15 psi gauge differential across the membrane and has been tested to vibration loads of more than 500 G using the Proton launch vibration spectrum. On computer command, a sensor seal is opened by rapidly heating its surface metallization. The sudden temperature increase thermally stresses the nitride film, which decomposes into micron sized particles, exposing the chemical thin-film. These nitride particles are chemically inert, and have negligible impact on the experiment.

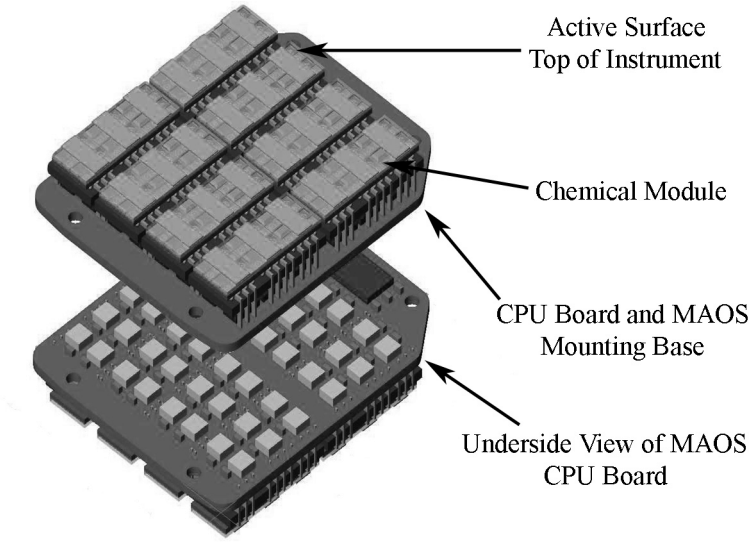

Figure 3. The Mars Atmospheric Oxidant Sensor (described in chapter 6).

The micro-machined sealing system was fully designed, tested and delivered as part of the MOx flight instrument, however, there is a high financial cost associated with the fabrication and integration of this system. Additionally, there is some level of risk associated with the system since mechanical failure or leaking of the seals represents an instru-

ment failure mode. Even in the absence of membrane failure or leakage, a low level of film oxidation is unavoidable during sensor fabrication. As part of this thesis, a sensor that uses in situ deposition of the thin-film sensing material has been developed. The use of in situ deposition of chemical films for oxidation sensors represents a new approach to increasing sensor shelf life and sensitivity while minimizing instrument risk and cost.

1.6 The Atacama Desert as a Mars analog test site

The part of the Atacama region between 22° S and 26° S is extremely arid; its total rainfall of only a few millimeters over decades (McKay et al., 2003) makes it one of the driest deserts in the world. These conditions have existed in the region for 10-15 Myrs (Ericksen, 1983), making one of the best analogs on Earth for the present dry conditions on Mars. It has been reported that soils from certain regions of the Chilean Atacama Desert have some characteristics that are similar to the surface materials tested by the Viking Landers. Navarro-González et al. (2003) demonstrated that the quantity and diversity of

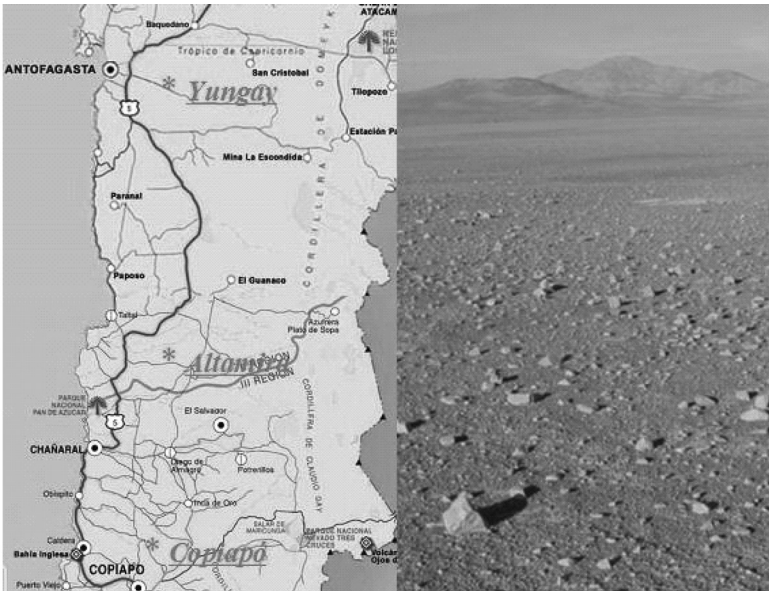

Figure 4. A map of the Chilean pacific coast showing the Atacama Desert. The photo shows the local geology at the field site near Yungay (24°4'50" S).

heterotrophic bacteria increase as a function of local water availability in the Atacama, and that for some soil samples collected in the driest regions, no culturable bacteria was isolated. Additionally, Navarro-González et al. (2003) reported that pyrolysis-GCMS analysis of soils collected from these regions revealed extremely low levels of organic matter. Although the mechanism resulting in the low level of organics in these regions was not established by Navarro-González (2003), the condition of organic-depleted, near-sterile soil offers an interesting Earth analog of the martian surface material, as the Viking Gas Exchange (GEx) experiment and Labeled Release (LR) experiment were unable to demonstrate the presence of culturable bacteria (Klein, 1978; Klein, 1979), and the Viking pyrolysis-GCMS was unable to detect organic compounds (Biemann et al., 1977; Biemann and Lavoie, 1979).

As part of this thesis, field experiments that are designed to develop and validate instrumental methods and measurement strategies for the in situ characterization of oxidation mechanisms, kinetics, and carbon cycling on Mars have been performed. The major mechanisms that have resulted in the low levels of organics in Atacama soils remain unknown; the same is true for Mars. The instrumental approach developed correlates chemical reaction rates with dust abundance, UV flux, humidity, and temperature, allowing discrimination between the competing hypotheses of oxidant formation and reactivity mechanisms. Comparative studies of Atacama field and Mars data sets allow formation mechanisms and properties of oxidants and their role in the carbon chemistry of these environments to be characterized.

The field test site (figure 4) is near an environmental monitoring station (24°4'50" S) established by McKay et al. (2003) in 1994. The station, which is near the abandoned nitrate mine of Yungay, collected temperature, wind direction, relative humidity, and rainfall data over a four-year period. The region has a temperate climate with a mean temperature between 10°C and 30°C. During the collection period the only significant rain event resulted in only 2.3 mm of precipitation. Although dew occurs more frequently than rain, it is not a significant source of soil moisture. The site is near the eastern limit of coast fog incursion as determined by Rech et. al. (2003), and therefore the soil formation may have been strongly influenced by marine deposition. Rech et al. (2003), using $\delta^{34}S$ and $^{87}Sr/^{86}Sr$ values, proposed that the marine influence is restricted to locations where marine fog can penetrate, i.e. where the altitude of the Coastal Cordillera is less than 1000 m. This excludes in general, locations above 1300 m and more than 90 km inland.

A striking feature of the Atacama Desert are large nitrate deposits, probably of atmospheric origin (Bohlke et al., 1997), that have not been biologically decomposed. These salt deposits are also known to contain highly oxidizing species, including iodates (IO_3^-), chromates (CrO_4^{-2}), and the only known naturally occurring exploitable deposits of perchlorate (ClO_4^-) (Ericksen, 1981). There are significant differences between the chemical composition and mineralogy of the Atacama Desert and the surface of Mars. However, the oxidizing compounds found in Atacama soils are likely formed by photochemical reactions at the soil/atmosphere interface, analogous to the presumed photochemical origin

of martian oxidants. Due to differences in water availability, solar flux, and soil composition, specific mechanisms and reaction products may differ, but similar chemical processes may be occurring both in the Atacama and on Mars.

1.7 Outline and conclusions of this thesis

The focus of this PhD thesis is the proposition that a key to understanding martian carbon chemistry and the ultimate fate of organics lies not only in identifying soil oxidants but, perhaps more importantly, in characterizing the dominant reaction mechanisms and kinetics of soil reactivity and organic decomposition that are occurring on the planet. These processes may have decomposed or modified organic material that might have survived from an early biotic period. There is a need to understand these processes to determine how and where to look for unaltered organic material. This thesis takes a multifaceted approach to characterizing reactive chemical processes occurring in the martian regolith. The approach includes:

- laboratory based experimental modeling and simulations of martian surface chemistry using data returned from previous Mars missions;
- comparative studies of terrestrial extreme environments and Mars to further understand of the formation mechanisms and properties of oxidants and their role in the carbon chemistry of these environments;
- the design, development, and field validation of instrumental methods and measurement strategies for the in situ characterization of oxidation mechanisms, kinetics, and carbon cycling on Mars.

In the Viking Labeled Release Experiment (Levin and Straat, 1977), an aqueous medium containing several organic compounds labeled with ^{14}C was introduced to a martian surface sample that had been place in a sealed chamber. The experiment was designed to measure metabolic activity, however, a rapid release of CO_2 was observed and attributed to the chemical decomposition of the organic medium instead of biological activity (Klein, 1977). Levin and Straat demonstrated that hydrogen peroxide could reproduce the results of the Viking LR experiment, although they concluded that to explain the thermal stability of the LR results, the peroxide would have to be complexed with the surface material in some unidentified manner. In **chapter 2**, we demonstrate that some transition metal compounds are capable of complexing hydrogen peroxide forming species that behave much as the Viking biology samples did. Titanium dioxide (anatase) exposed to hydrogen peroxide reproduces both the decomposition of organics seen in the Viking LR

experiment as well as the oxygen release seen in the Viking GEx experiment. We conclude that these responses are due to the formation of different types of chemisorbed species on the titanium dioxide. Complexation occurs at Ti^{4+} sites and the formation of similar species would also be expected to occur on other titanium containing minerals such as rutile, ilmenite and sphene.

Carbonates have been spectroscopically identified at a level of 2-5% on the martian surface (Bandfield et al., 2003). However, there is a discrepancy in the literature concerning the stability of carbonates on Mars in the current UV surface environment. On the basis of experiments in which natural calcite crystal (99.94%) decomposed when exposed under vacuum to UV light, Mukhin et al. (1996) reported that photodecomposition of carbonates occurs on Mars. This is at odds with the work of Booth and Kieffer (1978) which showed that carbonates form under conditions similar to those on Mars even with UV light present. In **chapter 3**, we report on experimental investigations of the effect of UV light on the stability of calcium carbonate in a simulated martian atmosphere. We conclude that given the expected stability of carbonate on Mars and our inability to detect carbonate decomposition, the 2-5% carbonate detected by Bandfield et al. (2003) represents an inventory unaltered by UV photodecomposition.

In **chapter 4**, we report the results of experiments which examine the degradation kinetics of aqueous organic substrates using Atacama soils as Mars analogs. We compare our results with direct information on the kinetic behavior of Mars soils in contact with organic compounds in aqueous systems obtained from Viking data. We find that the decomposition of organic compounds in our experiments is dominated by soil surface catalysis and that the overall rate of organic decomposition by some Atacama samples exceeds that of the Viking soils. In the Viking biology experiments, surface catalysis was one of multiple types of oxidative processes that occurred, but it was not the dominate process.

In **chapter 5**, the acid-base equilibration kinetics of soils collected in the Chilean Atacama Desert is compared to information on the acid-base chemistry of martian surface samples derived from the Viking experiments. When experimentally wetted, the pH of both the Viking surface samples collected from the dry-core of the Atacama desert (the Yungay region) underwent a rapid shift, similar in magnitude, from acidic to slightly basic. This shift was not observed in samples collected from wetter regions of the Atacama or from the subsurface at Yungay. This pH response is attributed to the dry deposition and accumulation of atmospheric acid aerosols, including H_2SO_4, and acid precursors on the soil surface at the Yungay and Viking sites. We concluded that in the Atacama and on Mars, extremely low pH resulting from acid accumulation, combined with limited water availability and high oxidation potential, results in acid-mediated reactions at the soil surface during transient wetting events.

The Mars Atmospheric Oxidant Sensor (MAOS) is described in **chapter 6**. MAOS, is a chemometric sensor array that measures the oxidation rate of chemical thin-films that are sensitive to particular types of oxidants, or that emulate some characteristics of pre-biotic and biotic materials. The thin-film reactants include highly electropositive metals, semiconductors, and a set of organic functional groups. MAOS is designed to control the temperature of the sensors and their exposure to dust and ultraviolet light which allows the instrument to discriminate among leading hypotheses for oxidant production. By monitoring differences in film reactions among different sensor combinations, MAOS quantifies the relative contribution of soil-borne oxidants, UV photoxidation, and gaseous oxidants to the chemical reactivity of the Mars surface environment.

Field experiments using the MAOS technologies performed in the Atacama Desert are described in **chapter 7**. Test results indicate distinct reaction patterns for each of the different sensor deployment modes. Reactivity is highest and reaction kinetics are fastest for sensors exposed to atmospheric dust. We conclude that the observed response is consistent with the deposition of dry-acid on the sensors and that the origin of the chemical reactivity is atmospheric dust reactions. In the Atacama region where the instrument was tested, atmospheric sulfur dioxide and nitrogen oxides are oxidized through gas phase reactions into sulfuric acid and nitric acid, which then adsorb onto aerosols and deposit as dry particles. These acids are strongly oxidizing and react with soil components, including organics, when solvated by atmospheric water vapor during periods of high nighttime relative humidity. These results represent the first field validation of the MAOS technology. A version of MAOS has been selected for inclusion in ESA's ExoMars Pasteur payload, a Mars mission currently scheduled for 2011.

In **chapter 8**, an oxidation sensor that uses in situ deposition of thin-film sensing materials is described. The use of in situ deposition of chemical films for oxidation sensors represents a new approach to increasing sensor shelf life and sensitivity while minimizing instrument risk and cost. The sensor is designed to characterize atmospheric oxidation rates on Mars and diurnal variations in these rates. The sensor also provides a proof-of - concept demonstration of in situ deposition of thin-film sensing materials on Mars as risk mitigation strategy and fabrication cost savings by eliminating the need for hermetic sealing of the chemical sensor. The sensor's operating principle is based on the thermal deposition of thin silver films onto a sapphire substrate and the monitoring of changes in film resistance during both deposition and post-deposition oxidation by atmospheric gases. By depositing fresh films at different times (e.g. sunrise, midday, sundown, midnight) diurnal variations in chemical activity can be mapped. The sensor was incorporated into the ESA Beagle 2 Mars Mission as part of the lander's Environmental Sensor Suite.

References

Bada, J.L., Glavin, D.P., McDonald, G.D., Becker, L., 1998. A search for endogenous amino acids in martian meteorite ALH84001. Science 279, 362-365.

Bandfield, J.L., Glotch, T.D., Christensen, P.R., 2003. Spectroscopic detection of carbonate minerals in the martian dust. Science 301, 1085-1087.

Barth, C.A.A., Stewart, I.F., Bougher, S.W., Hunten, D.M., Bauer, S.J., Nagy, A.F., 1992. Aeronomy of the current martian atmosphere. In: Kieffer, H.H., Jakosky, B.M., Snyder, C.W., Matthews, M.S. (Eds.), Mars, University of Arizona Press, Tucson, 1054-1089.

Benner, S.A., Devine, K.G., Matveeva, L.N., Powell, D.H., 2000. The missing organic molecules on Mars. Proc. Natl. Acad. Sci., USA 97, 2425-2430.

Biemann, K., Lavoie, J.M., 1979. Some final conclusions and supporting experiments related to the search for organic compounds on the surface on Mars. J. Geophys. Res. 84, 8383-8390.

Biemann, K., Oro, J., Toulmin III, P., Orgel, L.E., Nier, A.O., Anderson, D.M., Simmonds, P.G., Flory, D., Diaz, A.V., Ruchneck, D.R., Biller, J.E., LaFleur, A.L., 1977. The search for organic substances and inorganic volatile compounds in the surface of Mars. J. Geophys. Res. 82, 4641-4658.

Bohlke, J.K., Ericksen, G.E., Revesz, K., 1997. Stable isotopic evidence for an atmospheric origin of desert nitrate deposits in northern Chile and southern California, USA. Chemical Geology 136, 135-152.

Bullock, M.A., Stoker, C.R., McKay, C.P., Zent, A.P., 1994. A coupled soil-atmosphere model of H_2O_2 on Mars. Icarus 107, 142-154.

Christensen, P.R., et al., 2003. J. Geophys. Res. 108, 8084.

Chun, S.F., Pang, K.D., Cutts, J.A., Ajello, J.M., 1978. Photocatalytic oxidation of organic compounds on Mars. Nature 274, 875-876.

Costard, F. Forget, F. Mangold, N. Peulvast, J.P., 2002. Formation of recent martian debris flows by melting of near-surface ground ice at high obliquity. *Science*, 295, 110-113.

Encrenaz, Th., Bezard, B., Greathouse, T.K., Richter, M.J., Lacy, J.H., Atreya, S.K., Wong, A.S., Lebonnois, Lefevre, F., Forget, F., 2004. Hydrogn peroxide on Mars; evidence for spatial and seasonal variations. *Icarus*, 170, 424-429.

Ericksen, G.E., 1981. Geology and origin of the Chilean nitrate deposits. US Geological Survey Professional Paper, 1188.

Ericksen, G.E., 1983. The Chilean nitrate deposits. American Scientist 71, 366-374.

Flynn, G.J., 1996. The delivery of organic matter from asteroids and comets to the early surface of Mars. Earth, Moon, and Planets 72, 469-474.

Formisano, V., Atreya, S., Encrenaz, T. Ignatiev, N., Gluranna, M., 2004. Detection of methane in the atmosphere of Mars. Science 306, 1758-1761.

Glavin D. P., Schubert M., Botta O., Kminek G., and Bada J. L. 2001. Detecting pyrolysis products from bacteria on Mars. Earth and Planetary Science Letters 185, 1-5.

Grunthaner, F.J., Ricco A., Butler, M.A., Lane, A.L., McKay, C.P., Zent, A.P., Quinn, R.C., Murray, B., Klein, H.P., Levin, G.V., Terhune, R.W., Homer, M.L., Ksendzov, A., Niedermann, P., 1995. Investigating the surface chemistry of Mars. Analytical Chemistry 67, 605A-610A.

Haber, J., 1996. Selectivity in heterogeneous catalytic oxidation of hydrocarbons. In: Warren, B.K., Oyama, S.T., (Eds.), Heterogeneous Hydrocarbon Oxidation, ACS Symposium Series 638, 21-34.

Horowitz, N.H., Hobby, G.L., Hubard, J.S., 1977. Viking on Mars: the carbon assimilation experiment. J. Geophys. Res. 82, 4659-4667.

Hunten, D.M., 1974. Aeronomy of the lower atmosphere of Mars. Rev. Geophys. Space Phys. 12, 529-535.

Hunten, D.M., 1979. Possible oxidant sources in the atmosphere and surface of Mars. J. Mol. Evol., 14, 57-64.

Jull, A.J.T., Courtney, C., Jeffrey, D.A., Beck, J.W., 1998. Isotopic evidence for a terrestrial source of organic compounds found in martian meteorites Allan Hills 84001 and Elephant Moraine 79001. Science 279, 366-369.

Klein, H.P., 1978. The Viking biological experiments on Mars. Icarus 34, 666–674.

Klein, H.P., 1979. The Viking mission and the search for life on Mars. Rev. Geophys. Space Phys. 17, 1655-1662.

Klingelhöfer, G., Morris, R.V., Bernhart, B., Schroder, C., Rodionov, D.S, de Souza, P.A., Yen, A., Geller, R., Evlanov, E.N., Zubkov, B. Foh, J., Bonnes, U., Kankeleit, E., Gütlich, P., Ming, D.W., Renz, F., Wdowiak, T. Squyres, S.W., Arvidson, R.E., 2004. Jarosite and hematite at Meridiani Planum from Opportunity's mössbauer spectrometer. Science 304 1740-1745.

Levin, G.V, Levin, R.L., 1998. Liquid water and life on Mars. *Proc. SPIE*, 3441, 30-41.

Levin, G.V., Straat, P.A., 1977. Recent results from the Viking labeled release experiment on Mars. J. Geophys. Res. 82, 4663-4668.

Mallin, M.C., Edgett, K.S., 2000. Evidence for recent groundwater seepage and surface runoff on Mars. Science, 288, 2330-2335.

McDonald, G.D., deVanssay, E., Buckley, J.R., 1998. Oxidation of organic macromolecules by hydrogen peroxide: implications for stability of biomarkers on Mars. Icarus 132, 170-175.

McKay, C.P., Grunthaner, F.J., Lane, A.L., Herring, M., Bartmann, R.K., Ricco, A.J., Butler, M.A., Murray, B.C., Quinn, R.C., Zent, A.P., Klein, H.P., Levin, G.V., 1998. The Mars oxidant experiment (MOx) for Mars '96. Planetary and Space Science 46, 769-777.

McKay, C.P., Friedmann, E.I., Gomez-Silva, B., Cáceres-Villanueva, L., Andersen, D.T., Landheim, R., 2003. Temperature and moisture conditions for life in the extreme arid region of the Atacama Desert: four years of observations including the El Nino of 1997-1998. Astrobiology 3, 393-406.

McKay, D.S., Gibson, E.K., Thomas-Keprta, K.L., Vali, H., Romanek, C.S., Clemett, S.J., Chiller, X.D.F., Maechling, C.R., Zare, R.N., 1996. Search for past life on Mars: possible relic activity in martian meteorite ALH84001. Science 273, 924-930.

Mukhin, Koscheev, A.P.,. Dikov, Yu. P, Huth, J., Wanke H., 1996. Experimental simulations of the decomposition of carbonates and sulphates on Mars. Nature 379, 141-143.

Navarro-González, R., Rainey, F.A., Molina, P., Bagaley, D.R., Hollen, B.J., de la Rosa, J., Small, A.M., Quinn, R.C., Grunthaner, F.J., Caceres, L., Gomez-Silva, B., McKay, C.P., 2003. Mars-like soils in the Atacama Desert and the dry limit of microbial life. Science 302, 1018-1021.

Oyama, V.I., Berdahl, B.J., 1977. The Viking gas exchange experiment results from Chryse and Utopia surface samples. J. Geophys. Res. 82, 4669–4676.

Quinn, R.C., Orenberg, J., 1993. Simulations of the Viking gas exchange experiment using palagonite and Fe-rich montmorillonite as terrestrial analogs: implications for the surface composition of Mars. Geochim. Cosmochim. Acta 57, 4611-4618.

Quinn, R.C., Zent, A.P., 1999. Peroxide-modified titanium dioxide: a chemical analog to putative martian soil oxidants. Origins Life Evol. Biosph. 29, 59-72.

Rech, J.A., Quade, J., Hart, W.S., 2003. Isotopic evidence for the source of Ca and S in soil gypsum, anhydrite and calcite in the Atacama Desert, Chile. Geochim. Cosmochim. Acta 67, 575-586.

Skelley, A.M., Scherer, J.R., Aubery, A.D., Grover, W.H., Ivester, R.H.C., Ehrenfreund, P., Grunthaner, F.J., Bada, J.L., Mathies, R.A., 2005. Development and evaluation of a microdevice for amino acid biomarker detection and analysis on Mars. Proc. Nat. Acad. Sci. in press.

Squyres, S.W., Arvidson, R.E., Bell, J.F., et al., 2004a. The Sprit Rover's Athena science investigation at Gusev Crater, Mars. Science 305, 794-799.

Squyres, S.W., Grotzinger, J.P., Arvidsom, R.E., Bell, J.F., Calvin, W., Christensen, P.R., Clark, B.C., Crisp, J.A., Farrand, W.H., Herkenhoff, K.E., Johnson, J.R., Klingelhöfer, G., Knoll, A.H., McLennan, S.M., McSween, H.Y., Morris, R.V., Rice, J.W., Reider, R., Soderblom, L.A., 2004b. The Opportunity Rover's Athena science investigation at Meridiani Planum, Mars. 306, 1698-1703.

Sumner, D.Y., 2005. Poor preservation of potential organics in Meridiani Planum hematite-bearing sedimentary rocks. J. Geophys. Res. 109, E12007.

Toulmin, P. Baird, A.K., Clark, B.C., Keil, K. Rose, H.J., Christian, R.P., Evans, P.H., Kelliehr, W.C. 1977. Geochemical and minerlogical interpretation of the Viking inorganic chemical results. J. Geophys. Res. 84, 4625-4634.

Yen, A.S., Kim, S.S., Hecht, M.H., Frant, M.S., Murray, B., 2000. Evidence that the reactivity of the martian soil is due to superoxide ions. Science 289, 1909-1912.

Zent, A.P., McKay, C.P., 1994. The chemical reactivity of the martian soil and implications for future missions. Icarus 108, 146-157.

Zent, A.P., Quinn, R.C., Madou, M., 1998. A thermo-acoustic gas sensor array for photochemically critical species in the martian atmosphere. Planetary and Space Science 46, 795-803.

Zent, A.P., Quinn, R.C., Grunthaner, F.J., Hecht, M.H., Buehler, M.G., McKay, C.P., 2003. Mars atmospheric oxidant sensor (MAOS): an in situ heterogeneous chemistry analysis. Planetary and Space Science 51, 167-175.

Chapter 2

Peroxide-modified titanium dioxide: A chemical analog of putative martian soil oxidants

R. C. Quinn and A. P. Zent

Hydrogen peroxide chemisorbed on titanium dioxide (peroxide-modified titanium dioxide) is investigated as a chemical analog to the putative soil oxidants responsible for the chemical reactivity seen in the Viking biology experiments. When peroxide-modified titanium dioxide (anatase) was exposed to a solution similar to the Viking labeled release (LR) experiment organic medium, CO_2 gas was released into the sample cell headspace. Storage of these samples at 10°C for 48 hr prior to exposure to organics resulted in a positive response while storage for 7 days did not. In the Viking LR experiment, storage of the Martian surface samples for 2 sols (~49 hr) resulted in a positive response while storage for 141 sols essentially eliminated the initial rapid release of CO_2. Heating the peroxide-modified titanium dioxide to 50°C prior to exposure to organics resulted in a negative response. This is similar to, but not identical to, the Viking samples where heating to approximately 46°C diminished the response by 54–80% and heating to 51.5°C apparently eliminated the response. When exposed to water vapor, the peroxide-modified titanium dioxide samples release O_2 in a manner similar to the release seen in the Viking gas exchange experiment (GEx). Reactivity is retained upon heating at 50°C for three hours, distinguishing this active agent from the one responsible for the release of CO_2 from aqueous organics. The release of CO_2 by the peroxide modified titanium dioxide is attributed to the decomposition of organics by outer-sphere peroxide complexes associated with surface hydroxyl groups, while the release of O_2 upon humidification is attributed to more stable inner-sphere peroxide complexes associated with Ti^{4+} cations. Heating the peroxide-modified titanium dioxide to 145°C inhibited the release of O_2, while in the Viking experiments heating to this temperature diminished but did not eliminated the response. Although the thermal stability of the titanium-peroxide complexes in this work is

lower than the stability seen in the Viking experiments, it is expected that similar types of complexes will form in titanium containing minerals other than anatase and the stability of these complexes will vary with surface hydroxylation and mineralogy.

2.1 Introduction

Since the return of data from the Viking Landers in 1977, numerous hypotheses have been presented to explain the results of the Labeled Release (LR) and Gas Exchange (GEx) Experiments. These biology experiments were designed to test Martian surface samples for the presence of life by measuring metabolic activity and distinguishing it from physical or chemical activity (Oyama *et al*., 1976; Levin and Straat, 1976). In the Viking Gas Exchange Experiment (GEx), an attempt was made to identify microbial activity by using gas chromatography to measure the gas changes in the headspace above a soil sample after the addition of an aqueous nutrient medium designed to promote microbial growth. The primary result of this experiment was the release of oxygen in amounts ranging from 70 to 700 nmole cm^{-3} by the Martian surface samples upon introduction of water vapor into the sample cell. Heating the sample to 145°C was found to diminish but not eliminate the release of oxygen. The Labeled Release Experiment (LR) (Levin and Straat, 1976) attempted to detect metabolism or growth of microorganisms through radiorespirometry. In the LR experiment, a liquid medium containing several organic substrates labeled with C was introduced to the Martian surface sample. The major results of the LR were: ^{14}C-labeled CO_2 was rapidly released upon contact of the surface material with the solution; the reaction slowed down after only a small fraction of the added organic medium decomposed; preheating the samples to 160°C for three hours completely inhibited the release of $^{14}CO_2$ (Levin and Straat, 1977).

These results, combined with the failure of the Viking GCMS to detect organic compounds in tested surface samples, have generally lead investigators to the conclusion that the surface material was not biologically active under the experimental conditions, but was chemically reactive (for reviews see Klein, 1978; 1979; Zent and McKay, 1994). In a review article, Zent and McKay (1994) examined a suite of GEx and LR hypotheses (Table I) and concluded that the simplest and most consistent explanation involves a photochemically-produced oxidant which originates in the atmosphere and diffuses into the regolith in very small quantities. Heterogeneous chemical reactions between these photochemically-produced oxidants and the regolith then create surface complexes responsible for the results seen in the Viking biology experiments. The most likely candidate for the oxidant species are the various forms of odd-oxygen and odd-hydrogen expected to be photochemically produced in the Martian atmosphere.

For instance, Hunten (1979) calculated the H_2O_2 flux to the surface of Mars to be $2x10^9$ molecules cm^{-2} s^{-1} and suggested that this may be the source of the oxidant detected by the Viking biology experiments. Huguenin *et al*. (1979) and Huguenin (1982)

Table I
Explanations for the Viking Results

GEx oxygen release	
KO_2, ZnO_2	Ponnamperuma *et al*., 1977
MnO_2, irradiated	Blackburn *et al*., 1978
O_2 trapped in micropores	Nussinov *et al*., 1978
O plasma	Ballou *et al*., 1978
Activated halides	Zent and McKay, 1994
H_2O_2 formed on olivine and pyroxene	Huguenin *et al*., 1978
H_2O_2 adsorbed on Titanium dioxide	This Work
LR CO_2 release	
H_2O_2	Oro, 1979; Levin and Straat 1981
H_2O_2 adsorbed on Titanium dioxide	This Work
Peroxonitrate (NOO_2^-)	Pumb *et al*., 1989
Fe-rich smectite clays	Banin and Margulies, 1983

suggested that surface peroxides formed from the process of water frost dissociating into OH^- and H^+ on the surface of olivine and basalt could be responsible for both the LR and GEx results. In this model, the protons from the dissociated water frost migrate into the mineral lattices leaving the OH^- radicals on the surface to recombine into surface peroxides. Unfortunately, the experiments described by Huguenin failed to demonstrate the thermal stability of these surface peroxide groups, although allowing the frost to melt on the mineral surfaces did produce an oxygen release. Other interpretations of the LR results have also invoked hydrogen peroxide. Levin and Straat (1979; 1981) performed LR simulations using aqueous hydrogen peroxide mixed with Mars soil analogs and concluded that some of the tested mixtures can reproduce the kinetics and thermal information contained in the LR data, however, if H_2O_2 is responsible for the LR results, it would have to be complexed in an unknown way with the Martian surface material.

It is the objective of this study to investigate the complexation of hydrogen peroxide with titanium dioxide to determine if these complexes exhibit stability and reactivity that is similar to what was seen in the Viking biology experiments. Elemental analysis of the

Martian surface by the Viking XRF determined that the Martian surface material contains approximately 1% Ti, reported as TiO_2 (Clark *et al*., 1977). However, while the XRF analysis provided elemental abundance, no mineralogical characterization of the surface material was carried out. On earth, titanium is widely distributed in igneous rocks, with rutile being the most common form of naturally occurring TiO_2. Anatase, a low temperature form of TiO_2, is often formed as an alteration product of ilmenite ($FeTiO_3$) which is a common accessory mineral in igneous rocks. Another widespread accessory mineral containing titanium that is found in igneous rocks is sphene $CaTi[SiO_4](O,OH,F)$. For this work, we chose to use synthetic titanium dioxide (anatase) as the substrate for complexation with peroxide. Although the use of natural titanium containing samples would be preferable over synthetic samples, natural samples were avoided for several reasons. Through careful synthesis of samples, the microbial and organic contaminants that are commonly found in natural samples can be avoided. Organic compounds and microbes will not only react with hydrogen peroxide, they also can lead to false interpretations of any GEx or LR like activity. Additionally, through careful selection of the synthesis conditions the chemical state of the titanium dioxide surface can be controlled, leading to a better understanding of the chemical nature of the complexes that form. Since we are not using a mineral likely to be abundant on Mars, we are proposing a chemical analog for possible stabilization mechanisms of hydrogen peroxide on Mars, we are not proposing a mineralogical model. Of primary interest in this study is the chemical interaction of hydrogen peroxide with the Ti^{4+} cations that are present in the TiO_2 samples, and would also be expected be to present in titanium-containing minerals on Mars.

2.2 Experimental

2.2.1 Synthesis of titanium dioxide (anatase)

Samples of titanium dioxide (anatase) were prepared by hydrolysis of reagent grade titanium tetrachloride (Aldrich Chemical). 5.5 mL of $TiCl_4$ was slowly added to 100 cc of doubly-distilled water cooled in an ice bath. The pH of the resulting mixture was adjusted to 9 by the addition of ammonium hydroxide, and the solution was boiled for one hour. The resulting precipitate was washed with doubly-distilled water by filtering on a sintered glass funnel until free of chloride ions as determined by spot tests of acidified effluent with 0.1 N silver nitrate. The sample was then calcined at either 200 or 350°C for four hours. Calcination at 200°C removes molecular water from the sample, but leaves the majority of surface hydroxyl groups intact (creating a hydroxylated sample), while heating to 350°C removes molecular water as well as a large number of surface hydroxyl groups (creating a partially dehydroxylated sample). Munuera *et al.* (1978) determined that heat treatment of anatase at 350°C yields a surface with 2.8 OH groups per nm^2, while anatase heat-treated at 150 and 250°C contain 8.2 and 6.5 OH groups per nm^2 re-

spectively. Analysis of samples prepared in this manner have been determined to be predominately anatase type TiO_2 (Funaki and Saeki, 1956; Bauer 1963). The surface area of the partially dehydroxylated samples used in this work was determined to be 208 $m^2\ g^{-1}$ from N_2 adsorption isotherms measured at 77 K.

2.2.2 Decomposition of aqueous organics

The fundamental result of the Viking LR experiment was the decomposition of aqueous organic compounds. Samples of peroxide-modified titanium dioxide were prepared and tested to see if sufficient reactivity was retained by the peroxide complexes to decompose the organics that were used in the LR experiment. Because of the difficulty in working with radioisotopes in the laboratory, the LR radioscopic technique was not used, and as such actual simulations of the LR experiment were not performed. Instead the decomposition of LR organics by the peroxide-modified TiO_2 was monitored by measuring CO_2 in the sample cell headspace using gas chromatography. Details of sample preparation and analysis are discussed below, while a discussion on how CO_2 release measured by GC compares to the LR technique is included in Section 3 (Results and Discussion).

Samples of TiO_2 (1.0 g) were suspended in freshly prepared 1% H_2O_2 solutions (prepared by dilution of Aldrich Chemical 30% H_2O_2) for 20–30 min. The samples were then filtered on sintered glass filters and washed with distilled water to remove excess H_2O_2. The total peroxide coverage was determined to be 7.2 x 10^{17} molecules m^{-2} from the difference in concentration (determined by titration with potassium permanganate) of the effluent and the original solution.

To prevent microbial contamination of the samples, all glassware was cleaned with Micro cleaning solution (International Products Inc.), rinsed with doubly-distilled water, and dried under vacuum at 160°C. Additionally, glassware was covered or sealed to prevent spore or microbe contamination during the synthesis. After synthesis, all samples were immediately transferred to a clean box with a continuous purge He atmosphere. Once transferred into the box, 0.1 g samples were placed into 8.6 cc glass sample vials and crimp sealed with rubber septa. The samples were stored in the dark at 10°C between analyses.

Sample analysis of headspace gases was carried out by extracting 1.0 mL of the cell headspace with a gas-tight syringe. The gas sample was then analyzed using a Varian 3400 GC fitted with a 6ft. x 1/8" o.d. HayeSep N column (column temperature 140°C) and thermal conductivity detector (detector 180°C, filament 220°C). Helium, delivered at 80 psi, was used as the carrier gas. A three-level calibration was done for CO_2 using 99.99% carbon dioxide.

Before injection of aqueous organics, the samples were incubated in the dark at 10°C for 48 hr and an initial headspace analysis was performed to verify that no atmospheric CO_2 contamination or sample outgassing had occurred. After this initial analysis, 0.5 mL

of an equal-molar solution of DL-alanine (Sigma, 99% minimum purity), formic acid (Aldrich, 99+% purity), glycine (Sigma, 99+% purity), glycolic acid (Sigma, 98% minimum purity) and DL-lactic acid (Sigma, sodium salt 60% (w/w) syrup 98%) was added to the test cells (total molarity 0.25, pH adjusted to 8.0 with KOH). After injection of the organic medium, the CO_2 level in the headspace was monitored for a period of 72 hours. In this work, both the sample size and the concentration of the organic solution was increased compared to the Viking experiments (6.5 mg as TiO_2 vs. 0.5 to 1.0 cc and 250 mM vs. 0.25 mM) to compensate for the lower sensitivity of the GC analysis relative to the LR radioisotopic technique. Later interpretations of the LR experiment indicate that the soil oxidant, not the nutrient, was the limiting reagent in the LR reaction (Levin and Straat, 1981). Since the total load of active hydrogen peroxide adsorbed on the TiO_2 samples was not known, the relative amount of nutrient used in this work was increased over the Viking LR to insure that the nutrient did not become the limiting reagent. Therefore, results are scaled based on the weight of TiO_2 used since the total amount of CO_2 released by the samples is related to the availability chemisorbed peroxide and not the amount of nutrient injected. This scaling is discussed further in Section 3 (Results and Discussion).

The thermal stability of the peroxide complexes was tested by heating samples (sealed in a helium atmosphere) at 50°C for three hours prior to addition of the organic solution and testing of headspace gases. Blank samples of titanium dioxide that had not been exposed to hydrogen peroxide, were analyzed in the same manner as the peroxide-modified samples.

2.2.3 Oxygen release upon humidification

The primary result of the Viking GEx was the rapid release of O_2 gas upon humidification of the Martian surface samples. In both the Viking GEx and this work changes in sample cell headspace composition were monitored using gas chromatography. Samples of TiO_2 (1.0 g) were suspended in approximately 30 mL of 3% H_2O_2 (Aldrich, stabilized, A.C.S. reagent grade) for 30 min, filtered on a covered sintered glass crucible in air and transferred into a 35 cc stainless steel sample cell. To prevent atmospheric oxygen from leaking into the cell, all seals were metal gasket compression type (conflat, Varian). The cell was equipped with two Nupro SS-4BK bellow-sealed valves. One valve allowed for the evacuation and sampling of cell gases, the other was used to introduce water vapor into the cell via a glass reservoir connected to the cell with a glass-to-metal transition tube. Doubly-distilled water de-gassed by at least 3 freeze-pump-thaw cycles was used for all experiments.

After transferring the sample into the cell, the cell was attached to a vacuum manifold and pumped to a pressure of 10^{-4} torr at room temperature for 16–20 hr. Samples were then heated to approximately 50°C under vacuum for an additional three hours to remove water from the sample and to test the thermal stability of the peroxide complexes. The

samples were then cooled to 10°C (the temperature of the Viking GEx test cell) and, as was done in the Viking GEx, the sample cell was filled to 200 torr with He. After filling with He, the samples were equilibrated for 16 hr before testing.

The gases in the headspace were separated, identified and quantified using a Varian 3400 GC gas chromatograph. A poropak Q 100/120 mesh 7.6 m x 1 mm i.d. column (column temperature 25°C) capable of separating N_2, O_2, Ar/CO, and CO_2 was used to insure that air contamination in the cell could be recognized. Helium carrier gas was delivered at a pressure of 80 psi with a flow rate of 30 cc min^{-1}. A thermal conductivity detector was used for detecting gases eluted from the column. A three-level calibration was done for O_2 using 99.9% pure oxygen.

2.3 Results and Discussion

2.3.1 Carbon dioxide release

Figure 1 compares the carbon dioxide released from the organic nutrient by two replicate samples of partially dehydroxylated (350°C synthesis) peroxide-modified titanium dioxide with the results of the Viking LR VL-1 cycle one and VL-2 cycle one samples (Levin and Straat, 1979). To facilitate comparison, the release of CO_2 by the peroxide-modified TiO_2 is reported as nmoles of CO_2 released per 0.0065 g of titanium dioxide. The Viking LR utilized 0.5 cm^3 of Martian surface material, which corresponds to 0.0065 g of titanium (as TiO_2) in each sample, assuming a density of 1.3 g cm^{-3} (Oyama *et al*., 1977) and a 1% titanium content by weight (Clark *et al*., 1977).

The use of GC instead of the LR radioisotopic technique to monitor the release of CO_2 affects the interpretation and comparison of results. Analysis by GC required extraction of headspace gas at periodic intervals and continuous measurement of the release of CO_2 was not possible as it was with the LR experiment. Therefore, no comparison between the kinetics of CO_2 release by the peroxide modified TiO_2 with the kinetics observed in the first few hours of the LR experiment can be made. However, general trends occurring over the first 72 hr can be compared.

The Viking LR experiments were characterized by a rapid release of CO_2 from the nutrient medium during the first 24 hr followed by a slower prolonged increase over the next few sols. As can be seen in Figure 1, during the first 24 hr of the Viking experiments the VL-1 sample decomposed approximately 14 nmoles of nutrient while the VL-2 sample decomposed approximately 18 nmoles. In contrast, for the peroxide-modified TiO_2 (partially dehydroxylated), a smaller amount of CO_2 was released into the headspace (when scaled by weight as describe above), during the first 24 hr, 10 nmoles of CO_2 from sample TiO_2-A and 2 nmoles from sample TiO_2-B. In addition, after the first 24 hr, the rate of CO_2 released by the Viking samples decreased, while the rate of release by these TiO_2 samples did not. Although partially dehydroxylated samples do result in the release

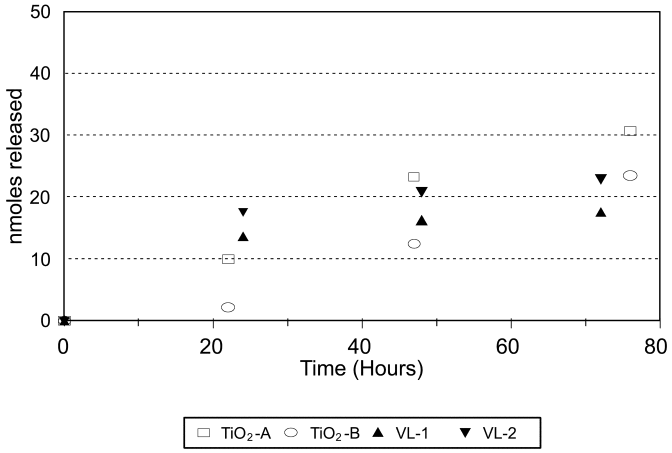

Figure 1. Carbon dioxide changes upon introduction of organic nutrient medium to the peroxide-modified titanium dioxide (partially dehydroxylated anatase) containing sample cell compared to the results of the Viking LR-1 cycle one and VL-2 cycle one samples.

of CO_2 into the cell headspace, the initial rate of release appears to be some what slower and the release fails to level off at the same rate seen in Viking LR results.

In the case of hydroxylated samples, the rate of CO_2 release differed slightly from the partially dehydroxylated samples. Figure 2 compares the carbon dioxide released by hydroxylated samples of peroxide-modified titanium dioxide with the results of the VL-1 cycle one and the VL-2 cycle one. During the first 24 hr, sample TiO_2-C released (scaled by relative weight as described above) approximately 18 nmoles of CO_2 while sample D released 16 nmoles. This compares to approximately 14 nmole for VL-1 cycle one and approximately 18 for nmoles VL-2 cycle one. Additionally, unlike the partially dehydroxylated samples, the release from the hydroxylated samples starts to decrease after the first 24 hr as is seen in the Viking results. No CO_2 was released by titanium dioxide samples that were exposed to the organic solution (and stored in the dark) but not exposed to hydrogen peroxide, indicating that the decomposition of the organic medium is due to the presence of H_2O_2 complexes and not due to the inherent catalytic activity of TiO_2 or microbial contamination.

The ability of peroxide-modified titanium dioxide to reproduce the Viking LR results is apparently influenced by the hydroxylation state of the sample. This is indicative of different types of peroxide complexes forming on the surface titanium dioxide, which is consistent with other studies of peroxide-modified titanium dioxide (Boonstra and Mutsaers, 1975; Munuera *et al*., 1980; Klissurski *et al*., 1990). It has also been found that the same types of complexes form from exposure of TiO_2 to vapor phase or aqueous hydro-

gen peroxide (Boonstra and Mutsaers, 1975). This is important since on Mars the source of soil peroxide-complexes would likely be from hydrogen peroxide that is photochemically produced in the atmosphere and diffuses into the soil where complexation then occurs.

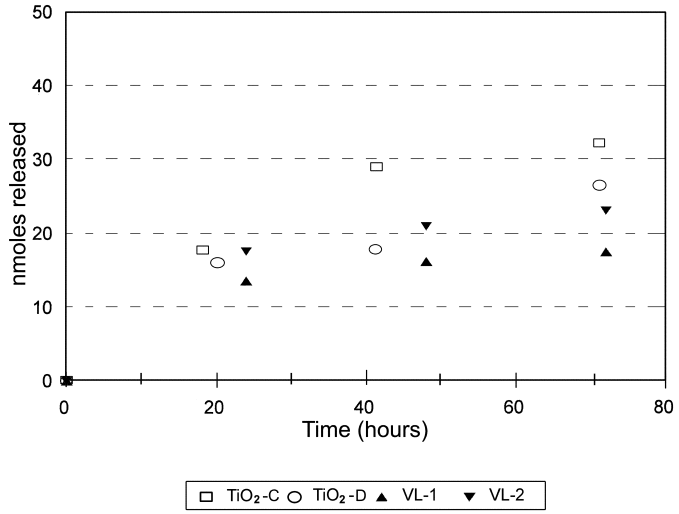

Figure 2. Carbon dioxide changes upon introduction of organic nutrient medium to the peroxide- modified titanium dioxide (hydroxylated anatase) containing sample cell compared to the results of the Viking LR-1 cycle one and VL-2 cycle one samples.

When exposed to either vapor phase or aqueous hydrogen peroxide, different types of peroxide complexes form on the surface of titanium dioxide. One of these types is inner-sphere peroxo-complexes of Ti^{4+} ions, where the H_2O_2 molecules act as bidentate ligands saturating the coordinative capacity of the Ti^{4+} ions originally in a 4-fold coordination scheme (Munuera *et al*., 1980). The bonding in these complexes is coordinative in nature and gives peroxide-modified titanium a characteristic bright yellow color. Another type of complex that forms is outersphere complexes associated with surface hydroxyl groups. These complexes are tightly bonded to the surface through hydrogen bonding (Munuera *et al*., 1980). The number and type of complexes that form depends on the hydroxylation state of the titanium dioxide, with the hydroxylated samples containing a greater number of surface hydroxyl groups and therefore more outer-sphere complexes than the partially dehydroxylated samples. Likewise, the partially dehydroxylated samples have a greater

number of inner-sphere complexes than the hydroxylated sample. It is likely that the less tightly bonded, outer-sphere peroxide complexes on the surface of the titanium dioxide are responsible for the initial rapid release of CO_2 by the hydroxylated samples.

In the Viking LR experiment, three samples were heat-treated for three hours prior to injection of the nutrient medium. Sample VL-2 cycle four was heated at approximately 46°C (accurate to within only a few degrees), and exhibited a 54–80% decrease in CO_2 release compared to the unheated Viking samples (Levin and Straat, 1977, 1979). Sample VL-2 cycle two was heated at 51.5°C for three hours, (again accurate to within a few degrees) and in this case, the release of CO_2 was essentially eliminated. In addition, unusual kinetics which could not be traced to instrument anomalies were seen for the very small amounts of CO_2 detected in the cell (Levin and Straat, 1977). The third sterilized sample VL-1, cycle two, which was heated to 160°C, exhibited essentially no initial release of CO_2 when exposed to the nutrient medium.

Given the uncertainty in the accuracy of the Viking temperature measurements, it can be said that the LR oxidant decomposes at about 50°C. In this study, samples heated to 50°C for three hours released no detectable amount of CO_2. This is consistent with the direct measurement of the thermal stability of outer-sphere peroxide complexes on titanium dioxide which are completely desorbed at about 50°C (Boonstra and Mutsaers, 1975; Munuera *et al*., 1980; Klissurski *et al*., 1990).

The lifetime of the peroxide complex at 10°C was also investigated. In the Viking LR experiments, samples stored for 2 sols (~49 hr) at 10°C in the dark produced positive responses while the initial rapid release of CO_2 was essentially eliminated after storage for 141 sols. In this work, the responses reported are for samples stored for 48 hr in a He atmosphere at 10°C in the dark before introduction of the nutrient medium. Samples that were stored for 7 days exhibited a negative response consistent with the Viking results.

2.3.2 Oxygen release

Figure 3 shows oxygen released upon humidification by peroxide-modified titanium dioxide samples compared to the results of the Viking GEx VL-1 Sandy Flats and VL-2 Beta samples (Oyama and Berdahl, 1977). For comparison the amount O_2 released by the peroxide-modified titanium dioxide is scaled by weight and reported as nmoles released per 0.013 g of TiO_2. The Viking GEx utilized 1.0 cm^3 of Martian surface material, which corresponds to 0.013 g of titanium (as TiO_2) in each sample, assuming a density of 1.3 g cm^{-3} (Oyama *et al*., 1977) and a 1% titanium content by weight (Clark *et al*., 1977).

Upon humidification of the peroxide-modified anatase samples in the simulated GEx experiments, the O_2 level in the headspace rapidly increased. Control samples of TiO_2 not exposed to peroxide did not exhibit any release of oxygen. The general trend for O_2 changes in the headspace of the peroxide-modified titanium dioxide samples in this work is similar to the increase in oxygen seen in the Viking VL-1 cycle one and VL-2 cycle one

data where an initial rapid release of O_2 gas was seen during the first 24 hr after exposure to water vapor (Figure 3).

The decomposition of organics in this work has been attributed to outer-sphere peroxide groups on the surface of a hydroxylated anatase sample. This is based on the thermal stability of these complexes reported in the literature (Boonstra and Mutsaers, 1975; Munuera *et al*., 1980; Klissurski *et al*., 1990) and the negative result obtained with these samples after heating at 50°C for three hours. In the case of the humidification experiments, all samples were heated under vacuum at 50°C for three hours prior to use. This heat treatment was done to remove physically adsorbed water from the surface of the

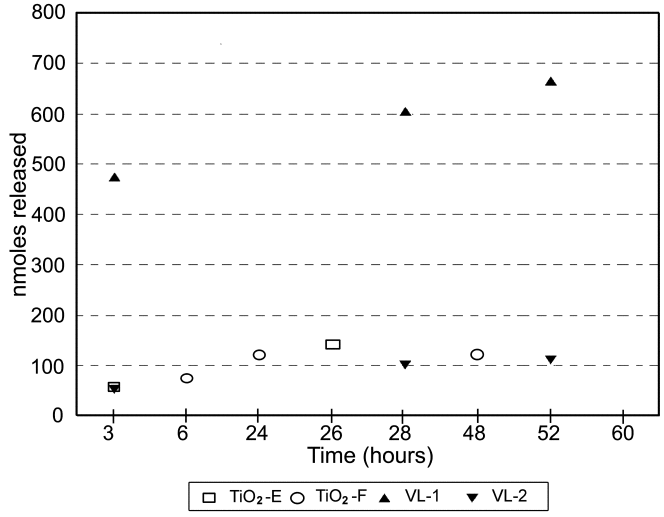

Figure 3. Oxygen release from peroxide-modified titanium dioxide upon humidification compared to the Viking VL-1 Sandy Flats and VL-2 Beta samples.

sample. Since samples of peroxide-modified titanium dioxide heated to 50°C released O_2 upon humidification, but did not decompose organics, it appears that different species are responsible for these two responses although their origin is the same (complexed hydrogen peroxide). This is consistent with conclusions drawn from the results of the Viking Biology experiments (Klein, 1977; 1979). It should be noted however, that in both the Viking LR experiments and the CO_2 release experiments in this work, the sample cell was sealed during the heating procedure. Thus, the stability of the oxidant may have been af-

fected by exposure to high water vapor concentrations during the heating process (Horowitz, 1986).

An average of 120 nmoles of O_2 (scaled by relative wt. of TiO_2) were released by the peroxide-modified titanium dioxide in this work which is consistent with the VL2 GEx results. Table II compares values reported in the literature for the temperature stability of inner-sphere peroxide complexes on anatase with the samples used in this work. In this work, all the peroxide complexes desorbed at temperatures below 120°C, and not surprisingly samples heated to 145C° did not release O_2 upon humidification. However, peroxide desorption occurs over a broad temperature range with variations in the upper and lower temperature limits that depend on mineralogy and hydroxylation state (Boonstra and Mutsaers, 1975; Munuera *et al*., 1980; Klissurski *et al*., 1990).

Table II
Stability of inner-sphere peroxide complexes on TiO_2

	Surface coverage	Desorption range
Klissurski *et al*., 1990	1.5×10^{13} molecules cm^{-2}	75–170 °C
Boonstra and Mutsaers, 1975	1.7×10^{14} molecules cm^{-2}	50–150 °C
Munuera *et al*., 1980	1.0×10^{14} molecules cm^{-2}	150–200 °C
This work	7.2×10^{13} molecules cm^{-2}	50–120 °C

The total amount of O_2 released by the TiO_2 represents a fraction of the total chemisorbed peroxide. The number of inner-sphere peroxide groups present on the surface of the anatase is approximately 7 x 10^{17} molecules m^{-2}, which corresponds to a release of 1572 nmoles of O_2 for a 0.013 g sample if all groups decompose to form water and O_2. Furthermore, the TiO_2 samples retained their bright yellow color after humidification, which indicated that at least some of the inner-sphere peroxide groups remained. One possible explanation for the release of O_2 in amounts that correspond to only approximately 10% of the chemisorbed hydrogen peroxide, is that during the sample dehydration process, some of peroxide groups may partially decompose or migrate to sites previously occupied by water molecules. Upon re-hydration of the anatase sample, water displaces the peroxide and it decomposes into H_2O and O_2. On Mars, the surface coverage of physically adsorbed water is only a fraction of a monolayer (Zent and Quinn, 1995). Under these conditions, it is possible that peroxide may adsorb onto sites that would be occupied by molecular water at higher temperatures and higher water vapor abundance. When the dry Martian surface sample is exposed to 100% humidity at 10°C in the gas exchange experiment, several monolayers of physically-adsorbed water form on the surface, displacing peroxide. Once desorbed from the surface, the peroxide decomposes (catalyzed by iron oxide and other components of the surface material) and releases oxygen into the headspace.

2.4 Conclusions

Levin and Straat (1981) demonstrated that hydrogen peroxide could reproduce the results of the Viking LR experiment, although they concluded the peroxide would have to be complexed with the surface material in some unidentified manner. We have demonstrated that hydrogen peroxide complexes with titanium dioxide and retains the ability to decompose the same organics used in the Viking LR experiment and release O_2 when humidified as was seen in the Viking GEx. This complexation of peroxide with titanium dioxide imparts stability which is similar, although not identical, to that seen in the Viking samples. The outer-sphere peroxide complexes on titanium dioxide which are most probably responsible for the release of CO_2 in this work decompose at approximately 50°C. In the Viking LR experiments, heating to 46°C (plus or minus several degrees) decreased the signal by as much as 80%, and heating to 51.5°C (plus or minus several degrees) may have eliminated the response altogether (Levin and Straat, 1977). Storage of the peroxide modified titanium dioxide samples at 10°C for 48 hr prior to exposure to organics resulted in a positive response while storage for 7 days did not. In the Viking LR experiment, storage of the Martian surface samples for 2 sols (~49 hr) resulted in a positive response while storage for 141 sols essentially eliminated the initial rapid release of CO_2.

Oxygen release by the peroxide-modified titanium dioxide apparently is related to the presence of the more stable inner-sphere peroxo-complexes. The ability of these samples to release O_2 upon humidification was seen in samples that were heated at 50°C for three hours, distinguishing these complexes from the complexes responsible for the release of CO_2 which was eliminated by prolonged heating at 50°C. This is somewhat consistent with the findings of the Viking experiment where activity was diminished but not eliminated in samples heated to 145°C. Although the samples used in this work heated to 145°C did not exhibit a release of O_2 upon humidification as seen in the Viking samples, other researchers have demonstrated that chemisorbed hydrogen peroxide in some case is stable above 145°C (Table II). Since the chemisorption occurs at Ti^{4+} sites it is reasonable to expect that the same type of chemisorption will occur on titanium containing minerals other that anatase such as rutile, ilmenite and sphene, although the stability and surface coverage of the peroxide groups is expected to differ some what with variations in hydroxylation state and mineralogy.

Acknowledgements

This work was supported by the NASA Exobiology Program.

References

Ballou, E. V., Wood, P. C., Wydeven, T., Lehwalt, M. E. and Mack, R. E., 1978. *Nature* 271, 644.

Banin, A. and Margules, L., 1983. *Nature* 305, 523.

Blackburn, T. R., Holland, H. D. and Ceaser, G. P., 1979. *J. Geophys. Res.* 84, 8391.

Boonstra, A. H. and Mutsaers, C. A. H. A., 1975. *J. Phys. Chem.* 79, 1940.

Brauer, G., 1963. *Handbook of Preparative Inorganic Chemistry,* Vol. 1, Academic Press, pp. 1216–1217.

Clark, B. C., Baird, A. K., Rose Jr., H. J., Toulimin III, P., Christian, R. P., Kelliher, W. C., Castro, A. J., Rowe, C. D., Kiel, K. and Huss, G. R., 1977. *J. Geophys. Res.* 82, 4577.

Funaki, K. and Saeki, Y., 1956. *Kogyo Kagaku Zasshi* 59, 1295.

Horowitz, N. H., 1986. *To Utopia and Back, The Search for Life in the Solar System*, Freeman, New York.

Hunten, D., 1979. *J. Mol. Evol.* 14, 57–64.

Huguenin, R. L., Miller, K. J. and Harwood, W. S., 1979. *J. Mol. Evol.* 14, 103.

Klein, H. P., 1978. *Icarus* 34, 666.

Klein, H. P., 1979. *Rev. Geophysics and Space Res.* 17, 1655.

Klissurski, D., Hadjiivanov, K., Kantcheva, M. and Gyurova, L., 1990. *J. C. S. Faraday I.* 86, 385.

Levin, G. V. and Straat, P. A., 1976. *Origins of Life* 7, 293.

Levin, G. V. and Straat, P. A., 1977. *J. Geophys. Res.* 82, 4663.

Levin, G. V. and Straat, P. A., 1979. *J. Mol. Evol.* 14, 167.

Levin, G. V. and Straat, P. A., 1981. *Icarus* 45, 494.

Nussinov, M. D., Chernyak, Y. B. and Ettinger, J. L., 1978. *Nature* 274, 859.

Munuera, G., Rives-Arnau, V. and Saucedo, A., 1979. *J.C.S. Faraday I.* 75, 736.

Munuera, G., Gonzales-Elipe, A. R. and Soria, J., Sanz, J., 1980. *J.C.S. Faraday I.* 76, 1535.

Oro, J. and Holzer, G., 1979. *J. Mol. Evol.* 14, 153.

Oyama, V. I., Berdahl, B. J., Carle, G. C. and Lehwalt, M. E., 1976. *Origins of Life* 7, 313.

Oyama, V. I. and Berdahl, B. J., 1977. *J. Geophys. Res.* 82, 4669.

Oyama, V. I., Berdahl, B. J. and Carle, G. C., 1977. *Nature* 265, 110.

Plumb, R. C., Tantayanon, R., Libby, M. and Xu, W. W., 1989. *Nature* 338, 633.

Ponnamperuma, C., Shimoyama, A., Yamada, M., Hobo, T. and Pal, R., 1977. *Science* 197, 455.

Zent, A. P. and McKay, C. P., 1994. *Icarus* 108, 146.

Zent, A. P. and Quinn, R. C., 1995. *J. Geophys. Res.* 100, 5341.

Chapter 3

The photochemical stability of carbonates on Mars

R. C. Quinn, A. P. Zent, C. P. McKay

Carbonates, predominately $MgCO_3$, have been spectroscopically identified at a level of 2-5% in Martian dust (Bandfield et al., 2003). However, in spite of this observation, and a large number of climate studies that suggest one to several bars of CO_2 should be sequestered in carbonate rocks, no outcrop-scale exposures of carbonate have been detected anywhere on Mars to date. To address one hypothesis for this long-standing puzzle, the effect of UV light on the stability of calcium carbonate in a simulated martian atmosphere was experimentally investigated. Using ^{13}C-labeled calcite we found no experimental evidence of the UV photodecomposition of calcium carbonate in a simulated martian atmosphere. Extrapolating the lower limit of detection of our experimental system to an upper limit of carbonate decomposition on Mars yields a quantum efficiency of 3.5×10^{-8} molecules/photon over the wavelength interval of 190-390 nm and a maximum UV photodecomposition rate of 1.2×10^{-13} kg m^{-2} s^{-1} from a calcite surface. The maximum loss of bulk calcite due to this process would be 2.5 nm yr^{-1}. However, calcite is expected to be thermodynamically stable on the surface of Mars and potential UV photodecomposition reaction mechanisms indicate that while calcium carbonate may decompose under vacuum, it would be stable in a CO_2 atmosphere. Given the expected stability of carbonate on Mars and our inability to detect carbonate decomposition, we conclude that it is unlikely that the apparent absence of extensive carbonate deposits on the martian surface is due to UV photodecomposition of calcite in the current environment.

Chapter 3

3.1 Introduction

3.1.1 Formation of carbonates on Mars

As has been discussed extensively in the literature, it is thought that Mars may have once had a thick CO_2 atmosphere, which is now in the form of carbonate deposits. There are two lines of evidence that suggest that Mars had a thicker atmosphere during the Noachian epoch (3.8 Gyr ago). First is the evidence of much higher erosion rates in the Noachian terrain compared to younger terrains. Carr (1992) has estimated that the erosion rate on Noachian surfaces was 2-10 μm yr^{-1}, a value comparable to the low end of terrestrial erosion rates. Post-Noachian erosion rates are on the order of 0.02 μm yr^{-1} ($2x10^{-8}$ m yr^{-1}). The second line of evidence is the presence of fluvial channels on the Noachian surface, indicating a stable flow of liquid water.

Both of these lines of evidence suggest that Mars had a thicker, warmer atmosphere at the end of the Noachian than it does today. Paradoxically, these warmer conditions existed when the solar luminosity was about 0.8 of its present value. For many years, it was generally believed that a several-bar atmosphere of CO_2 would provide an adequate greenhouse effect to allow for surface conditions consistent with a hydrological cycle and the concomitant fluvial and erosion features (e.g. Pollack et al., 1987; Fanale et al., 1991). However, over time the thick CO_2 atmosphere would be removed through the precipitation of carbonate resulting from the formation of CO_3^{-2} by dissolved CO_2 and the dissolution of cations from silicate rocks. The formation of carbonate would result in a net loss of CO_2 from the atmosphere, which would continue until the atmospheric pressure approached the triple point of water and liquid water was no longer formed (Kahn, 1985).

Theoretical models suggest that carbonate formation would proceed for 10 to 100 million years before the thick CO_2 atmosphere would be reduced to current surface pressures (Pollack et al., 1987; McKay and Davis, 1991; Haberle et al., 1994). Recycling of carbonate has been suggested as the mechanism by which a thick atmosphere was maintained during the Noachian; Pollack et al. (1987) and Schaefer (1990) suggested volcanic recycling, while Carr (1989) suggested impact recycling. The drop-off of recycling due to lower heat flow or the cessation of impacts would account for the drop in atmospheric pressure and the lowering of temperatures at the end of the Noachian. Without plate tectonics to subduct carbonate sediments and thereby decompose them to CO_2, Mars had no mechanism to recycle carbonates and the planet quickly cooled to its current state. Along these lines, Griffith and Shock (1995) have suggested that rainfall is not necessary to form carbonates and that hydrothermal systems could have formed massive carbonate deposits.

The entire thick CO_2 hypothesis was thrown into question when Kasting (1991) pointed out that a thick CO_2 atmosphere on early Mars would not be able to warm the surface sufficiently to allow for water to flow, due to the condensation of the atmospheric CO_2. To warm Mars to a globally averaged temperature of 273 K early in its history, when the solar luminosity was 0.8 times its present value, requires an atmospheric pres-

sure of about 3-5 bars of CO_2 (Pollack et al., 1987). However, at these high levels the partial pressure of CO_2 in the upper atmosphere exceeds its saturation point. The resulting condensation changes the temperature lapse rate, with the net effect of cooling the planet's surface. Hence, there is a limit to the amount of greenhouse warming that is possible with a CO_2 and H_2O atmosphere. This effect had been previously noted by Gierasch and Toon (1973) but was not properly incorporated into greenhouse models of Mars until 1991. Thus theoretical models imply that the CO_2 greenhouse could not warm Mars to temperatures above -50°C early in its history. Unless they invoke greenhouse gases other than CO_2, such as CH_4, current climate models cannot adequately explain the hypothesized surface conditions on Mars during the Noachian or the existence of channels on younger terrain. However, recent models which include the effects of clouds (Forget and Pierrehumbert, 1997; Mischna et al., 2000) show that carbon dioxide clouds could result in a net warming and generate surface temperatures near freezing.

3.1.2 The effect of UV light on carbonate formation and stability

Carbonates, predominately $MgCO_3$, have been spectroscopically identified at a level of 2-5% in martian dust (Bandfield et al., 2003). However, there is a discrepancy in the literature concerning the stability of carbonates on Mars in the current UV surface environment. Mukhin et al. (1996) reported that photodecomposition of carbonates occurs on Mars, on the basis of experiments in which natural calcite crystal (99.94%) decomposed when exposed under vacuum to UV light. This is at odds with the work of Booth and Kieffer (1978) which showed that carbonates form under conditions similar to those on Mars even with UV light present. To resolve this discrepancy, we have carried out a series of experiments to investigate the temperature dependence of UV-induced carbonate decomposition in a simulated Mars atmosphere (at a pressure of 10 mbar).

3.2 Materials and methods

3.2.1 Experimental apparatus

Experiments were carried out in ultrahigh-vacuum-compatible 34.5 cc stainless steel reaction cells. Each cell utilized a stainless steel bellows valve for introduction and extraction of headspace gases, and a 2.54 cm UV grade-sapphire view port for illumination of samples. All seals were conflat-type metal compression seals, ensuring a leak-tight system. The reactions cells used for UV exposures is shown in Fig. 1. After preparing a sample (described in section 2.2), the cell was fitted into an aluminum cold-block which was temperature controlled using a FTS Systems recirculating cooler with a lower temperature limit of 173K. A Photon Technologies International 150-watt Xe arc lamp with

an ellipsoid reflector was used to illuminate the samples. A 18 cm water filter cooled with recirculating water was used to prevent IR heating of the samples during illumination. The entire system (lamp, filter, cell, and cold block) was enclosed in a glove bag purged with dry nitrogen to prevent condensation of water ice on the surface of the cell windows during illumination and to minimize UV adsorption by gases in the optical path between the lamp and sample cell.

3.2.2. Sample preparation

99.6% purity labeled calcium carbonate, 99.1% ^{13}C, (Isotec Inc.) was used to allow carbonate decomposition to be differentiated from the CO_2 present in the simulated Mars atmosphere used in the experiments. The samples were identified to be calcite by X-ray diffraction analysis. 0.5-gram samples of the $Ca^{13}CO_3$ were placed in planchets and lightly pressed to yield a flat and uniform surface area and sealed in the sample cells. The sealed cells were attached to a turbo-pumped high-vacuum system (base pressure 10^{-8} torr) with an oil-free diaphragm foreline pump and baked out under vacuum to remove

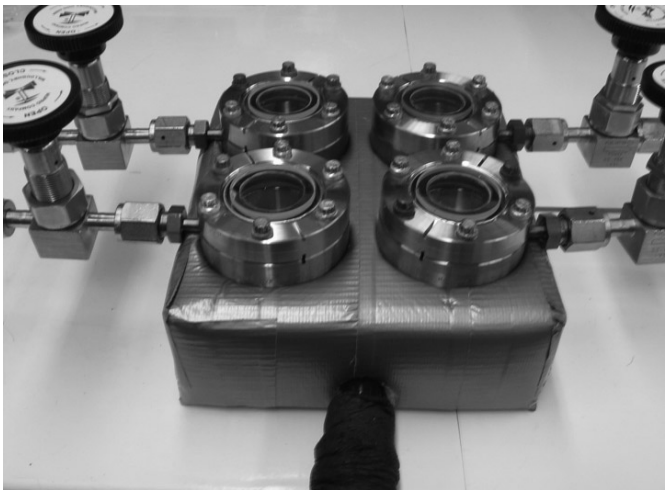

Figure 1. UV photolysis sample cells fitted in a temperature controlled aluminum block. The cells are ultra-high vacuum compatible with UV-grade sapphire view-ports. A Xe lamp was used to simulate Mars solar flux.

adsorbed gases and surface contaminants. After sample bake-out, the sample cells were filled to 10 mbar with a simulated martian atmosphere gas mixture consisting of 97.27% CO_2, 2.7% N_2, and 0.13% O_2 (AirGas Inc).

3.2.3 Experimental procedure

Experiments were run for periods of up to 70 hours at four cell temperatures: 423K, 323K, 278K, and 243K. In each experiment the lamp was positioned to provide a UV flux of no more than ~10^{17} photons $cm^{-2}s^{-1}$. After the UV exposure period was completed, the cells were allowed to warm to room temperature and then analyzed using a Stanford Research Systems Residual Gas Analyzer (quadrupole mass spectrometer). Samples of headspace gases were admitted from the cells into the RGA through a leak valve. Production of $^{13}CO_2$ was monitored by analyzing changes in the 44/45 ($^{12}CO_2^+$)/($^{13}CO_2^+$) mass ratio.

3.2.4 Calibrations

The Photon Technologies International UV lamp with a 150-watt Xe short arc lamp (Ushio Inc.) was calibrated using an Ultra Violet Products (UVP) radiometer and sensors calibrated with standards traceable to the National Physics Laboratory (UK). A comparison of the calibrated spectrum of the Xe lamp to the UV flux at the surface of Mars (Khun and Atreya, 1979) is shown in Fig. 2. For all runs, the flux used to calculate either the quantum yield or the lower limit of detection was determined from the run UV calibration curve for wavelengths below 390 nm.

The mass spectrometer used for analyzing the sample headspace gases was calibrated using 99.9% purity ^{13}C labeled CO_2 (Isotec Inc.). The total ^{13}C content in the standard gas equaled 99.1 atom % and ^{12}C content equaled 0.9 atom %. Ar/O_2 and N_2 contamination was less than 50 ppm, CO contamination less than 20 ppm, and total hydrocarbon content less than 20 ppm. Calibration curves were created by plotting the ($^{13}CO_2^+$)/($^{12}CO_2^+$) mass ratio (45/44) against the delivery pressure of $^{13}CO_2$ standard. The standards were introduced into the RGA system through a leak valve in the same manner as for sample analysis. For each experiment, three background measurements were taken of simulated Mars atmosphere mixture without added $^{13}CO_2$. The standard deviation of these background measurements was used to determine the lower limit of detection (LLD = 2σ) for each experiment. A linear detector response was observed over the range of 0 to 0.2 mbar (0 to 1.7 x 10^{17} molecules) of $^{13}CO_2$ added to the sample cells. A representative calibration curve is shown in Fig. 3.

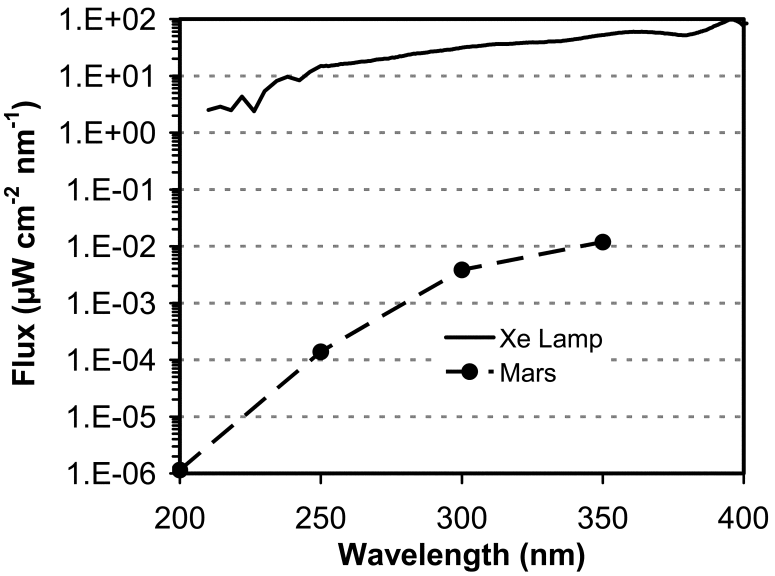

Figure 2. Representative spectral output of Xe lamp used to irradiate samples compared to the radiation incident on the martian surface for 50°N latitude in the spring. Mars spectrum adapted from Khun and Atreya (1979).

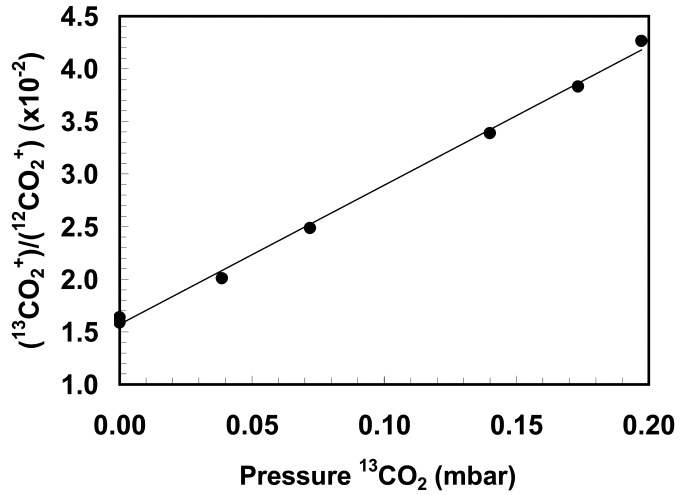

Figure 3. Example of a typical quadrupole mass spectrometer (RGA) $^{13}CO_2$ calibration curve.

3.3 Results

A summary of run conditions and results is given in table 1. From one of the high temperature runs (423K), a maximum quantum yield for carbonate decomposition can be calculated to be $3x10^{-7}$ molecules/photon. However, although a quantum yield can be calculated, we attribute all measured production of $^{13}CO_2$ in the high temperature experiments not to UV decomposition but to a thermal release of adsorbed or trapped $^{13}CO_2$ from the carbonate sample. To analyze this thermal effect, it is useful to divide the experiment runs into two sets based on sample pre-run treatment. Although all samples were pumped down overnight to the 10^{-8} mbar range, each was subjected to a different thermal treatment during the pump-down procedure. As table 1 shows, three irradiated samples and a blank run (consisting of a non-illuminated sample cell containing $Ca^{13}CO_3$ and Mars gas mixture) were held at room temperature during the pump-down, while four other samples were baked out during pump-down. Other than the experimental run carried out at 423K, only one other run (carried out at 323K) and the blank run had measured 45/44 mass ratios that exceeded two standard deviations of the baseline. The run temperatures for both of these samples exceeded the bake-out temperature, while the blank was held at room temperature and not subjected to UV exposure. The other sample held at room temperature during pump-down had a 45/44 ratio of less than one sigma; however, it was held at subambient temperatures (i.e. it did not exceed its bake-out temperature) during the course of the experiment. In samples that were not baked out, $^{13}CO_2$ was released (or possibly exchanged with the headspace $^{12}CO_2$) even if the sample was not exposed to UV radiation, unless the sample was cooled during the experiment.

These results can be compared to the samples that received high-temperature bake-out during sample pump-down. Samples B1 and B2 were each baked out at 490K, while samples B3 and A4 were baked out at 625K and 675K respectively. Three of the baked

Table 1

Experiment	Mass Ratio 45/44 ($x10^{-2}$)			Bakeout Temp. (K)	Run Temp. (K)	UV Flux (Photons $s^{-1}cm^{-2}$)	Exposure Time (hours)	LLD Quantum Efficiency (molecules/photon)
	Baseline	LLD	Measured					
High Temp/No Bakeout	1.25	1.32	1.60	293	423	$4.5x10^{17}$	45	$2.6x10^{-7*}$
High Temp/No Bakeout	1.25	1.32	1.34	293	324	$1.3x10^{17}$	48	$2.2x10^{-7}$
High Temp + Bakeout	1.25	1.32	1.21	675	325	$1.3X10^{17}$	48	$2.2x10^{-7}$
Low Temp/No Bakeout	1.25	1.32	1.26	293	245	$1.3x10^{17}$	48	$2.2x10^{-7}$
Low Temp + Bakeout	1.61	1.66	1.60	625	278	$8.6x10^{16}$	11	$1.7x10^{-6}$
Low Temp + Bakeout	1.61	1.66	1.61	490	278	$5.4x10^{15}$	11	$2.6x10^{-6}$
Low Temp + Bakeout	1.61	1.66	1.63	490	278	$6.3x10^{16}$	70	$3.5x10^{-8}$
Blank/No Bakeout	1.25	1.32	1.36	293	293	Dark	48	N/A

*Actual calculated quantum efficiency. In all other cases lower limit of detection reported.

out samples were held slightly below room temperature (~278K) during UV illumination. In all three cases the measured 45/44 ratios after illumination were less than one standard deviation of the baseline. A fourth sample, which was heat to 675K during pump-down, was heated during UV illumination to a temperature of 325K, substantially below its bake-out temperature. Again, in this case, as with the other samples that were baked out, the post-illumination 45/44 ratio was less than one standard deviation above the baseline.

In summary, we see no evidence for the UV decomposition of $CaCO_3$ in our experiments. Nevertheless, we cannot, of course, rule out that the reaction may be occurring at a rate below our LLD. However, as can be seen in table 1, even if this were the case, the upper limit of the quantum efficiency with which the UV decomposition of carbonate can take place is ~$3x10^{-8}$ molecules/photon.

3.4 Discussion

Our inability to detect the photodecomposition of carbonate in our experimental runs leads to two possible conclusions: that decomposition does not take place in a Mars atmosphere, or that decomposition is taking place with a quantum efficiency below $3.5x10^{-8}$ molecules/photon. Below we consider these two possibilities, examine why we expect carbonates to be stable on the surface of Mars, suggest possible mechanisms for the UV decomposition of carbonates, and discuss implications of carbonate UV-decomposition rates below $3.5x10^{-8}$ molecules/photon on the surface of Mars.

3.4.1 Thermodynamic effects of CO_2 partial pressure

The stability of carbonates on Mars has been the subject of considerable research (e.g. O'Connor, 1968; Gooding, 1978; Fegley and Treiman, 1992) that has yielded a detailed set of chemical equilibrium equations that can be solved for the stability fields of carbonates. Each of these studies concluded that not only are carbonates thermodynamically stable at the current CO_2 surface pressures on Mars, but that virtually all the available CO_2 should eventually be converted to carbonates.

Thermodynamically, the role of system CO_2 pressure can be examined by considering the heterogeneous formation (solid-gas) of carbonates on Mars in the absence of water. Although the case presented is simplified, it illustrates the important role of CO_2 partial pressure on carbonate stability. The heterogeneous decomposition of calcite can be represented by the reaction

$$CaCO_3 \rightarrow CaO + CO_2 + \Delta G_T^o \qquad (1)$$

where G^o is the Gibbs free energy of the reaction, which is a function of temperature (the Helmholz free energy defined for constant volume reactions). At low temperatures G^o is positive (130 kJ at 25°C), indicating that calcite is quite stable. However, at elevated temperatures G^o becomes negative and calcite decomposition proceeds with the formation of CaO according to Eq. 1. The Gibbs free energy of the reaction is given by:

$$\Delta G = \Delta H - T\Delta S \tag{2}$$

where ΔH is the enthalpy of formation and ΔS is the entropy. As temperature increases, the second term in Eq. 2 (TΔS) increases due to its explicit temperature dependence and because one of the reaction products, CO_2, is in the gas phase and the entropy is approximately linearly proportional to temperature. Thus, because ΔH is roughly temperature independent, as temperature increases the second term becomes dominant and eventually ΔG^o becomes negative.

A low and constant CO_2 partial pressure is implicit in the above discussion. (Strictly speaking, it is the fugacity that is low and constant, but for all conditions considered here, the fugacity is equal to the partial pressure to adequate accuracy). Of course, in a closed system calcite decomposition would result in the generation of CO_2 until equilibrium is reached, with the back reaction of Eq. 1 proceeding at the same rate as the forward reaction. Assuming that the activity coefficients of $CaCO_3$ and CaO are unity (as pure solids), the equilibrium partial pressure of CO_2 is given by

$$p^eCO_2 = \exp[-\Delta G°/RT] \tag{3}$$

where R is the universal gas constant. When the system partial pressure of CO_2 is not equal to its equilibrium value, a free energy difference is generated which drives the reaction toward the direction that will establish equilibrium. The value of this free energy is given by

$$\Delta G° = -RT \ln[pCO_2/p^eCO_2]. \tag{4}$$

At room temperature, $\Delta G°$ for the decomposition of carbonate is approximately 130 kJ $mole^{-1}$ (Stern and Weiss, 1969), so the expected equilibrium CO_2 partial pressure for the experiments carried out at room temperature in this work is approximately 10^{-23} bar. In both cases, the actual CO_2 partial pressure greatly exceeded this value, which should drive the reaction toward the formation of carbonate with the value of ΔG^o reduced by an amount given by Eq. 4. This value is equal to -120 kJ $mole^{-1}$ ($pCO_2 \sim 10$ mbar) in this work. There is considerably more (almost double) free energy driving the formation of carbonates, and resisting their decomposition, under the realistic P_{CO2} experimental conditions.

It is interesting to compare these free energy values with the activation energy reported for carbonate decomposition. Stern and Weise (1969) surveyed reported values of the activation energy and found that nearly all are approximately 167 kJ $mole^{-1}$. Thus, the energy of back reaction (formation of carbonates) in this work is comparable to the activation energy. It should be mentioned that our experiments examined only the possibility of carbonate decomposition and not the reverse reaction. Booth and Kieffer (1978), in a carefully conducted study, demonstrated the growth of carbonates on rock powder exposed to UV in the presence of CO_2 ranging from 100 to 500 mb. Another of their findings relevant to the discussion here is that the carbonate formation rate was proportional to the pressure of CO_2 over the range of 100 to 500 mb.

3.4.2 Effects of UV light on carbonate stability

However intriguing the thermodynamic discussion given above, it is an incomplete description in that it does not include the effects of UV light. Numerous studies have examined the generation of defects in carbonates by irradiation (e.g. Stoesser et al., 1996; Bartoll et al., 2000). These works are primarily concerned with radiation defects in relation to Electron Spin Resonance (ESR) spectroscopy dating. Most of these works examined the generation of defects by high-energy γ radiation; very few studies addressed the effects of UV light on the structure of calcium carbonate. In fact, we were able to find in the literature only one study that reported the generation of electronic defects in calcium carbonate by UV light (Bartoll et al., 2000).

As is the case with studies of the effects of high-energy irradiation of carbonates, Bartoll et al. (2000) examined the effects of UV/VIS light on carbonates in relation to ESR dating techniques. They found that radical species such as CO_2^- and CO_3^- could be generated by exposing synthetic and natural calcium carbonates to sunlight or a Hg (Xe) lamp. They also found that while these and other radical species normally observed in carbonates exposed to high energy radiation (α,β,γ) can be generated by exposure to lower-energy UV light, there are numerous subsequent reactions that take place, such as recombination and conversion into other centers. Bartoll et al. (2000) also found that the presence of manganese, iron, or zinc in the carbonate can serve as a sensitizer for the formation of radicals while at the same time causing optical bleaching of defects. Therefore, it is possible that in the Mukhin et al. (1996) work, UV irradiation resulted in the generation of electronic defects, including possible CO_2^- and CO_3^- radicals, and that these species subsequently formed CO_2 gas. However, several thermal, mechanical, and optical pathways exist through which photo-generated centers can recombine, convert, or be bleached, and although Bartoll et al. (2000) documented the bleaching and conversion of defects in calcium carbonate by UV light, they did not report the generation of CO_2 from any of the observed centers. They also did not specify whether there were any background gases present during the UV exposure. If in fact the exposure was carried out in air, or if

trace amounts of O_2 or CO_2 were present, CO_3^- could be formed through the generation of radicals from adsorbed O_2 and CO_2

$$O_{2\ \text{adsorbed}} + h\nu \rightarrow 2O^- \quad (5)$$

$$CO_{2\ \text{adsorbed}} + O^- \rightarrow CO_3^- \quad (6)$$

If CO_3^- radicals are formed on calcium carbonate by UV radiation, either by radical formation on the surface due to adsorbed gas or by defect formation in the lattice, there are several mechanisms by which these centers can recombine, convert, or react (especially if headspace gases are present). One probable mechanism that can result in the formation of CO_2 gas is photodetachment and photodissociation of the CO_3^- radical:

$$CO_3^- + h\nu \rightarrow CO_2 + O^- \quad (7)$$

This reaction has been studied extensively in the gas phase in the context of negative ion chemistry in the ionosphere (Moseley et al., 1974; Hiller and Vestal, 1980; Hunton et al., 1984). Mosely et al. (1974) reported that photodetachment thresholds for CO_3^- are above 3eV while photodissociation occurs between 2.35 and 2.71 eV. In these works, it has been found that when the reaction 7 is carried out at high CO_2 pressures, the O^- produced from the photodissociation undergoes recombination with CO_2 gas to reform CO_3^-.

$$2CO_2 + O^- \rightarrow CO_3^- + CO_2 \quad (8)$$

In these studies the rate of recombination is dependent on both the CO_2 pressure and the time the CO_3^- resides in the drift tube in which it is generated. As drift time increases, CO_2 pressure must decrease to prevent O^- from reacting with CO_2 to reform CO_3^-. Typically, the CO_2 pressure in the drift tube is kept below 0.1 torr to minimize conversion of CO_2 back into CO_3^- as the CO_3^- exits the drift tube.

In the case where the CO_3^- radical is generated as a surface defect on the carbonate crystal, reaction 7 can proceed at a rate limited by the rate of removal of CO_3^- from the surface through the formation of CO_2. When the reaction takes place at low CO_2 pressures, as was the case in the Mukhin work, the reaction 7 proceeds in the forward direction as written and results in the release of CO_2 gas from the carbonate surface. When the system CO_2 pressure is high, as was the case in this work (10 mbar), a steady state between reactions 7 and 8 can be established with no net production of CO_2. Because there is a finite number of CO_3^- centers that may form on the surface of the carbonate crystal, in our work the formation of $^{13}CO_2$ would be limited to the maximum number density of CO_3^- centers that can be formed on the crystal. After the initial formation of $^{13}CO_3^-$ sites and subsequent formation of $^{13}CO_2$, the centers will reform through suppressing the

$$2\ {}^{12}CO_2 + O^-_{\ surface} \rightarrow {}^{12}CO_3{}^-_{surface} + {}^{12}CO_2 \quad (9)$$

generation of new $^{13}CO_2$ centers and halting the generation of $^{13}CO_2$ at a level below the LLD. Likewise, on Mars the decomposition of calcite crystal would be suppressed by the maintenance of surface defect populations through reaction 8.

3.4.3 UV decomposition at quantum efficiencies less than $3x10^{-8}$

Although there was no experimental evidence for UV-induced carbonate decomposition using baked-out samples or in samples that were held at low run temperatures, it is possible that decomposition occurred at a rate below the experimental detection limit. Using $3.5x10^{-8}$ for the quantum efficiency of carbonate decomposition and the same value of UV photon flux at the surface of Mars used by Mukhin et al. (1996) ($2x10^{15}$ photons cm^{-2} s^{-1}), the upper limit of carbonate decomposition from bulk calcite (unmixed in the martian regolith) would be $1.2x10^{-13}$ kg m^{-2} s^{-1}, which corresponds to a maximum rate of photo-induced chemical weathering of 1.5 nm yr^{-1} (terrestrial year). Therefore, $1.5x10^{-9}$ m yr^{-1} is equal to $2.5x10^{-9}$ m yr^{-1} (Mars year), an order of magnitude less than the estimate of mechanical erosion/deposition by Carr (1992). Over geological time scales ($4x10^9$ Gyr terrestrial), this would be equivalent to the decomposition of 6.1 meters of a pure calcium carbonate outcrop, assuming that the reaction doesn't cease due to expected passivation of the carbonate surface.

An erosion rate of 0.02μm (Carr, 1992) would erode bulk carbonate outcrops and mix them with the regolith material faster than the outcrops could photodecompose. This abrasion and mixing would lead to the dispersal of carbonate fragments in the regolith and the burial of carbonate outcrops by wind-borne sediments. Once mixed with the regolith, carbonate photodecomposition would be limited to the photon penetration depth in the regolith; the rate-limiting process would be the rate at which unreacted carbonate is cycled to the surface by regolith mixing.

Although the rate at which the martian surface material is eroded and mechanically mixed is unknown, we can examine relative rates of erosion, mechanical mixing, and photodecomposition to assess the implications of potential low-rate loss of carbonate on the surface due to photodecomposition. For the purposes of this discussion, we restrict the use of the term "erosion" to the mechanical disaggregation and dispersal of carbonate outcrops, and use the term "deflation" to refer to stripping and removal of particulate regolith material. "Deposition" is assumed to be equal on both outcrops and regolith. The combined effects of deflation and deposition over many years results in "mixing" the regolith to some depth. Photodecomposition operates with equal quantum efficiency on both bulk carbonate outcrops, and on carbonate clasts in the regolith.

The first scenario is the photodecomposition of carbonate under conditions of low regolith mixing and erosion rates greater than 1.5 nm yr^{-1}. In this case, the rate at which a

carbonate outcrop is eroded and carbonate fragments subsequently diluted and buried in the regolith would exceed the photodecomposition loss rates and result in the accumulation of carbonate in the soil. For example, a post-Noachian erosion rate of 0.02 μm yr^{-1} (Carr, 1992) would yield a carbonate sedimentation rate of $1.7x10^{-6}$ kg m^{-2} yr^{-1}, (assuming that 3% of the eroded surface material is carbonate; $\rho = 2.8x10^{3}$ kg m^{-3}). Taking into account a maximum photodecomposition rate of carbonate of $1.1x10^{-7}$ kg m^{-2} yr^{-1}, (based on a 3% carbonate component in the soil and a photodecomposition quantum efficiency of $3.5x10^{-8}$), the result is a net accumulation of $1.6x10^{-6}$ kg m^{-2} yr^{-1} of carbonate in the

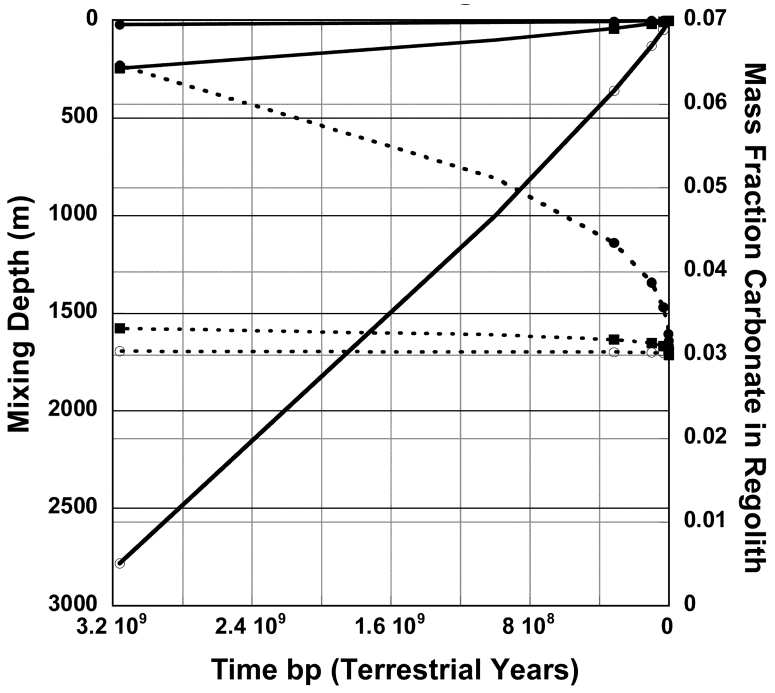

Figure 4. Weight % of carbonate at the visible surface of the regolith as a function of time for a photodecomposition rate of 1.5 nm yr^{-1} (dotted lines). Also shown for each case is the mixing relation between time and the depth of regolith stirring (solid line). The solid circles (●) are for stirring of 10m/Ga, the solid squares (■) for stirring 100/Ga, and the open circles(○), for stirring 1 km/Ga. All models are constrained to predict 3% at the current epoch.

regolith as the unreacted carbonate is buried by freshly eroded surface material. This scenario is however, not consistent with observations, which preclude 3% of the surface being exposed carbonate outcrop.

In the second scenario, the effective erosion rates are assumed to be effectively zero, based on the absence of identifiable carbonate outcrops. Photodecomposition will deplete the regolith of carbonate fragments at a rate that depends upon the depth and time scales that control regolith mixing. In Figure 4, the visible fraction of carbonates in the martian regolith dust is predicted, based upon three different regolith stirring relationships. We examine the effects of regolith stirring to 10m, 100m and 1 km over timescales of 1 Ga. The models are constrained to reproduce the current observation of 3% visible carbonate.

Where the entire 1 km of regolith is stirred over 1 Ga timescales, the maximum allowable photodecomposition rate is inadequate to reduce the visible carbonate in the regolith. Even at 3 Ga, the visible carbonate in the regolith is just over 3%. However, this process would have released almost 2 bars of CO_2 back into the atmosphere in 3Ga. Since that CO_2 is not visible in the atmosphere/cap system, and since the adsorbed reservoir, although unknown, is unlikely to be substantially greater than the CO_2 visible in the atmosphere+cap system (800Pa, Zent, 2005), this scenario would require that virtually all CO_2 be re-incorporated as subsurface carbonate.

Indeed even if regolith stirring is restricted to the upper 10 m over the past 1 Ga, the total CO_2 observed in the atmosphere+cap system would be released to the atmosphere in just over 1 Ga; even for this restrictive case, the very low limits on photodecomposition would predict CO_2 inventories that are greater than those observed. Therefore, either the actual photodecomposition rates are even smaller, or subsequent re-precipitation in unseen subsurface carbonate deposits are required to explain the observed exchangeable CO_2 inventory.

3.5 Conclusions

We have seen no evidence of UV-decomposition of $CaCO_3$ when calcite is exposed to UV light in a simulated martian atmosphere at 10 mbar. Based on the experimental lower limit of detection, the upper limit of photodecomposition on Mars is 3.5×10^{-8} molecules/photon. However, it is most likely that UV photodecomposition of $CaCO_3$ does not occur on Mars due to the high pressure of atmospheric CO_2. In vacuum, the decomposition of $CaCO_3$ may occur due to the photodetachment and photodissociation of CO_3^- radical defects generated by UV light. In a CO_2 atmosphere, the decomposition of $CaCO_3$ is suppressed by the reformation of the UV-generated CO_3^- by adsorbed CO_2 and surface O^- radicals.

In the event that photodecomposition is occurring at rates below 3.5×10^{-8} molecules/photon, the depth to which carbonate is decomposed in the regolith will be limited by the rate at which unreacted material is exposed through wind abrasion and the rate at

which mechanical mixing of the regolith can cycle carbonates to the surface. Based on our upper limit of photodecomposition on Mars, even for relatively shallow and slow mixing depths, the total CO_2 released to the atmosphere would be greater than can easily be accommodated in the observed exchangeable CO_2 reservoir, suggesting either that the carbonate photodecomposition rate is indeed well below our upper limit, or that subsequent re-precipitation to carbonate renders photodecomposition an insignificant branch of the current Martian carbon cycle.

Acknowledgements

This work was supported by the NASA Exobiology Program and NASA Ames/SETI Institute cooperative agreement NCC2-1408.

References

Bartoll, J., Stößer, R., and Nofz, M., 2000. Generation and conversion of electronic defects in calcium carbonates by UV/Vis light. *Appl. Rad. and Isotope,* 52, 1099-1105.

Blaney, D.L., and McCord, T.B., 1990. An observational search for carbonates on Mars. *J. Geophys. Res*., 94, 10,159-10,166.

Booth, M.C., and Kieffer, H.H., 1978. Carbonate formation in Mars-like environments. *J. Geophys. Res*., 83, 1809-1815.

Calvin, W.M, King, T.V.V., and Clark, R., 1994. Hydrous carbonates on Mars?: Evidence from Mariner 6/7 infrared spectrometer and ground-based telescopic spectra. *J. Geophys. Res.*, 99, 14,659-14,675.

Carr, M. H., 1989. Recharge of the early atmosphere of Mars by impact induced release of CO_2. *Icarus*, 79, 311-327.

Carr, M., 1992. Post-Noachian Erosion Rates: Implications for Mars Climate Change. In 23rd *Lunar and Planetary Science Conference Abstracts,* Lunar and Planetary Institute, Houston, pp. 205-206.

Clark, R.N., Swayze, G.A, Singer, R.B., and Pollack, J., 1990. High-resolution reflectance spectra of Mars in the 2.3 micrometer region: Evidence for the mineral scapolite. *J. Geophys. Res.*, 95, 14,463-14,480.

Clark, B.C., and Van Hart, D.C., 1981. The salts of Mars. *Icarus*, 45, 370-378.

Fanale, F.P., Postawko, S.E., Pollack, J.B., Carr, M.H., and Pepin, R. O., 1992. Mars: Epochal climate change and volatile history. In *Mars* (H.H. Kieffer, B.M. Jakosky, C.W. Snyder, and M.S. Matthews, Eds.), Univ. of Arizona Press, Tucson, pp. 1135-1179.

Fegley, B., and Treiman, A.H., 1992. *Chemistry of atmosphere-surface interactions on Venus and Mars, Venus and Mars : Atmosphere, Ionospheres, and Solar Wind Interactions.* AGU, Washington D.C., pp. 7-71.

Forget, F. and Pierrehumbert, R.T., 1997. Warming early Mars with carbon dioxide clouds that scatter infrared radiation. *Science,* 278, 1273-1276.

Gierasch, P.J. and Toon, O.B., 1973. Atmospheric pressure variation and the climate of Mars. *J. Atmos. Sci.*, 30, 1502-1508.

Gooding, J.L., 1978. Chemical weathering on Mars: Thermodynamic stabilities of primary minerals (and their alteration products) from mafic igneous rocks. *Icarus,* 33, 483-513.

Gooding, J.L., 1992. Soil mineralogy and chemistry on Mars: Possible clues from salts and clays in SNC meteorites. *Icarus,* 99, 28-41.

Greeley, R., Leach, R.N., Williams, S.H., White, B.R., Pollack, J.B., Krinsley, D.H., and Marshall, J.R., 1982. Rate of Wind Abrasion on Mars. *J. Geophys. Res*., 87, 10,009-10,024.

Griffith, L.L. and Shock, E.L., 1995. A geochemical model for the formation of hydrothermal carbonates on Mars. *Nature,* 377, 406-408.

Haberle, R.M., Tyler, D., McKay, C.P., and Davis, W.L., 1994. A model for the evolution of CO_2. *Icarus*, 109, 102-120.

Hiller, J.F. and Vestal, M.L., 1980. Tandem quadrupole study of laser photodissociation of CO^-_3. *J. Chem. Phys*., 72, 4713-4722.

Hunton, D.E., Hofmann, M., Lindeman, T.G., and Castleman, A.W., 1985. Photodissociation dymanics of CO^-_3. *J. Chem. Phys.*, 82, 134-149.

Jull A.J.T., Eastoe, C.J., Xue, S., and Herzog, G.F., 1995. Isotopic composition of carbonates in the SNC meteorites Allan Hills 84001 and Nakla. *Meteoritics*, 30, 311-318.

Kahn, R., 1985. The evolution of CO_2 on Mars, *Icarus*, 62, 175-190.

Kasting, J.F., 1991. CO_2 condensation and the climate of early Mars. *Icarus*, 94, 1- 13.

Khun, W.R. and Atreya, S.K., 1979. Solar Radiation Incident on the Martian Surface. *J. Mol. Evol.*, 14, 57-64.

Kirkland, L.E., Herr, K.C., Salisbury, J.W, McAfee, J.M., and Forney, P.B., 2001. Determining the TES Detection Limits for Minerals [Abstract 1864]. In 32st *Lunar and Planetary Science Conference Abstracts*, Lunar and Planetary Institute, Houston.

McKay, C.P. and Davis, W.L., 1991. Duration of liquid water habitats on early Mars. *Icarus,* 90, 214-221.

McKay, C.P., and Nedell, S.S., 1988. Are there carbonate deposits in Valles Marineris, Mars?, *Icarus*, 73, 142-148.

Mischna, M.A., Casting, J.F., Pavlov, A., and Freeman, R., 2000. Influence of carbon dioxide clouds on early martian climate. *Icarus*, 145, 546-554.

Moseley, J.T., Bennett, R.A., and Peterson, J.R., 1974. Photodissociation of CO^-_3. *Chem. Phys. Letters*, 26, 2, 288-291.

Mukhin, A.P., Koscheev, Dikov, Yu. P., Huth, J., and Wanke, H., 1996. Experimental simulations of the decomposition of carbonates and sulphates on Mars. Nature, 379, 141-143.

O'Connor, J.T., 1968. Mineral stability at the martian surface. *Geophys. Res*., 73, 5301-5311.

Pollack, J.B., Kasting, J.F., Richardson, S.M., and Poliakoff, K., 1987. The case for a wet, warm climate on early Mars. *Icarus*, 71, 203-224.

Pollack, J.B., Roush, T., Witteborn, F., Bregman, J., Wooden, D., Stoker, C., Toon, O.B., Rank, D., Dalton, B., and Freedman, R., 1990. Thermal emission spectra of Mars (5.4 -10.5 um): Evidence for sulfates, carbonates, and hydrates. *J. Geophys. Res*., 95, 14,595-14,628.

Roush, T.L., Blaney, D., McCord, T.B., and Singer, R.B., 1986. Carbonates on Mars: Searching the Mariner 6 and 7 IRS measurements. In 17th *Lunar and Planetary Science*, Lunar and Planetary Institute, Houston, pp. 732-733.

Schaefer, M.W., 1993. Volcanic recycling of carbonates on Mars. *Geophys. Res. Lett*., 20, 827-830.

Stoesser, R., Bartool, J., Schirrmeister, L., Ernst, R., and Lueck, R., 1996. ESR of trapped holes and electrons in natural and synthetic carbonates, silicates and aluminosilicates. *Appl. Radiat. Isot*., 47, 1489-1496.

Stern, K.H., and Weise, E.L., 1969. High temperature properties and decomposition of inorganic salts, Part 2. Carbonates. *NSRDS-NBS*, 30, p.32.

Stoker, C.R. and Bullock, M.A., 1997. Organic degradation under simulated Martian conditions. *J. Geophys. Res.*, 102, 10,881-10,888.

Wright, I.P., Grady, M.M., and Pillinger, C.T., 1992. Chassigny and the nakhlites: Carbon-bearing components and their relationship to martian environmental conditions. *Geochim. Cosmochim. Acta*, 56, 817-826.

Zent, A. P., 2005. An historical search for thin films of H_2O at the Phoenix Landing site. *J. Geophys. Res.,* submitted.

Chapter 4

Aqueous decomposition of organic compounds in the Atacama Desert and in martian soils

R.C. Quinn, P. Ehrenfreund, F.G. Grunthaner, C.L. Taylor, A.P. Zent

The discovery of the existence of present-day near-surface ground ice on Mars and evidence of past aqueous processes at the Mar Exploration Rover Opportunity site raises the possibility of the presence of liquid water or thin-films of water at soil/ice interfaces on the planet. These environments are potentially vastly different from the desiccated soils sampled by the Viking landers and the stability of organic compounds in these systems is unknown. We report the results of experiments which examine the degradation kinetics of aqueous organic substrates using Atacama soils as Mars analogs. We compare our results with direct information on the kinetic behavior of Mars soils in contact with organic compounds in aqueous systems obtained from Viking data. We find that the decomposition of organic compounds in our experiments is dominated by soil surface catalysis and that the overall rate of organic decomposition by some Atacama samples exceeds that of the Viking soils. However, in the Viking biology experiments, surface catalysis was one of multiple types of oxidative processes that occurred, but it was not the dominate processes. In situ, organic decomposition on Mars, and in the Atacama, may be dominated by active photochemical mechanisms. Soil and water ice may serve as a sink for photochemically produced oxidizing species resulting in accelerated organic decomposition kinetics during transient wetting events.

4.1 Introduction

Remotely obtained images of Mars have provided ample evidence of a history of liquid water on the planet's surface. One striking example of this evidence are the images collected by the Mars Global Surveyor which indicate the presence of gullies that can be explained by ground water seepage and surface runoff (Malin and Edgett, 2000). More recently, the NASA Mars Exploration Rovers were sent to regions which based on remote imaging, appeared to have been altered by the presence of liquid water (Squyers et al.,

2004). The Opportunity rover landed at Meridiani Planum, which was selected as a landing site on the basis of Thermal Emission Spectrometer (TES) data returned by Mars Global Surveyor. The TES data indicated that the surface at Meridiani Planum contains course grained hematite (15 to 20%) which may have formed in liquid water (Christensen et al., 2000). Data returned from the Opportunity payload confirmed a history of aqueous processes at the site including, sulfur-rich sedimentary rocks thought to have deposited in shallow surface water and hematite-rich spherules thought to be concretions formed in liquid water (Squyers et al., 2004).

While there is abundant evidence that liquid water was present on the surface of Mars at some point in its history, this is not the case for organic compounds. Recently, methane has been detected in the atmosphere of Mars at a mixing ratio of 10 ± 5 parts per billion by volume (ppbv) by the Planetary Infrared Fourier Spectrometer on the European Space Agency Mars Express spacecraft (Formisano et al., 2004). Aside from trace amounts of atmospheric methane, no other organic chemicals have been detected on the surface or in the atmosphere of Mars. The most comprehensive search for organic compounds on Mars, which was carried out using the Viking Gas Chromatograph Mass Spectrometer (GCMS), revealed that the surface material was depleted of organic compounds (Biemann and Lavoie, 1979). Recently, Sumner (2004) pointed out that organics are expected to be unstable in the types of aqueous environments in which the sedimentary deposits observed at the MER typically form. Squyers et al. (2004) have concluded that the sediments observed with the Opportunity payload at the Meridiani Planum site formed in shallow surface water followed by evaporation and desiccation. Sulfur salts are abundant in outcrops and jarosite has been identified using Opportunity's Mössbauer spectrometer (Klingelhöfer et al., 2004). The detection of jarosite is significant since it forms in strongly acidic and oxidizing aqueous environments. The important discussion presented by Sumner (2004) is primarily based on the expected thermodynamic stability of organic compounds at the MER site and does not comprehensively address the kinetics of aqueous systems on Mars. In this paper, we report the results of experiments which examined the degradation kinetics of organic substrates using Atacama soils as Mars analogs and compare the results to organic chemical decomposition rates observed with Mars soils during the Viking biology experiments.

The choice of Atacama soils as Mars analogs was based on the research of Navarro-González et al. (2003) which demonstrated that the quantity and diversity of heterotrophic bacteria increase and the level of organic compounds decrease, as a function of local water availability in the Atacama. They also reported the observation of active decomposition of organics by soils in incubation experiments patterned after the labeled release experiment (LR), which was one of the Viking biology experiments. Additionally, Skelley et al. (2005), using the Mars Organic Analyzer, found extremely low levels of amino acids in soils collected from the Yungay region of the Atacama, which is consistent with the results of Navarro-González (2003).

On Mars and in the Atacama, active photochemical processes are likely to be the most active pathway for the decomposition of organics (Quinn et al., 2005). Radiation can be adsorbed in soils by both organic (if present) and inorganic chromophores, a process that initiates free radical reactions that can chemically alter organic compounds and mineral surfaces. Multiple contributing mechanistic pathways are likely in soil systems; three of the most common are:

1. Nitrate Photochemistry

$$NO_3^- + \text{light} \rightarrow NO_3^{-}{}^* \rightarrow NO_2^- + O(3P) \quad (1)$$

or

$$NO_3^- + \text{light} \rightarrow NO_3^{-}{}^* \rightarrow NO_2 + \cdot O^- \quad (2)$$

$$\cdot O^- + H_2O \rightarrow \cdot OH + OH^- \quad (3)$$

2. Fenton or Photo-Fenton reactions

$$Fe(III) + H_2O_2 \rightarrow Fe(II) + HO_2/O_2^- + H^+ \quad (4)$$

$$Fe(II) + H_2O_2 \rightarrow Fe(III) + \cdot OH + OH^- \quad (5)$$

or

$$Fe\ (III) + \mu v \rightarrow Fe(II) + H_2O_2 \rightarrow Fe\ (III) + \cdot OH + OH^- \quad (6)$$

3. Metal Oxide Photochemistry

$$MeOx + \mu v \rightarrow \cdot O_2^- \rightarrow \cdot OH \quad (7)$$

The key radical precursors and radicals in these reactions are superoxide, hydrogen peroxide, and the OH radical. Superoxide has been suggested as an explanation for the Viking Biology Gas Exchange experiment results (Chun, 1978; Yen, 2000), while the OH radical as shown in this work, and suggested by others is capable of oxidizing organic compounds on Mars (Atkinson, 1986; Benner, 2000). As indicated by the above reactions, these species can also oxidize and reduce other soil components, including transition metals, sulfur compounds, and nitrogen compounds. In the Atacama nitrate photochemistry is likely to play an important role in the desert's carbon cycle, while on Mars fenton reac-

tions and metal-oxide photochemistry are likely to be important (Quinn et al., 2005). Additional pathways exist for the generation of reactive species in soils, including the production of singlet oxygen through the creation of excited states in soil humic acids (Zepp, 1992). Singlet oxygen reacts at significant rates with several types of furans, sulfides, amines, polynuclear aromatics, hydrocarbons, and other electron-rich compounds. In aqueous systems and in the presence of UV light, these reactions, along with reactions 1 through 7 shown above, are highly efficient in decomposing organic compounds.

We compare our results using Atacama soils with direct information on the kinetic behavior of Mars soils in contact with organic compounds in aqueous systems obtained from Viking data. The Viking landers performed an in situ search for life on the surface of Mars using substrate-induced respiration tests. In these biology experiments, changes in headspace gases were monitored after the addition of an aqueous solution of organic compounds into a sealed cell containing a sample of Mars surface material (Levin and Straat, 1976; Oyama and Berdahl, 1976). Results of substrate-induced respiration tests often depend on the choice of substrate and each of the Viking biology experiments utilized a different set of organic substrates. In all of the Viking biology experiments, oxidative abiotic decomposition of organics was observed resulting from multiple oxidative processes with different reaction kinetics (Klein, 1978; 1979). In this paper we compare possible mechanisms and kinetics for the decomposition of organics in the Viking biology experiments with the oxidative behavior of Atacama soils. We also discuss the relevance of these observations to the stability of organics during aqueous processes that may be currently occurring on Mars.

4.2 Methods and Materials

4.2.1 Atacama samples

Samples were collected from hilltops near S 24° 4’ 9.6”, W 69° 51’ 58.1” which is located in the Yungay region of the Atacama desert. This location corresponds to the collection site for sample AT02-03 in the Navarro-Gonzalez et al. (2003) study. The site is near an environmental monitoring station (24°4'50" S) established by McKay et al. (2003). The region has a temperate climate with a mean temperature between 10°C and 30°C. During a four year collection period spanning from 1994 to 1998 McKay et al. (2003) reported one significant rain event which resulted in only 2.3 mm of precipitation.

Two types of samples were collected for this study (table 1). One type (surface samples) consists of scrapings, removed from the top of a gypsum-rich surface crust, approximately 5-6 mm thick. The second sample type (subsurface samples) is taken from a fluffy particulate layer, 3-4 cm thick, directly beneath the crust at a nearby location. Both samples are dominated by gypsum and anhydrite. Samples were collected and immediately sealed in stainless steel storage containers with metal compression seals to provide a

clean, hermetically sealed transport system from the field site to the lab for analysis (Figure 1). Prior to use, the containers were wrapped in aluminum foil and sterilized by baking out in air at 350°C, the containers remained wrapped until used at the collection site in the field. Sterile scoops were used to collect the soil samples. Extreme care was used to seal the containers in the field and to transport the soil back to the laboratory for analysis. Due to the low relative humidity (<10%) at the time of sample collection, and the potential for water to modify the chemical activity of the soil, exposure to lab humidity levels was avoided. In the lab, the soil was handled only in controlled-atmosphere glove boxes while monitoring the relative humidity, which was always kept below 2%.

Figure 1. The sample collection site near S 24° 4' 9.6", W 69° 51' 58.1" in the Yungay region of the Atacama. Samples were collected and immediately sealed in sterile stainless steel storage containers with metal compression seals to provide a clean, hermetic transport system from the field site to the lab for analysis.

4.2.2 Substrate induced organic decomposition experiments

Soil samples (1 cc) were transferred from the transport containers and sealed under dry nitrogen in sterile 55 cc vials and crimp-sealed with sterile rubber septa. Three different sets of organic substrates were used: a 50 mM ^{13}C-labled sodium formate solution; a 5 mM L-alanine and 5 mM D-glucose solution (biotic substrate); and a 5 mM D-alanine and

5 mM L-glucose solution (abiotic substrate). The different combinations of enantiomers were used to distinguish biotic from abiotic responses. All organics were obtained from IsoTec Inc. and were 99+% 13-C labeled, except for the L-glucose which was obtained from Cambridge Isotope Laboratories. The organic substrate (either 1 or 0.2 cc) was introduced into the sample vial using a 1 cc sterile syringe with a sterile 0.2 µm filter. Extracted headspace samples were analyzed for the production of $^{13}CO_2$ using an HP 5900 gas chromatograph with a 5972 mass selective detector. Measured levels of $^{12}CO_2$ were used to correct for the natural abundance of $^{13}CO_2$ present in the sample cells.

There were three differences between this method and the method of Navarro-Gonzalez et al. (2003). (1) We analyzed samples more frequently to obtain kinetic data. (2) A larger sample vial was used to allow more frequent headspace sampling. (3) Experiments were carried out in which 0.2 cc of organic solution was added to 1 cc of soil (Viking LR mixing ratios).

4.3 Results

The average total measured $^{13}CO_2$ present in the headspace 3 and 5 days after wetting with organic media is shown in table 1. Over the course of the experiments, no production of $^{13}CO_2$ was observed in vials which contained the organic substrate solutions but no soil. The total number of moles of $^{13}CO_2$ produced by the subsurface samples is consistent with the values reported by Navarro-Gonzalez et al. (2003) for single sample measurements taken 3 to 5 days after substrate injection. However, the quantity of $^{13}CO_2$ present in the headspace of the surface sample cells is substantially different from the subsurface sam ples. The time dependence of the headspace $^{13}CO_2$ levels for these samples is shown in figure 2.

Table 1.
Experimental results listing amounts of formate, alanine, and glucose decomposed by two types of Atacama soils (surface and subsurface) after 3 to 5 days of incubation.

	Formate	D-Alanine + L-Glucose	L-Alanine + D-Glucose
	micromoles	micromoles	micromoles
Subsurface Samples Day 3	4.5	0.6	
Subsurface Samples Day 5	7.8	0.7	
Surface Samples Day 3	1.1	0.2	0.4
Surface Samples Day 5	2.4	0.95	1.1
Navarro-Gonzalez Day 3-5	3-12	~0.4	~0.4
Hematite + H2O2 Day 3	6.5	0.3	
Hematite + H2O2 Day 4	6.9	0.3	

The observed differences in the samples are not due to experimental measurement errors. A three level calibration of the instrument was performed twice a day and performance was validated by repeated injections of the same standards. Additionally, as can be seen by comparing figure 2a and 2b, the $^{13}CO_2$ release pattern was consistent between replicate samples of a given soil type (surface or subsurface). It is not possible to quantita-

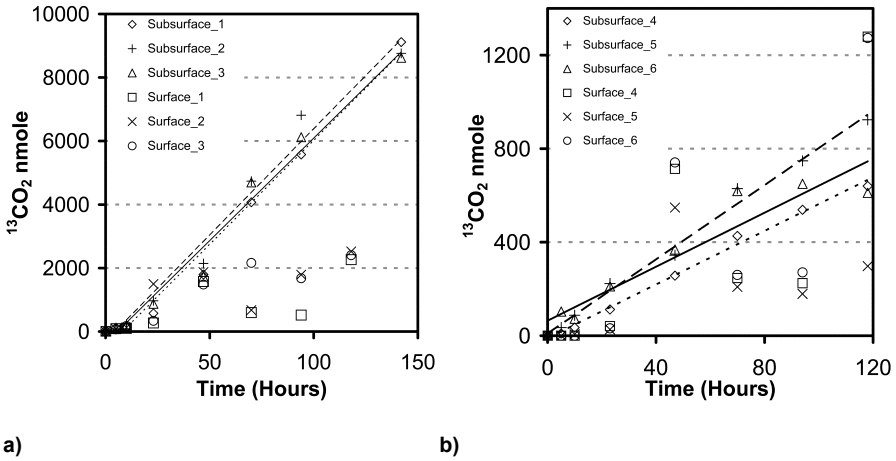

Figure 2. The measured $^{13}CO_2$ present in the headspace as a function of time for both surface and subsurface Atacama samples. 2a shows the decomposition of sodium formate and 2b the decomposition of the D-alanine and L-glucose mixture. The $^{13}CO_2$ release pattern was consistent between replicate samples of a given soil type (surface or subsurface).

tively explain the differences between the observed headspace $^{13}CO_2$ levels for the two sample types. However, the levels of headspace gases shown in figures 2 and 3 are not corrected for changes in solubility that may have occurred over the duration of the experiment. It is likely CO_2 solubility in the surface sample varied over the course of the experiment due to shifts in carbonate equilibrium and resulted in the fluctuation of headspace $^{13}CO_2$. Substantial differences in the pH equilibration kinetics between surface and subsurface soil samples collected in the Yungay region have been reported by Quinn et al. (2005). Additionally, variable levels of $^{12}CO_2$ present in the surface sample cells also indicate that the $^{13}CO_2$ shifts were due to pH changes and carbonate equilibrium shifts.

Comparison of the levels of $^{13}CO_2$ in samples with L-alanine and D-glucose (biotic) substrate to the samples with D-alanine and L-glucose (abiotic) substrate indicate that if biological activity played a role in the production of $^{13}CO_2$ in experiments, the contribution was insignificant relative to abiotic processes (figure 3).

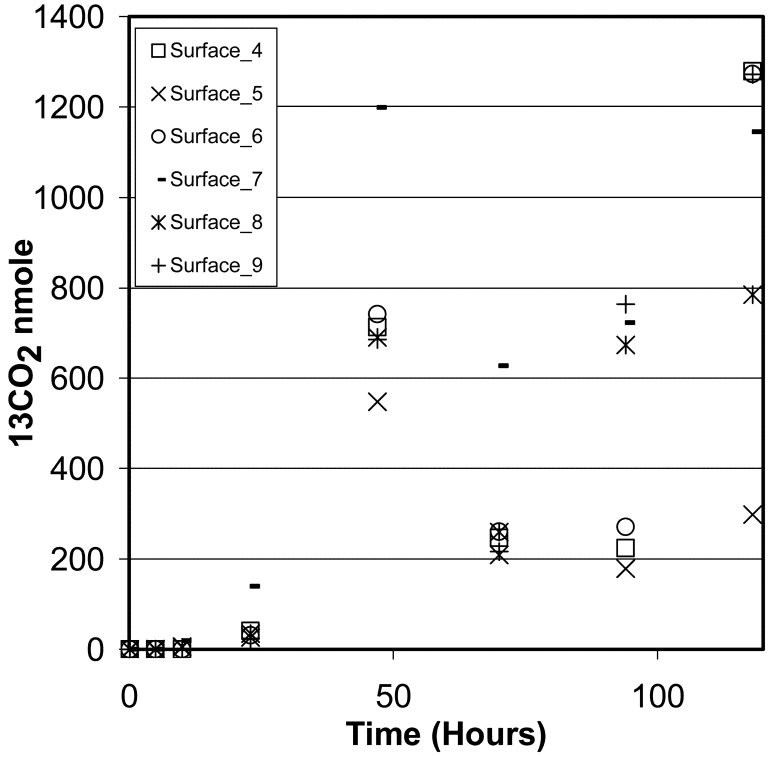

Figure 3. Comparison of the levels of $^{13}CO_2$ in samples with the abiotic substrate D-alanine and L-glucose (sample 4-6) to the samples with the biotic substrate L-alanine and D-glucose (samples 7-9). The amount of decomposition was equal for both substrate types indicating that contribution of biological activity, if any, was insignificant relative to abiotic processes.

4.4 Discussion

4.4.1 Formate decomposition kinetics

Insights into the extent to which the oxidative behavior of Atacama soils in aqueous systems may be analogous to martian surface materials can be obtained by comparing the substrate-induced production of $^{13}CO_2$ in the Yungay subsurface samples to Viking LR results. In the Viking LR experiment, radioactive gas evolution was monitored after the addition of a ^{14}C-labeled aqueous organic substrate into a sealed test cell that contained a martian surface sample (Levin and Straat, 1976).

Two distinct $^{14}CO_2$ evolution patterns were observed. First, a rapid release of $^{14}CO_2$ occurred over the first 24-48 hours of the experiment which has been attributed to a thermally labile oxidant. This initial rapid release was apparently reduced by heating the surface sample to 50ºC (and eliminated by heating the sample to 160º) in the sealed sample cell prior to introduction of the organic substrates. The second pattern of $^{14}CO_2$ evolution was a slower log-linear release observed after the first oxidative reaction ceased.

The responses of the Viking lander 1 cycle 1 sample and subsurface samples (after sodium formate addition) is shown in figure 4. The initial rapid $^{14}CO_2$ release pattern in the Viking LR has been interpreted as the complete decomposition of the sodium formate (30 nmoles) component of the substrate. This was followed by the slower decomposition of other substrate components, which were 14C-labeled: glycine, DL-alanine, sodium lactate, and calcium glycolate. This slower release has been attributed to substrate decomposition by γFe_2O_3 (hematite) in the martian surface sample while the initial rapid release

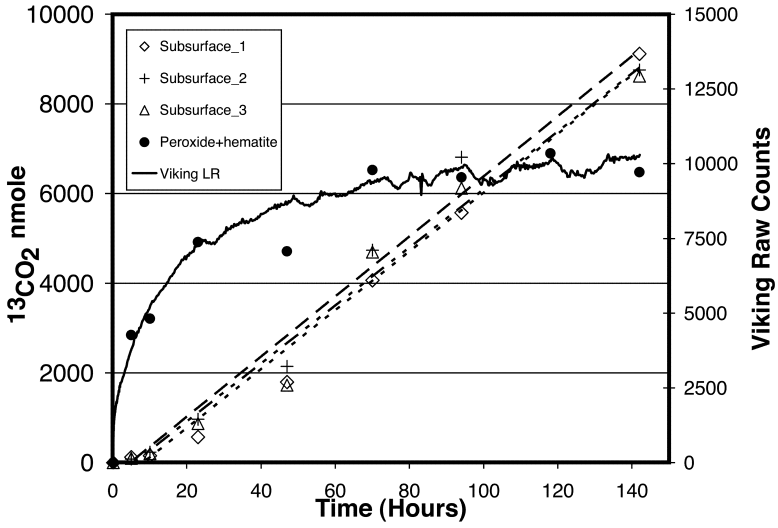

Figure 4. The responses of the Viking lander 1 cycle 1 sample and Atacama subsurface samples (after sodium formate addition). The initial rapid $^{14}CO_2$ release pattern in the Viking LR is shown as raw counts and has been interpreted as the complete decomposition of the sodium formate (30 nmoles) component of the substrate. This was followed by the slower decomposition of other substrate components. The kinetics of formate decomposition by the Atacama subsurface is dominate by soil surface catalysis, while decomposition due to OH radicals dominates the Viking results. Hydrogen peroxide in the presence of hematite mimics the LR response.

has been attributed to H_2O_2 in the presence of γFe_2O_3 (Klein, 1978, 1979). As can be seen in figure 4, the kinetics of formate decomposition by the Yungay subsurface samples differ from the Viking LR results. Other explanations for the LR results have been proposed (see Zent and McKay (1994) for a review). However, H_2O_2 together with hematite has been shown to reproduce both the kinetics and thermal characteristics of the LR experiment and is used as a model system here for comparisons with Atacama soils.

Recently, sodium formate has been used by soil scientists as a probe molecule to measure production of OH radicals in soil systems on earth (Kwan and Volker, 2002; Southworth and Voelker, 2003). An Fe(III)-initiated chain reaction involving hydrogen peroxide (fenton reaction) results in decomposition of formate by OH radicals. The kinetics of this reaction, which closely mimic the LR results, is shown in figure 4. The (partial) mechanism for this reaction sequence includes the following steps:

$$Fe(III) + H_2O_2 \rightarrow Fe(II) + HO_2/O_2^- + H^+ \quad (8)$$

$$Fe(II) + H_2O_2 \rightarrow Fe(III) + \cdot OH + OH^- \quad (9)$$

$$Fe(III) + HO_2/O_2^- \rightarrow Fe(II) + O_2 + H^+ \quad (10)$$

$$\cdot OH + HCOOH/HCOO^- \rightarrow CO_2 + O_2^- + H^+ \quad (11)$$

Evidence of this reaction is absent in the Yungay soil samples. It should be noted that Oyama and Berdahl (1979) proposed a different mechanism at the time of the Viking experiments to explain the peroxide induced decomposition of formate in the LR. This hypothetical mechanism, which also has the same kinetics as the LR response, involves the formation of an iron peroxy acid derivative by HOO^- which then reacts with available formate to produce H_2O and CO_2.

4.4.2 Surface catalyzed organic decomposition

Although the kinetics of formate decomposition by the Yungay soil samples in the laboratory experiments is not consistent with the LR results or an OH radical decomposition mechanism, a significant rate of formate decomposition is observed. In fact, overtime the overall rate of formate decomposition by the Yungay soil exceeds the rate of decomposition by the peroxide-hematite system. In the peroxide-hematite system, formate was added in excess relative to the peroxide and initial reaction kinetics were governed by ·OH production. Once production of ·OH ceased, formate decomposition slowed and the rate became governed by catalytic decomposition.

The ability of the Yungay soil and the peroxide-hematite system to decompose organics that are more complex than formate can be seen in figure 5. In this experiment, a 5 mM mixture of D-alanine and L-glucose was added to the samples. In the first 48 hours, the total $^{13}CO_2$ produced by the peroxide-hematite system is approximately equal to the amount produced by surface catalysis in the Yungay sample. This was not the case when formate was the added substrate (figure 4) and is due to the slower reaction kinetics of OH radicals with glucose and alanine than with formate. Once OH radical production stopped in the peroxide-hematite sample, the rate of both the formate and D-alanine/L-glucose decomposition, was greater in the Yungay samples. This suggests that when wetted, the Yungay subsurface sample is a more active catalyst for organic chemical decomposition than the Viking soil samples. Catalytic decomposition of organics in the LR has been attributed to the presence of iron oxide in the Mars surface sample. As can be seen in figures 4 and 5, the catalytic properties of iron oxide alone are insufficient to explain the high rate of catalysis observed in the Yungay subsurface samples. Bulk chemical analysis of these soils show that significant quantities of redox active transition metals including manganese, cesium, and copper are present at ppm levels. These catalytic species are

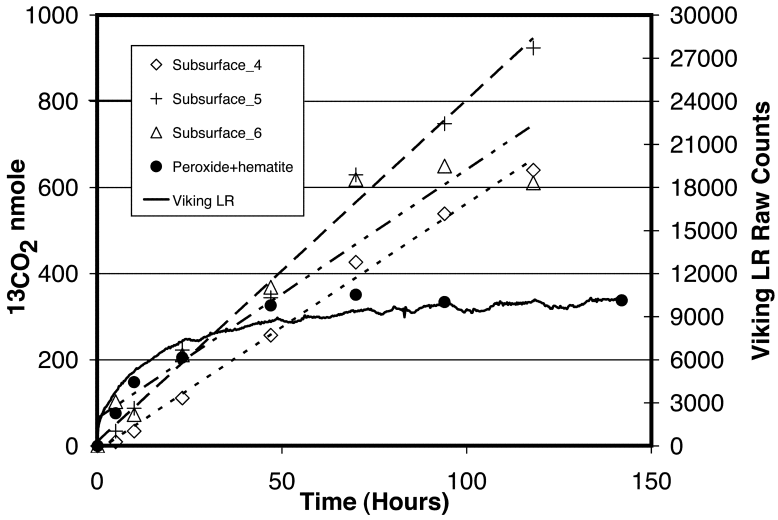

Figure 5. The response of D-alanine and L-glucose added to the Atacama samples. The total $^{13}CO_2$ produced by the Atacama soils exceeds the production by the peroxide-hematite sample. This suggests that even in the absence of OH radicals, when wetted, the Atacama sample is a more active catalyst for organic chemical decomposition than the Viking soil samples.

frequently used in low temperature wet air oxidation processes for the conversion of organic compounds into CO_2 and H_2O (Lin et al., 2002). Determination of the activity of these species in Yungay soils is difficult due to the high ionic strength and complex nature of the soil solutions. However, we are further analyzing these soils and performing electrochemical studies to determine the dominate redox couples and catalytic pathways in these aqueous systems.

4.4.3 Oxidant chemistry in aqueous systems on Mars

Photochemical processes occurring in liquid water can efficiently decompose organic compounds and even in ice containing soils on Mars, the outlook for the survival of organics may not be good. The discovery of the existence of present-day near-surface ground ice on Mars (Boynton et al., 2002) has resulted in the theoretical reconsideration, from a geochemical and astrobiological perspective, of the implications of both the possibility of liquid water or thin-films of water at soil/ice interfaces. This environment is potentially vastly different from the desiccated soils sampled by the Viking landers; moreover, because the ice may be relict of outflow events to the northern plains, or might otherwise preserve materials that characterize organic chemistry and climatic evolution, it represents a high-priority target for future missions.

Creation of a liquid H_2O phase in ice-containing soils on Mars may occur as a result of partial melting during diurnal or seasonal obliquity variations. Additionally, the formation of a liquid or liquid-like phase does not require bulk melting of the ice. It is also possible that significant chemical weathering or alteration may occur in permanently frozen soils due to the low temperature formation of liquid-like layers at the soil/ice interface. The presence of unfrozen water on Mars, even if transient, can have important impacts on organic chemical alteration rates. The factors that can influence the amount of unfrozen water in a soil sample include: temperature, pressure, chemical and mineralogical composition, surface area and porosity, exchangeable ions, and solute concentration and composition. It is known that a nonfreezing layer in clays and silicates can be present at temperatures below -50^0C (Turvo and Leboda, 1999).

Examination of the terrestrial record indicates that ice may not be an impervious barrier to highly reactive radicals and radical precursors. Evidence for recent liquid water (Malin and Edgett, 2000; Christensen, 2003) at midlatitudes suggests the possibility of periodic freeze/thaw in limited locations across the martian surface. Laboratory literature suggests that generation of reactive species can be accelerated in freeze/thaw systems (Betterton and Anderson 2001). H_2O_2 is soluble in H_2O, occurs naturally in terrestrial ice, is known to oxidize insoluble particulates in ice (Neftel et al., 1986), and is known to occur in the martian atmosphere (e.g. Krasnopolsky, 2003). H_2O_2 is incorporated into polar ice on Earth in amounts ranging from 150 to ~0.1 ppb (100 ppb H_2O_2 in ice = $3x10^{15}$ cm^{-3} or 5 nmoles cm^{-3}) (Neftel et al., 1986). The H_2O_2 profile falls off slowly with age

throughout the Holocene in both the Greenland and Antarctic ice sheets, indicating that there is a chemical sink for the species in the ice. The nature of the sink is not precisely clear, but correlation of H_2O_2 depletion with insoluble inclusions suggests that the H_2O_2 is migrating along dislocations caused by the presence of particles. Conklin et al. (1993) inferred bulk diffusion coefficients for H_2O_2 in ice varying from $4.4x10^{-14}$ m^2s^{-1} at -3°C to $2.9x10^{-16}$ m^2 s^{-1} at -45°C.

Dilute aqueous solutions of oxidizable species can react rapidly during freezing (Betterton and Anderson 2001). This result is likely due to a freeze-concentration effect that occurs when reactants are concentrated into liquid micropockets ahead of the advancing ice front. This process may be significant where freeze/thaw cycles occur naturally, especially where oxidants can accumulate near ice surfaces. Oxidation by H_2O_2 is also accelerated on freezing (Betterton and Anderson, 2001). A dilute peroxide solution can concentrate to the 40% range in the first freezing cycle, and the freezing point of a fraction in the 40% range is -40 to -50°C (e.g. Schumb et al., 1955). The maximum concentration achievable by repeatedly fractionally freezing peroxide is about 60%. This suggests that on Mars peroxide may quickly concentrate and remain in the liquid phase even at very low temperatures, which would yield both high reactivity and mobility. The major inhibitor of this process would be the catalytic decomposition of any liquid H_2O_2 by iron cations in the system. However, catalytic decomposition of H_2O_2 in soil and ice can result in the formation of highly reactive OH radicals. It is unknown whether the ice-bearing soil on Mars contain significant concentrations of free-radicals or free-radical precursors. However, terrestrial polar ice cores contain hydrogen peroxide that has been incorporated through vapor phase deposition and/or precipitation at levels up to 150 ppb. This level of H_2O_2 is only slightly less than the concentration of soil oxidants needed to explain the Viking biology results. It is also possible that low levels of H_2O_2 may concentrate through fractional freezing processes that may occur if the soil undergoes freeze-thaw cycles on Mars.

4.5 Conclusions

We have measured the decomposition rates of organic compounds in aqueous solution added to Atacama soils collected from 2-3 cm below the surface in the arid core of the desert. Our results show that the primary decomposition of organics in the Atacama Desert is dominated by surface catalysis. This is different from Mars soils as indicated by the Viking biology experiments. Surface catalysis was one of multiple oxidative processes observed in the Viking biology experiments, but it was not the dominate mechanism. Although other explanations have been suggested for the Viking labeled release results, our results are consistent with the decomposition of added formate by OH radicals as primary decomposition mechanism. Surface catalysis of organics was observed in the Viking biol-

ogy experiments but the reaction kinetics for these reactions is slower than for decomposition by OH radicals.

Overall, the reaction kinetics for the catalytic decomposition of organics in aqueous experiments was faster in Atacama soils than would be expected for Viking-like Mars soils. In the Atacama and on Mars, the catalytic soil mechanisms active during transient wetting events may play an important role in the destruction of organics in these environments. These decomposition mechanisms are expected to be active when dew and fog, and (less frequent) rain, is present in the Atacama.

Photochemical processes are also likely to provide active pathways of organic chemical decomposition in the Atacama and on Mars. These processes result in the production of H_2O_2 and oxidizing radical species which are highly active in aqueous systems. On Mars, H_2O_2 and radicals may be preserved in ground ice and react with organics during freeze thaw cycles or when thin-films of water form on soil surfaces. As a consequence, it is possible that the stability of organic compounds will be lower, and the rate of decomposition will be higher, in aqueous environments than in desiccated environments on Mars.

Acknowledgements

This work was supported by the NASA Mars Fundamental Research program, the NASA Astrobiology Science and Technology for Exploring Planets program, and NASA Ames/SETI Institute cooperative agreement NCC2-1408. Pascale Ehrenfreund acknowledges grant NWO VI 016.023.003.

References

Atkinson, R.,1986. Kinetics and mechanisms of the gas-phase reactions of the hydroxyl radical with organic compounds under atmospheric conditions, *Chem. Rev.*, 86, 69-201.

Benner, S. A., K. G. Devine, L. N. Matveeva, D. H. Powell, 2000. The missing organic molecules on Mars, *Proc. Natl. Acad. Sci.*, USA, 97, 2425-2430.

Betterton, E. A., D. J. Anderson, 2001. Autooxidation of N(III), S(IV) and other species in frozen solution, - A possible pathway for enhanced chemical transformation in freezing systems, *J. Atomos Chem.*, 40, 171-189.

Biemann, K., J. M. Lavoie, 1979. Some final conclusions and supporting experiments related to the search for organic compounds on the surface on Mars, *J.Geophys. Res.,* 84, 8385-8390.

Boynton, W. V., W. C. Feldman, S. W. Squyres, T. H. Prettyman, J. Brückner, L. G. Evans, R. C. Reedy, R. Starr, J. R. Arnold, D. M. Drake, P. A. J. Englert, A. E. Metzger, I. Mitrofanov, J. I. Trombka, C. D'Uston, H. Wänke, O. Gasnault, D. K. Hamara, D. M. Janes, R. L. Marcialis, S. Maurice, I. Mikheeva, G. J. Taylor, R. Tokar, C. Shinohara, 2002. Distribution of hydrogen in the near surface of Mars: Evidence for subsurface ice deposits, *Science*, 297, 81-85.

Christensen, P. R., 2003. Formation of recent martian gullies through melting of extensive water-rich snow deposits, *Nature*, 422, 45-48.

Chun, S. F., K. D. Pang, J. A. Cutts, J. M. Ajello, 1978. Photocatalytic oxidation of organic compounds on Mars, *Nature*, 274, 875-876.

Conklin, M. H., A. Sigg, A. Neftel, R. C. Bales, 1993. Atmoshere-snow transfer function for H_2O_2: Microphysical considerations, *J. Geophys. Res*., 98, 18,367-18,376.

Formisano, V., S. Atreya, T. Encrenaz, N. Ignatiev, M. Giurana, 2004. Detection of Methane in the Atmosphere of Mars, *Nature,* 306, 1758-1761.

Grunthaner, F. J., A. Ricco, M. A. Butler, A. L. Lane, C. P. McKay, A. P. Zent, R. C. Quinn, B. Murray, H. P. Klein, G. V. Levin, R. W. Terhune, M. L. Homer, A. Ksendzov, and P. Niedermann, 1995. Investigating the surface chemistry of Mars. *Analytical Chemistry*, 67, 605A-610A.

Klein, H. P., 1978. The Viking biological experiments on Mars. *Icarus*, 34, 666–674.

Klein, H. P., 1979. The Viking mission and the search for life on Mars. *Rev. Geophys. Space Phys*., 17, 1655 - 1662.

Klingelhöfer, G., R.V. Morris, B. Bernhart, C. Schroder, D.S. Rodionov, P.A. de Souza, A. Yen, R. Geller, E.N. Evlanov, B. Zubkov, J. Foh, U. Bonnes, E. Kankeleit, P. Gütlich, D.W. Ming, F. Renz, T. Wdowiak, S.W. Squyres, R.E. Arvidson, 2004. Jarosite and hematite at Meridiani Planum from Opportunity's mössbauer spectrometer, *Science*, 304, 1740-1745.

Krasnopolsky, V. A., G. L. Bjoraker, M. J. Mumma, D. E. Jennings, 1997. High resolution spectroscopy of Mars at 3.7 and 8 um: A sensitive search for H_2O_2, H_2CO, HCl, and CH_4, and detection of HDO, *J. Geophys. Res.*, 102, 6525-6534.

Kwan, W. P., B. M. Voelker, 2002. Decomposition of hydrogen peroxide compounds in the presence of dissolved iron and ferrihydrite, *Environ. Sci. Technol.* 36, 1467-1476.

Levin, G. V. and P. A. Straat, 1977. Recent results from the Viking Labeled Release Experiment on Mars, *J. Geophys. Res.*, 82, 4663 - 4667.

Lin, S.S., C.L. Chen, D.J. Chang, C.C. Chen, 2002. Catalytic wet air oxidation of phenol by various CeO_2 catalysts, *Water res.*, 36, 3009-3014.

Malin, M. C., K. S. Edgett, 2000. Evidence for recent groundwater seepage and surface runoff on Mars, *Scienc*e, 288, 2330-2335.

McDonald, G. D., E. Vanssay, J. R. Buckley, 1998. Oxidation of organic macromolecules by hydrogen peroxide: Implications for stability of biomarkers on Mars, *Icarus*, 132, 170-175.

McKay, C.P., E.I. Friedmann, B. Gomez-Silva, L. Cáceres-Villanueva, D.T. Andersen, R. Landheim, 2003. Temperature and moisture conditions for life in the extreme arid region of the Atacama Desert: four years of observations including the El Nino of 1997-1998, Astrobiology, 3, 393-406.

Navarro-Gonzalez, R., F. A. Rainey, P. Molina, D. R. Bagaley, B. J. Hollen, J. de la Rosa, A. M. Small, R. C. Quinn, F. J. Grunthaner, L. Caceres, B. Gomez-Silva, C. P. McKay, 2003. Mars-like soils in the Atacama Desert and the dry limit of microbial life, *Science*, 302, 1018-1021.

Neftel, A., P. Jacob, D. Klockow, 1986. Long-term record of hydrogen peroxide in polar ice cores, *Tellus, Ser. B*, 38B, 262-270.

Oyama, V. I., B. J. Berdahl, 1977. The Viking Gas Exchange Experiment results from Chryse and Utopia surface samples, *Journal of Geophysics Research*, 82, 4669–4676.

Quinn, R.C., C.L. Taylor, A.P. Zent, C.P. McKay, F.J. Grunthaner, 2005. Dry acid deposition and accumulation at the Viking Lander sites and in the Atacama Desert, Chile. *Icarus*, submitted.

Schumb, W. C., C. N. Satterfield, R. L. Wentworth, 1955. *Hydrogen Peroxide*, Reinhold Publlishing, New York.

Skelley, A.M., J.R. Scherer, A.D. Aubery, W.H. Grover, R.H.C Ivester, P. Ehrenfreund, F.J. Grunthaner, J.L. Bada, R.A. Mathies, 2005. Development and evaluation of a microdevice for amino acid biomarker detection and analysis on Mars, Proc. Nat. Acad. Sci. in press.

Southworth, B. A., B. M. Voelker, 2003. Hydroxyl radical production via the photo-Fenton reaction in the presence of fulvic acid, *Environmental Science & Technology*, 37, 1130-1136.

Squyers, S.W., J.P. Grotzinger, R.E. Arvidsom, J.F. Bell, W. Calvin, P.R. Christensen, B.C. Clark, J.A. Crisp, W.H. Farrand, K.E. Herkenhoff, J.R. Johnson, G. Klingelhöfer, A.H. Knoll, S.M. McLennan, H.Y. McSween, R.V. Morris, J.W Rice, R. Reider, L.A. Soderblom, 2004. *Science*, 306, 1709-1714.

Sumner, D.Y., 2004. Poor preservation of potential organis in Meridiiani Planum hematite bearing sedimentary rocks. *J. Geophys. Res.*, 109, E12007.

Turov, V. V., Leboda, R., 1999. Application of 1H NMR spectroscopy method for determination of characteristics of thin layers of water adsorbed on the surface of dispersed and porous adsorbents, *Adv. Colloid Interface Sci*., 79, 173-211

Yen, A. S., S. S. Kim, M. H. Hecht, M. S. Frant, and B. Murray, 2000. Evidence that the reactivity of the martian soil is due to superoxide ions, *Science*, 289, 1909-1912.

Zent, A. P. and C. P. McKay, 1994. The chemical reactivity of the martian soil and implications for future missions, *Icarus*, 108, 146–157.

Zepp, R. G., B. C. Faust, J. Holgné, 1992. Hydroxyl radical formation in aqueous reactions (pH 3-8) of iron(II) with hydrogen peroxide: The photo-Fenton reaction, *Environ. Sci. Technol.*, 26, 313-319.

Zhou, X., K. Mopper (1990). Determination of photochemically produced hydroxyl radicals in seawater and freshwater, *Marine Chemistry,* 30, 71-88.

Chapter 5

Dry acid deposition and accumulation at the Viking lander sites and in the Atacama Desert, Chile

R. C. Quinn, F. J. Grunthaner, C. L. Taylor, A. P. Zent, C. P. McKay

We have measured the pH of soil samples collected along a north-south transect (24°S to 28°S; ~ 70°W) in the Chilean Atacama Desert and compared the magnitude and kinetics of pH shifts in these soils upon wetting with pH changes occurring in Viking martian surface samples wetted in the Labeled Release experiment. We quantified the pH changes occurring when the Viking 1 LR cycle 2 experiment surface sample was wetted by converting the quantity of CO_2 adsorbed or desorbed due to pH shifts to equivalent H^+ using carbon dioxide/carbonic acid equilibrium calculations. Soil pH is known to play a role in a number of processes that may explain the results of Navarro-González et al. (2003), who reported the discovery of "Viking-like" soils in the Yungay region of the Atacama Desert. Soil pH can affect the solubility of soil components (which determines the availability of nutrients and toxins), soil microorganism population diversity and activity, and soil organic chemical degradation mechanisms. On Mars, the Viking Gas Chromatograph Mass Spectrometer (GCMS) failed to detect organic compounds in the surface material at the Viking sites, and the Viking Biology Experiments failed to detect microbial life. Similarly, Navarro-González et al. (2003) reported the inability to detect organic compounds in Yungay soil samples using flash pyrolysis-GCMS, as well as the inability to isolate culturable bacterial from these samples. When experimentally wetted, the pH of both the Viking and Yungay surface samples underwent a rapid shift, similar in magnitude, from acidic to slightly basic. This shift was not observed in samples collected from wetter regions of the Atacama or from the subsurface at Yungay. We attribute this pH response to the dry deposition and accumulation of atmospheric acid aerosols, including H_2SO_4, and acid precursors on the soil surface at the Yungay and Viking sites. The pH response of the Yungay soils also indicates a higher level of acidity, with slower equili-

bration kinetics as water availability decreases. In the Atacama and on Mars, extremely low pH resulting from acid accumulation, combined with limited water availability and high oxidation potential, may result in acid-mediated reactions at the soil surface during transient wetting events. These soil acids are expected to play a significant role in the oxidizing nature of the soils, the formation of mineral surface coatings, and the chemical modification of organics in the surface material.

5.1 Introduction

It has been discovered recently that soils from certain regions of the Chilean Atacama Desert have some characteristics that are similar to the surface materials tested by the Viking Landers. Navarro-González et al. (2003) demonstrated that the quantity and diversity of heterotrophic bacteria increase as a function of local water availability in the Atacama, and that for some soil samples collected in the driest regions, no culturable bacteria could be isolated. Additionally, Navarro-González et al. (2003) reported that pyrolysis-GCMS analysis of soils collected from these regions revealed extremely low levels of organic matter. Although the mechanism resulting in the low level of organics in these regions was not established by Navarro-González, the condition of organic-depleted, near-sterile soil offers an interesting Earth analog of the martian surface material, as the Viking Gas Exchange (GEx) experiment and Labeled Release (LR) experiment were unable to demonstrate the presence of culturable bacteria (Klein, 1978; Klein, 1979), and the Viking pyrolysis-GCMS was unable to detect organic compounds (Biemann et al., 1977; Biemann and Lavoie, 1979).

In this work we examine the acid-base equilibration kinetics of soils collected in the Chilean Atacama Desert and compare these results to information on the acid-base chemistry of martian surface samples derived from the Viking experiments. Soil pH is of interest because it plays a direct role in a number of processes that affect both soil organic chemistry and soil biological load. Soil parameters that are typically pH-dependant include the solubility of soil components (which determines the availability of plant nutrients and toxins); soil microorganism population diversity; and activity; and organic chemical degradation mechanisms.

The recent discovery at the Mars Exploration Rover (MER) Opportunity site of jarosite (Kerr, 2004), which typically forms in strongly acidic-sulfate rich environments, heightens the importance of performing the aqueous electrochemical measurements in-situ. The first direct measurement of pH and other electrochemical properties of the martian surface material will be performed by the Mars Environmental Compatibility Assessment (MECA) wet chemical laboratory (Kounaves et al., 2003) on the 2007 NASA Phoenix Mission. Currently, the only experimental information on the chemical behavior of the martian surface in aqueous systems is indirect and must be deduced from the Viking biology experiments. These experiments demonstrated that the martian surface mate-

rial at both landing sites, Chryse and Utopia, was chemically active when introduced to aqueous systems (Klein et al., 1976). The primary experimental results leading to this conclusion include the release of oxygen from samples that were wetted with either water vapor or liquid water in the GEX experiment (Oyama et al., 1977; Oyama and Berdahl, 1977) and the decomposition of components of an aqueous solution of organic chemicals in the LR experiment (Levin and Straat, 1976; Levin and Straat, 1977; Levin and Straat, 1979). Thermal treatments of samples in these biology experiments revealed that multiple reactants were present in the surface material and that a minimum of three oxidizing species are needed to explain the experimental results of both the GEX and LR (Klein, 1978; Klein, 1979).

Although examined less than the data that indicates that the martian surface material is oxidizing, the first information on the acid-base chemistry of the surface material was also returned by the Viking Biology experiments. Viking did not measure pH directly, but examination of CO_2 partitioning between the headspace and aqueous phases in the biology experiments has yielded limited insight into the acid-base chemistry of the surface material at the landing sites. Oyama et al. (1977) concluded that the surface material at the Viking site had a weak acidic nature. The experimental evidence that indicates the presence of this acidic component is the release of CO_2 from the soil prior to the wet mode in the GEX, an initial small CO_2 peak in the Pyrolytic Release Experiment (PR) (Horowitz et al., 1977), and the release of $^{14}CO_2$ from the heat-sterilized VL 1 cycle 2 sample (injection 1). The observation of higher background counts in the LR experiment after the sterilization treatment led Oyama et al. (1977) to suggest that the acidic component may be $H_2SO_4 \cdot 2H_2O$, and that it is semi-volatile when heated during the sterilization sequence.

The initial increase in headspace CO_2 levels seen in the Viking biology experiments has been attributed to an acidic soil component, however, the magnitude of CO_2 uptake subsequent to any initial CO_2 release during the GEX and LR indicates that the acid component is neutralized upon wetting. Oyama et al., 1977 attributed this resorption of desorbed CO_2 to the generation of hydroxyl ions from the reaction of soil superoxides with water. Simulations of the GEX have indicated that after neutralization of the acidic components, the overall pH of the aqueous soil mixtures tested by Viking were slightly (pH = 7.4) to moderately (pH = 8.7) basic (Quinn and Orenberg, 1993). Although the samples analyzed by Viking represent the current chemical state of the surface at the site, and not the past or subsurface state, it is interesting to note that jarosite would be expected to form in an aqueous acidic surface environment but not in an alkaline environment.

5.2 Experimental

5.2.1 Atacama samples

Soil samples were collected along a north-south transect (~ 70° W longitude) in the Atacama Desert, which is located along the northern Chilean Pacific coast (from 30°S to 20°S latitude). The samples were collected at sites along a climatic gradient from more southern humid regions (28°S) near Copiapo to the most arid region in the north (24°S) near Yungay. Table 1 lists the sample identification numbers and the locations of sample collection sites. The surface samples tested were identical to the samples analyzed by Navarro-Gonzalez et al. (2003) and use the same identification numbers.

Table 1
Sample collection location and equilibrated pH and E_H values.

Sample ID	Latitude South	Longitude West	Collection Depth (cm)	Equilibrated pH	Equilibrated E_H
AT02-03	24° 4' 10"	69° 51' 59"	Surface	6.8	532
AT02-29	24° 34' 26"	69° 47' 45"	Surface	7.9	420
AT02-27	25° 4' 6"	69° 53' 17"	Surface	5.9	624
AT02-16	25° 18' 17"	69° 50' 32"	Surface	7.5	620
AT02-24	25° 45' 37"	70° 11' 47"	Surface	7.8	607
AT02-22	28° 7' 5"	69° 55' 58"	Surface	8.6	342
AT03-S1	24° 4' 10"	69° 51' 59"	0.5 - 3.5	7.7	600
AT03-SP1	24° 4' 10"	69° 51' 59"	28	8.5	443
AT03-SP2	24° 4' 10"	69° 51' 59"	46	8.0	473
AT03-SP3	24° 4' 10"	69° 51' 59"	56	7.9	449
AT03-SP4	24° 4' 10"	69° 51' 59"	70	8.1	466
AT03-SP5	24° 4' 10"	69° 51' 59"	85	8.1	502
AT02-SP6	24° 4' 10"	69° 51' 59"	95	8.1	519
AT02-SP7	24° 4' 10"	69° 51' 59"	102	8.3	450
AT02-SP8	24° 4' 10"	69° 51' 59"	110	8.2	384
AT02-SP9	24° 4' 10"	69° 51' 59"	130	7.4	503
AT02-SP10	24° 4' 10"	69° 51' 59"	141	8.0	344

5.2.2 Atacama sample measurements

Measurements of the liquid phase pH, oxidation-reduction potential (E_H), and temperature were taken using a Thermo-Orion 635 Meter with a model 61-78 probe. For pH calibrations, premixed Thermo-Orion buffer solutions were used (pH 4, 7 and 10) and for ORP calibration, Thermo-Orion ORP standard was used to calibrate to the standard hydrogen electrode. The probe uses an integral temperature sensor to automatically compensate measurements for temperature. Measurements were made by adding Atacama soil to high-purity (18 Mohm) Milli-Q water in a 1:2 (wt:wt) soil-to-water ratio. In our experimental method, we begin measuring the E_H-pH of the soil as it is introduced to water and continue taking measurements as a function of time until equilibrium is approached. The release of oxygen in the GEX, the decomposition of organics in the LR, and the sorption of CO_2 in both experiments were rapid processes. Since our goal is to better understand and make comparisons to the Viking results, the E_H and pH values achieved upon the initial wetting of the soil is key to understanding the chemical behavior of the soils.

Non-aqueous pH-E_H measurements were made using a Thermo Orion pH/ISE meter (model 920A plus) with a Ross Ultra pH electrode (Thermo Orion model 8102BNU), a platinum redox electrode (Thermo Orion model 97-78-BN), and an automatic temperature compensation probe (Thermo Orion model 917006). Aldrich 99.5+% acetonitrile degassed with nitrogen was used in a 1:2 (wt:wt) soil-to-solvent ratio.

Ground level atmospheric NO_2, NO_x, SO_2, and O_3 were measured using Ogawa passive sample collectors obtained from Rupprecht and Patashnick Co., Inc. (Albany, NY). During each collection period, three replicate measurements of each type were performed at the AT02-03 site. The collection period was six consecutive days during the month of May and the results represent time weighted averages. Sensor collection pads were analyzed by Inter Mountain Laboratories Air Science, Inc. (Sheridan, WY) using ion chromatography and the standard operating procedures provided with the sensors.

The soluble ion content of the Atacama soils was determined at the NASA Jet Propulsion Analytical Laboratory by aqueous solvent extraction using a 1:2 soil-to-water ratio by weight and analysis by either atomic emission spectroscopy or ion chromatography.

5.2.3 Labeled Release experiment data reduction

Viking LR data was obtained from the NASA Planetary Data System. The data sets contain the counts recorded by a solid-state beta detector as a function of time resulting from the presence of $^{14}CO_2$ (g) in the sample cell headspace. In the LR, an aqueous solution of $^{14}CO_2$-labeled organics was introduced into the sample cell, with the corresponding changes in headspace $^{14}CO_2$ levels reflecting organic decomposition and CO_2 adsorption and desorption from the soil/solution mixture. To determine the magnitude of the pH shifts resulting in CO_2 sorption, the quantity of CO_2 absorbed or desorbed was converted

to equivalent H^+ using carbon dioxide/carbonic acid equilibrium calculations. $^{14}CO_2$ quantities in the LR cell headspace were calculated by taking 10,000 detector counts to correspond to 65% of one of the labeled aqueous substrates, which equals18.85 nmoles of $^{14}CO_2$ (Klein et al., 1976). At the start of a LR experiment, Mars atmosphere was trapped at 7.6 mBar and 0.132 cm^3 of starting gas at 8.505 Bar with a partial CO_2 pressure of 2.84% was added, resulting in 13.73 mBar of unlabeled CO_2 in the headspace. The total CO_2 change in the headspace was then calculated based on $^{14}CO_2$ partial pressures derived from LR detector response. Proportional partitioning of both labeled and unlabeled CO_2 with the aqueous phase was assumed. This calculation was applied to headspace changes that occurred in the Viking 1 LR cycle 2 experiment. In this experiment, the sample was heated to 160°C and cooled prior to nutrient injection, resulting in the deactivation of the chemical component responsible for the decomposition of the nutrient seen in other LR experiments (Levin and Straat, 1976).

The change in H^+ present in the soil solution was calculated using:

$$\text{Total}[CO_2(aq)] = \frac{[CO_2(aq)_H]([H^+]^2 + [H^+]K_{a1} + K_{a1}K_{a2})}{[H^+]^2} \quad (1)$$

to solve for $[H^+]$ and multiplying by the volume of injected LR solution. In equation 1, total$[CO_2(aq)]$ is the change in aqueous CO_2, assumed to be equal and opposite to the calculated change in headspace CO_2, $[CO_2(aq)_H]$ is the calculated Henry's law concentration of CO_2 (aq) given by:

$$[CO_2(aq)_H] = K_{CO2} * pCO_2 \quad (2)$$

where pCO_2 is the partial pressure of CO_2 in the LR cell headspace and K_{CO2} is the Henry's law constant for CO_2 at 10°C (5.39 X 10^{-2} Mole/L·Atm) . K_{a1} (3.42 x10^{-7} Mole/L·Atm) and K_{a2} (2.9 x 10^{-11}) are the equilibrium constants for carbon dioxide and carbonic acid acid-base equilibria at 10°C:

$$K_{a1} = \frac{[H^+][HCO_3^-]}{[CO_2\,(aq)]} \quad (3)$$

$$K_{a2} = \frac{[H^+][CO_3^{2-}]}{[HCO_3^-]} \quad (4)$$

5.3 Results and Discussion

5.3.1 pH response of Atacama soils

The sample identifier, collection depth, equilibrated pH, and equilibrated E_H, are listed in table 1. As seen in this table, all of the tested soils are oxidizing with equilibrated pH values ranging from 5.9 to 8.5. Additionally, the values do not follow a simple north-south gradient, instead reflecting the local microenvironment at the sample sites.

The AT02-03 (Yungay) site is located in the dry core of the Atacama Desert. This region appears to be nearly devoid of life, including hypolithic algae that are found in other arid deserts on Earth. An environmental monitoring station (24° 4' 50"S) established by McKay et al. (2003) in 1994 near the AT02-03 site collected temperature, wind direction, relative humidity, and rainfall data for a four-year period. The region has a temperate climate, with a mean temperature between 10°C and 30°C. During the collection period the only significant rain event resulted in just 2.3 mm of precipitation. Although dew occurs more frequently than rain, it is not a significant source of soil moisture.

A striking feature of this region is the large amounts of nitrate deposits, probably of atmospheric origin (Bohlke et al., 1997), that have not been biologically decomposed. These salt deposits are also known to contain highly oxidizing species, including iodates (IO_3^-), chromates (CrO_4^{-2}), and the only known naturally occurring deposits of perchlorate (ClO_4^-) (Ericksen, 1981; Ericksen, 1983). These oxidizing compounds are likely formed by photochemical reactions at the soil/atmosphere interface, analogous to the possible photochemical origin of martian oxidants. Due to differences in water availability, solar flux, soil composition, and atmospheric composition, specific mechanisms and reaction products may differ, but it appears that similar photochemical processes may be occurring both in the Atacama and on Mars.

Figure 1 shows the change in pH as a function of time as the Atacama surface soils collected along the north-south transect are introduced to water. A unique pH response occurred in the surface samples collected at the Yungay site compared to the samples collected at the other sites. The Yungay samples showed a rapid shift to an acidic pH followed by an equilibration to a more basic pH. This shift was consistently seen in surface samples collected at the AT02-03 site and was never observed in samples from the other collection sites. The initial pH of three Yungay surface samples shown in figure 1 reached 4.9 ± 0.2 when added to water. The variation in starting pH for the water used in each run is due to the difficulting in obtaining an accurate pH in deionized water. In all runs 18 MΩ water was used. The lowest initial pH observed after soil addition in tested Yungay samples was 4.3. Figure 2 shows the change in pH as a function of time for samples collected from a soil pit dug at the Yungay site. The sample collection depth is listed in table 1. The unique response of a rapid shift to an acid pH followed by neutralization seen in the Yungay surface samples was not observed in samples collected from subsurface horizons.

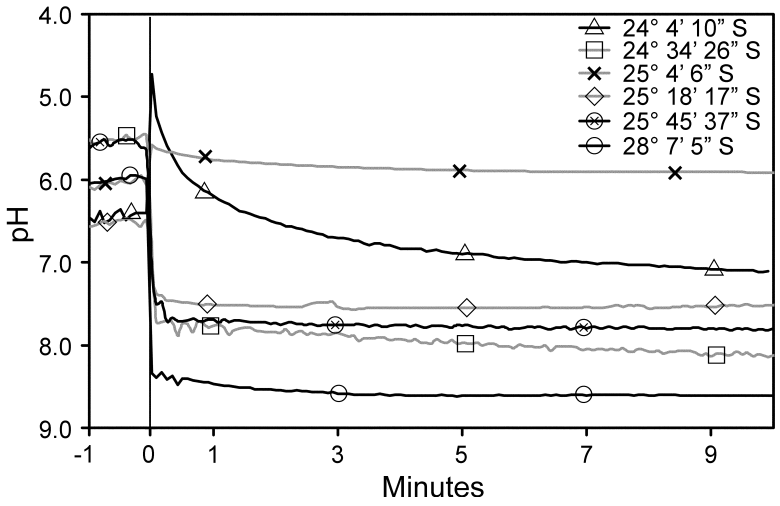

Figure 1. The pH response of Atacama surface soils when wetted. A rapid shift from acidic to slightly basic was observed for surface sample collected in the Yungay region (24° 4' 10" S). Soil was added at T=0.

The surface horizon AT02-03 consists of scrapings, removed from the top of a gypsum-rich surface crust, approximately 5-6 mm thick. Small quartz and plagioclase grains, derived from the surrounding terrain, typically rest atop the crust layer, but were not included in the surface sample analyzed here. Sample AT03-S1 is taken from a fluffy particulate layer, 3-4 cm thick, directly beneath the crust at a nearby location. Both AT02-03 and the underlying AT03-S1 are dominated by gypsum and anhydrite. Lower strata are also dominated by gypsum and anhydrite, which becomes less predominant at greater depth. At 122 cm, a horizon comprising halite and nitratine ($NaNO_3$), both highly soluble species, indicates the limits of ground-water infiltration.

We attribute the pH response observed in the Yungay surface samples to the presence of a soluble acid that is rapidly neutralized by soil components after dissolution. No evidence of this species was seen in surface samples collected from the wetter desert regions. The pH response of surface soils collected at the Yungay site is consistent with the dry deposition and accumulation of atmospheric acid aerosols and acid precursors on the soil surface at the Yungay site. The absence of this acid component in the sub-surface samples is consistent with a water transport mechanism for soil horizon formation. It appears that the low moisture levels at Yungay result in acids accumulating at the surface; accumulation would be expected to continue until offset by the periodic addition of sufficient amounts of water (either through rain or heavy fog) to cause dissolution and neutralization through soil cation exchange processes.

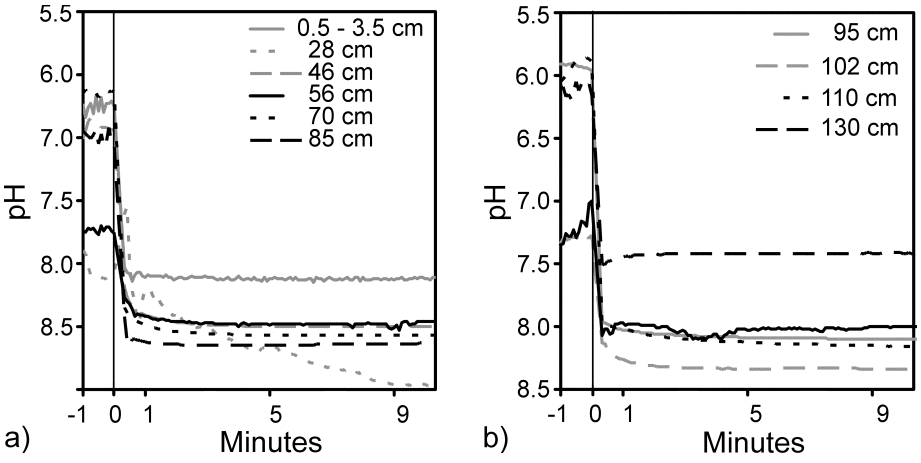

Figure 2. The change in pH as a function of time for samples collected from a soil pit dug at the Yungay site. The unique response of a rapid shift to an acid pH followed by neutralization seen in the Yungay surface samples was not observed in samples collected from subsurface horizons.

5.3.2 pH responses in the Viking labeled release experiment

The Viking Labeled Release (LR) experiment (Levin and Straat, 1976) was designed to detect hetrotrophic life by monitoring for evolution of radioactive gases after the introduction of a dilute aqueous solution of organic substrates labeled with ^{14}C. Upon initial introduction of the LR solution to a martian surface sample, a rapid increase in headspace $^{14}CO_2$ (g) was observed. This response is shown in figure 3 for the Viking Lander 1 Cycle 1 sample. A second injection of LR solution approximately 165 hours after the first injection resulted in a small $^{14}CO_2$ spike followed by $^{14}CO_2$ uptake. This initial CO_2 release can be explained by the presence of a small amount of hydrogen peroxide in the soil (Klein, 1976), although other explanations have been proposed (reviewed by Zent and McKay, 1993). Low levels of hydrogen peroxide are photochemically produced in the martian atmosphere (Encrenaz et al., 2004), diffuse into subsurface regions (Bullock et al., 1994) and may adsorb onto soil surfaces, where they are stabilized (Quinn and Zent, 1999). The presence of hydrogen peroxide is also consistent with the thermal stability of the active agent in the LR. A "positive" LR response was not observed in a sample heated to 160°C (VL1 cycle 2), while the response in a sample heated to 46°C (VL2 cycle 4) was 54-80% less than that observed in unheated samples.

Figure 3 shows as raw counts the response of the Viking Lander 1 cycle 2 LR sample, which was heated to 160°C for three hours and cooled prior to solution injection. In this experiment an instantaneous release of $^{14}CO_2$ occurred, followed by a rapid re-uptake of $^{14}CO_2$ into the solution. This response has been attributed to surficial acidity due to a thin coat of sulfuric acid that is neutralized by strongly basic alkali and alkaline earth metal hydroxides formed during wetting (Oyama et al. 1977). In figure 4 this response of the VL1 Cycle 2 sample is plotted as moles of aqueous H^+ (calculated using equation 1) in the soil solution as a function of time, overlaid with a pH data for Yungay surface samples (also reported as moles of aqueous H^+ in the soil solution). The total moles of aqueous H^+ in the Atacama soil solution was normalized to the 0.5 cc Viking LR sample volume.

We estimate that the initial pH of the soil at VL1 C2 soil reached 4 upon wetting. The higher background counts seen in the LR experiment after heating the sample indicates that some of the acid component may have volatilized prior to wetting. There is no way to determinate if a significant loss of the acid component occurred during heating, but if

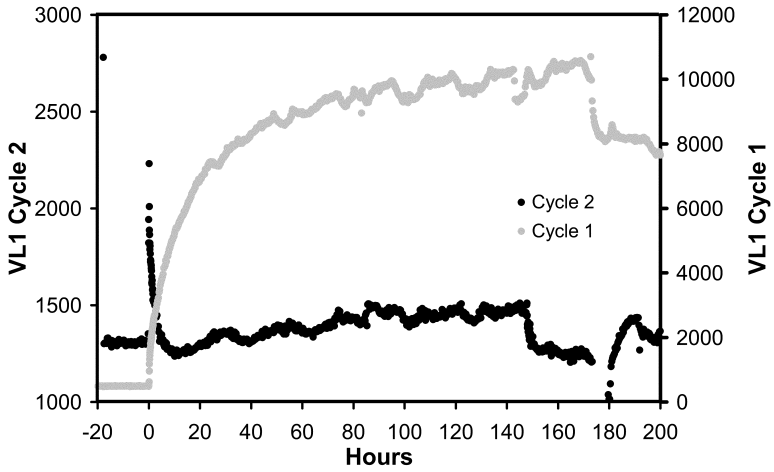

Figure 3. Response of the Viking Lander 1 Labeled Release experiment cycles 1 and 2. CO_2 changes in sample cell headspace are shown as raw counts recorded by the LR solid state beta detector. The cycle 2 sample was heated for 3 hours at 160°C prior to solution addition.

there was substantial loss, then the initial pH of an unheated surface sample would be below 4. The number of moles of H^+ released into solution by the Yungay soil is comparable to the amount released by the VL1 C2 sample. The measured kinetics, however, are different. These differences can be explained by the different measurement techniques

used to derive the H^+ changes. Figure 4 shows three plots of the equivalent H^+ released by Atacama soil solutions. The first curve shows moles of H^+ as a function of time for a stirred solution at 24°C, the second an un-stirred solution at 20°C, and the third an un-stirred solution at 4°C. As expected for measurements taken with a pH electrode, the equilibration times decrease with increasing temperature and stirring. Since the H^+ change in LR samples was derived from changes in CO_2 headspace concentrations, the kinetics are determined by CO_2 sorption rates and would be diffusion controlled. Under these conditions, several factors in addition to temperature and physical mixing will affect the apparent equilibration rate, and therefore the measured response rate, including sample surface area, sample porosity, and cell geometry.

Based on the data derivable from Viking, the response of the Yungay samples upon wetting is consistent with the LR observations and can be explained by the rapid solvation of an acid followed by neutralization. A decrease in pH was not seen in the Yungay samples following the addition of a second aliquot of water. In the LR VL1 C2 experiment, headspace $^{14}CO_2$ did not increase after the second injection. In both cases, this is consistent with neutralization of an acid component.

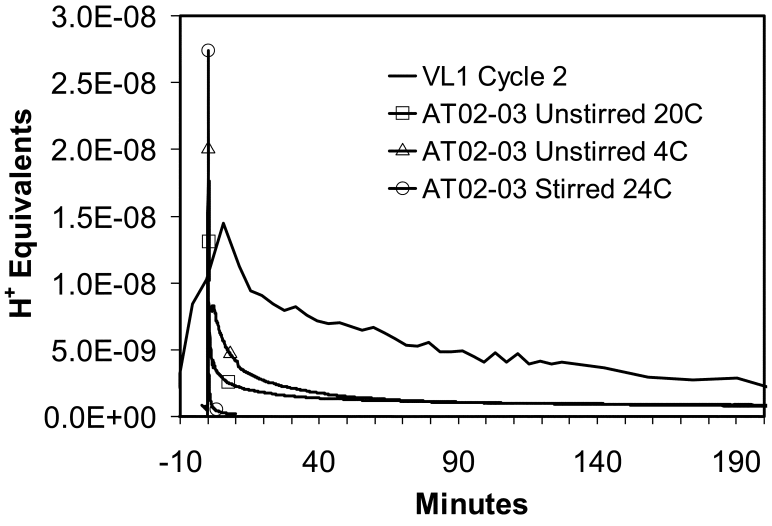

Figure 4. Response of the VL1 cycle 2 labeled release sample and Yungay surface samples shown as H^+ equivalents.

5.3.3 Acid deposition and accumulation

Dry and wet acid deposition can occur through multiple processes in terrestrial environments. On earth, the most common mechanisms involve atmospheric oxidation of NO_x and SO_2 released from both anthropogenic and natural sources. Atmospheric sulfur dioxide and nitrogen oxides are oxidized through gas phase or aqueous phase (in fog or clouds) into sulfuric acid and nitric acid which then can deposits either as dry particles or in aqueous precipitation. While multiple pathways of atmospheric SO_2 oxidation exist, the most common mechanism of gas-phase dry sulfuric acid formation is oxidation of SO_2 by OH radicals photochemically produced in the atmosphere:

$$O_3 + h\nu \rightarrow O(^1D) + O_2$$

$$O(^1D) + H_2O \rightarrow 2OH\cdot$$

$$SO_2 + OH\cdot + M \rightarrow HOSO_2 + M$$

$$HOSO_2 + O_2 \rightarrow HO_2 + SO_3$$

$$SO_3 + H_2O \rightarrow H_2SO_4$$

Sulfuric acid can then adsorb onto aerosols, which can then deposit onto soil surfaces. Nitric acid formation also occurs through a similar reaction with OH radicals:

$$OH\cdot + NO_2 + M \rightarrow HNO_3 + M$$

Although typically a minor formation mechanism, NO_2 may also react after sunset with O_3 (photochemically produced during daylight hours) to form nitric acid:

$$NO_2 + O_3 \rightarrow NO_3 + O_2$$

$$NO_3 + NO_2 \rightarrow N_2O_5$$

$$N_2O_5 + H_2O \rightarrow 2HNO_3$$

In fog, aqueous-phase-formation sulfuric acid is typically dominated by hydrogen peroxide oxidation:

$$SO_2 + H_2O_2 \rightarrow H_2SO_4$$

In hyper-arid environments such as the Atacama it may be possible for ground-level fogs, which are common, to contribute to dry acid deposition through evaporative condensation of acid on aerosol surfaces that settle on soil surfaces.

Results of soluble ion analysis of the Atacama soils and ground level atmospheric NO_2, NO_x, SO_2, and O_3 measurements at the Yungay site are shown in tables 2 and 3. Levels of soluble $SO_4^{=}$, NO_3^{-}, and Cl^{-} are highest at the Yungay site compared to the other soils, and suggest either higher rates of atmospheric deposition or lower rates of removal from the surface layers compared to the other sites. Based on the annual amount of precipitation at these sites and the pH response of the Yungay soils, a slower rate of removal from the surface is expected. The ground-level atmospheric NO_2, NO_x, SO_2, and O_3 levels, combined with the soluble ion data, indicate that both H_2SO_4 and HNO_3 are depositing on the soil surface at Yungay, while the soluble ion data indicate that an HCl contribution to soil acidity is also possible. The presence of a gypsum/anhydrite "surface crust" is typical at the Yungay site and is also indicative of acid deposition processes. Although the presence of exchangeable cations provide the soil with a significant buffering capacity, allowing rapid neutralization of the acid when sufficiently wetted, the low moisture levels at the Yungay site favor acid accumulation over neutralization.

Table 2
Atacama soil aqueous ion concentrations (parts-per-million).

Cations	Na	K	Mg	Ca	Fe	Sr
AT02-03	391	262	106	2.94E+04	0.4	102
AT02 16	130	146	23	5.40E+03	0.4	33
AT02 22	148	78	5.5	226	4.3	1.3
AT02 24	154	202	59	5.10E+03	0.2	1.6
AT02 27	236	472	105	5.80E+03	0.3	17
AT02 29	183	64	19	82	24	0.4
Anions	**F**	**Cl**	**NO3**	**PO4**	**SO4**	
AT02-03	56.3	26.2	82.1	10.9	6.35E+04	
AT02 16	2.4	9.1	13.8	3.6	1.10E+04	
AT02 22	nd	3.1	8.6	9.8	5.5	
AT02 24	nd	30.1	10.7	2	1.06E+04	
AT02 27	19.5	6.4	53.6	9.7	1.39E+04	
AT02 29	0.75	4.1	5.2	9.4	32.6	

Atmospheric models of Mars predict the presence of low levels of H_2O_2, O_3, ·OH, and H_2O near the planet's surface (Hunten, 1979). The presence of these gases, the high sulfur levels measured in Mars soils, and the presence of a "duricrust" point to accumulation of acid on the surface. In laboratory studies, Banin et al. (1997) examined the potential influence of acidic volatiles on the formation of the martian surface soils and concluded that the pH of the soil may be below neutrality and buffered by acidic species. Banin et al. (1997) did not examine the results of the Viking biology experiments for evidence of acid accumulation. As examined in this paper, the CO_2 sorption responses in the Viking Biology Experiments indicate that local water availability is insufficient to neutralize these soil acids rela-

Table 3
Ground-level atmospheric trace gas concentrations at the AT02-03 (Yungay) collection site (parts-per-billion).

Collection Period (min)	NO_x ppb	NO_2 ppb	SO_2 ppb	O_3 ppb
8440	1.7 ± 0.2	0.3 ± 0.2	4.9 ± 1.3	5.0 ± 1.9

tive to accumulation rates. However, when larger amounts of water are added to the system as was done in the GEX and LR experiments, the acid component is rapidly neutralized.

5.3.4 Adsorbed water and effective soil pH

The samples examined in the LR experiments were wetted to a level of 20% water by weight during the first injection and the Atacama samples studied in this work were wetted to levels of 200% water by weight. Under these conditions the soil suspensions were initially weakly acidic. When exposed to smaller amounts of water the effective pH at the soil surface will become strongly acidic. Environmental conditions in the Atacama and on Mars make transient low levels of water exposure more likely than complete soil wetting. Under these conditions, even if the accumulated load of soil acid is relatively low, the effective pH of the soil surface may be extremely acidic. In the Atacama these conditions occur when ground fog or dew is present, while on Mars mobile-thin films of water would be expected to form at soil/ice interfaces, with the thickness of the layer being a function of both ice temperature and soil composition. On Mars, small amounts of adsorbed mobile water would also be expected to persist in soil from which ice has been removed through sublimation (Möhlmann, 2004).

The pH response of Yungay surface soil measured in acetonitrile is shown in figure 5. Although caution must be used when comparing aqueous and nonaqueous pH measurements, the aqueous pH response of the Yungay soil is also shown in figure 5. When making nonaqueous pH measurement, a low level of water must be present in the system for the electrode to function properly. The acetonitrile (a dipolar aprotic solvent) used in this work contained a minimum of 0.3% water by weight. The water content of the soil system under these conditions was as much as three orders of magnitude less than in the aqueous measurements. The pH response of the Yungay soils in acetonitrile indicates a higher level of acidity, with slower reaction kinetics as water availability decreases. Additionally, the limited water level resulted in a comparatively slow dissolution of the soil acid, and water availability was insufficient to allow neutralization through cation exchange with the soil.

In the Atacama and on Mars, extremely low pH resulting from acid accumulation, combined with limited water availability, may result in acid-mediated reactions at the soil surface during transient wetting events. The presence of soil acids can limit nutrient availability and cause soil toxicity by solvating metals, resulting in environments depleted of life. Low soil pH combined with high redox potential would be expected to play a significant role in the formation of surface mineral coatings and the chemical modification of organics in the surface material.

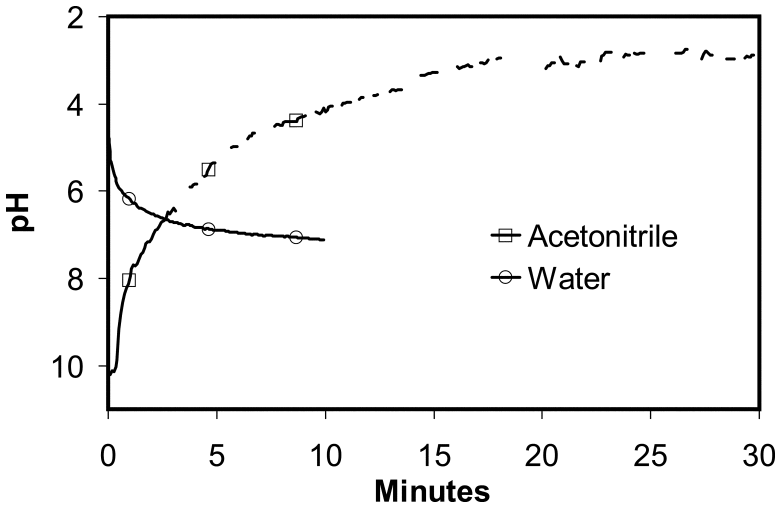

Figure 5. pH response of Yungay surface soils measured in acetonitrile and in water.

The oxidative processes that result in acid formation are intimately linked to other oxidative environmental processes, such as photo-Fenton reactions and nitrate photochemistry. The high levels of soil nitrate, combined with the presence of ground fog in the Atacama suggest that nitrate photochemistry may play a substantial role in the oxidative decomposition of organics in the soil. The photo-activation of soil nitrate in the presence of ground fog:

$$NO_3^- + h\nu \rightarrow NO_3^{*-} \rightarrow NO_2^- + O(3P) \rightarrow NO_2 \quad + \quad \cdot O^-$$

$$\cdot O^- + H_2O \rightarrow \cdot OH + OH^-$$

produces OH radicals which can then oxidatively destroy soil organics and oxidize inorganic soil components. On Mars, the high levels of iron present in the surface material suggest Fenton reactions may play a greater role in oxidative processes than soil-nitrate photochemistry. Möhlmann (2004) suggested that photo-Fenton-like processes in the martian soil would generate hydroxyl radicals that can oxidize most organic compounds. In contaminated soil systems on earth, Fenton's reagent, H_2O_2 plus Fe(II), is often used to oxidize organic pollutants. In the Fenton reaction, hydroxyl radicals are generated by the oxidation of Fe(II) to Fe(III) by H_2O_2. In the photo-Fenton reaction, the Fe(II) needed for the reaction to proceed is catalytically generated through the reduction of Fe(III) by UV. It is reasonable to expect that on Mars photo-Fenton-like reactions will occur and may play

a role in the oxidation of soil organics. However, on Mars Fenton reactions in the soil may dominate over photo-Fenton reactions. Treatment of contaminated soils on earth has shown that sufficient Fe(II) is generated by the slow reduction of Fe(III) by H_2O_2 to oxidize soil organics (Lu, 1990). On Mars, the Fenton-reaction should not be limited by lack of soil Fe(II). Therefore, in the absence of regolith mixing, Fenton-reactions will occur to a depth limited by the penetration of H_2O_2 and not limited by the penetration depth of UV radiation at the surface.

5.5 Summary and Conclusions

The measurements of the pH behavior of experimentally wetted Atacama soils indicate that dry deposition and accumulation of acids is occurring in soils in the Yungay region. The kinetic response of the Yungay soil pH is similar to the pH response of Viking soils inferred from the magnitude and kinetics of CO_2 sorption during the Viking LR experiment, indicating that the accumulation of dry acids has also occurred on Mars. The deposition of these acids in both the Yungay region and on Mars is likely the result of photochemical oxidation of acid precursors under dry atmospheric conditions. The accumulation of these acids on the surface of Mars and in the Atacama desert can profoundly impact inorganic and organic chemistry, as well as biologic potential. In these environments, chemical weathering would be expected to proceed under acidic conditions during episodic low-moisture wetting events. In both environments, likely wetting modes may involve small amounts of surface water. On Mars, thin-films of water may form at soil/ice interfaces either in regions where buried ice exists, during partial melting events, or as a result of frost formation (as was observed at the Viking 2 landing site). In the Atacama, the most common mode of soil wetting is the occasional occurrence of ground level fog. The results of this work indicate that in the presence of small amounts of liquid water, both Viking and Yungay soils are highly acidic. However, both the Viking and Yungay soil acids are rapidly neutralized by other soil components when sufficiently wetted (~1:1 soil to water by volume). This implies that for a Mars soil with an acid load and ion-exchange capacity similar to the present-day Viking surface material, different chemical weathering products would form under different wetting conditions. For example, it may be possible for jarosite to form during low-moisture wetting events in a present-day Viking surface environment, but not during bulk wetting of the surface material, since bulk wetting would result in a slightly basic aqueous system.

The surface environment at Yungay indicates the accumulation of sulfuric and nitric acids, while on Mars the accumulation of sulfuric acid would be expected. Both nitric and sulfuric acid are oxidizing; these acids, combined with other photochemically produced oxidizing species that are expected in these environments, such as H_2O_2, $\cdot O_2^-$, and $\cdot OH$, would aggressively attack organic compounds and can explain the low levels of organics and microbial populations found at Yungay in the Atacama as well as the apparent lack of

organics and microbial populations at the Viking Lander sites. Additionally, the rates of oxidative decomposition of organics would be expected to be highest in the presence of small amounts of liquid water, due to the formation of concentrated aqueous acids on soil surfaces. Small amounts of liquid water may also provide a mechanism to transport some of these oxidizers to sub-surface soils.

Acknowledgements

This work was supported by the NASA Mars Fundamental Research program, the NASA Astrobiology Science and Technology for Exploring Planets program, and NASA Ames/SETI Institute cooperative agreement NCC2-1408.

Chapter 5

References

Biemann, K., and Lavoie, J.M., 1979. Some final conclusions and supporting experiments related to the search for organic compounds on the surface on Mars. J. Geophys. Res. 84, 8385-8390.

Biemann, K., Oro, J., Toulmin, P., Orgel, L.E., Nier, A.O., Anderson, D.M., Simmonds, P.G., Flory, D., Diaz, A.V., Rushneck, D.R., Biller, J.E., Lafleur, A.L., 1977. The search for organic substances and inorganic volatile compounds in the surface of Mars. J. Geophys. Res. 82, 4641-4658.

Bohlke, J.K., Ericksen, G.E., Revesz, K., 1997. Stable isotopic evidence for an atmospheric origin of desert nitrate deposits in northern Chile and southern California, USA. Chemical Geology 136, 135-152.

Bullock, M.A., Stoker, C.R., McKay, C.P., Zent, A.P., 1994. A coupled soil-atmosphere model of H_2O_2 on Mars. Icarus 107, 142-154.

Encrenaz, Th., Bézard, B., Greathouse, T.K., Richter, M.J., Lacy, J.H., Atreya, S.K., Wong, A.S., Lebonnois, S., Lèfevreet, F., 2004. Hydrogen peroxide on Mars: evidence for spatial and seasonal variations. Icarus 170, 224-229.

Ericksen G.E., 1981. Geology and origin of the Chilean nitrate deposits. US Geological Survey Professional Paper 1188.

Ericksen, G.E., 1983. The Chilean nitrate deposits. American Scientist 71, 366-374.

Horowitz, N.H., Hobby, G.L., Hubard, J.S., 1977. Viking on Mars: The carbon assimilation experiment. J. Geophys. Res. 82, 4659-4667.

Hunten, D.M., 1979. Possible oxidant sources in the atmosphere and on the surface of Mars. J. Mol. Evol. 14, 71-78.

Kerr, R. A., 2004. A wet early Mars seen in salty deposits. Science 303, 1450.

Klein, H. P., 1978. The Viking biological experiments on Mars. Icarus 34, 666–674.

Klein, H. P., 1979. The Viking mission and the search for life on Mars. Rev. Geophys. Space Phys. 17, 1655-1662.

Klein, H.P., Horowitz, N.H., Levin, G.V., Oyama, V.I., Lederberg, J., Rich, A., Hubbard, J.S., Hobby, G.L., Straat, P.A., Berdahl, B.J., Carle, G.C., Brown, F.S., Johnson, R.D., 1976. The Viking biological investigation: Preliminary results. Science 194, 99-105.

Kounaves, S. P., Lukow, S.R., Comeau, B.P, Hecht, M.H., Grannan-Feldman, S.M., Manatt, K., West, S.J., Wen, X., Frant, M., Gillette, T., 2003. Mars Surveyor Program ’01 Mars Environmental Compatibility Assessment wet chemistry lab: A sensor array for chemical analysis of the Martian soil. J. Geophys. Res. 108, 5077-5089.

Levin, G.V. and Straat, P.A., 1976. Viking labeled release biology experiment: Interim results. Science 194, 1322-1329.

Levin, G.V. and Straat, P.A., 1977. Recent results from the Viking Labeled Release Experiment on Mars. J. Geophys. Res. 82, 4663-4667.

Levin, G.V. and Straat, P.A., 1979. Completion of the Viking labeled release experiment on Mars. J. Mol. Evol. 14, 167-183.

McKay, C.P., Friedmann, E.I., Gomez-Silva, B., Cáceres-Villanueva, Andersen, D.T., Landheim, R., Temperature and Mositure Conditions for Life in the Extreme Arid Region of the Atacama Desert: Four Years of Observations Including the El Nin0 of 1997-1998, 2003. Astrobiology 3, 393-406.

Mohlmann, D.T.F, 2004 Water in the upper martian surface at mid- and low-latitudes: presence, state, and consequences. Icarus 168, 318-323.

Navarro-González, R., Rainey, F.A., Molina, P., Bagaley, D.R., Hollen, B.J., de la Rosa, J., Small, A.M., Quinn, R.C., Grunthaner, F.J., Caceres, L., Gomez-Silva, B., McKay, C.P., 2003. Mars-like soils in the Atacama Desert and the dry limit of microbial life. Science 302, 1018-1021.

Oyama, V.I., Berdahl, B.J., Carle, G.C., 1977. Preliminary findings of the Viking gas exchange experiment and a model for Martian surface chemistry, Nature 365, 110-114.

Oyama, V. I., and Berdahl, B.J., 1977. The Viking Gas Exchange Experiment results from Chryse and Utopia surface samples. J. Geophys. Res. 82, 4669–4676.

Quinn, R.C. and Orenberg, J., 1993. Simulations of the Viking gas exchange experiment using palagonite and Fe-rich montmorillonite as terrestrial analogs: Implications for the surface composition of Mars, Geochim. Cosmochim. Acta 57, 4611-4618.

Quinn, R. C., and Zent, A.P., 1999. Peroxide modified titanium dioxide: A chemical analog to putative martian soil oxidants. Origins of Life and Evolution of the Biosphere 29, 59-72.

Zent, A. P. and McKay, C.P., 1994. The chemical reactivity of the martian soil and implications for future missions. Icarus 108, 146–157.

Chapter 6

Mars atmospheric oxidant sensor (MAOS): An in situ heterogeneous chemistry analysis

A.P. Zent, R.C. Quinn, F.J. Grunthaner, M.H. Hecht, M.G. Buehler, C.P. McKay, A.J. Ricco

We describe a chemometric array sensor, the Mars atmospheric oxidant sensor (MAOS, pronounced "mouse") that is designed to measure the oxidation rate of thin films on the martian surface. We select films that are sensitive to particular types of oxidants, that represent key elements in the martian soil, or that emulate prebiotic materials. Concern that naturally arising martian oxidants may have destroyed evidence of ancient life on Mars was raised by the Viking mission in the 1970s. The possibility that oxidants may limit the viability of biological habitats is particularly timely in the light of recent suggestions of contemporary flowing water on Mars. By controlling the temperature of the films, as well as their exposure to dust and ultraviolet light, MAOS will discriminate among leading hypotheses for oxidant production. MAOS weighs 55 g, fits in a 6×7×2 cm^3 envelope, and uses 250 mW power. Much of the enabling technology was developed for the MOx experiment, lost on the Russian Mars '96 mission.

6.1 Introduction

The planetary community is interested in life on other planets, as well as expanding the human presence into the solar system. On Mars, naturally arising oxidants may decompose organics relict of Mars' early history, and may affect human health and safety. In order to improve our chances of finding chemical evidence of life on Mars, and designing habitats and equipment that will function well on Mars' surface, we need to improve our understanding of these oxidants. We have developed, and describe here, a chemometric sensor array that we hope to use to characterize the oxidation potential of the Martian environment.

A quarter of a century ago, two Viking Landers were sent to Mars to seek evidence of life. However, the Viking experiments detected neither life nor organics in the martian

soil. Vigorous chemical activity was interpreted as the action of oxidizing species in the soil, rather than as biology. Viking was not designed to study oxidants. It is not possible to deduce from those results the nature and prevalence of the oxidizing species, nor whether they originated in the atmosphere or the bulk soil itself. Even the relationship between the absence of organics and the presence of oxidants may be considered circumstantial. Our chemiresistor-based oxidation potential sensor is referred to here as the Mars atmospheric oxidant sensor (MAOS, pronounced "mouse"). It weighs 55 g, fits in a 6 × 7 × 2 cm box, and uses, in normal operation, 250 mW power. The fundamental unit of MAOS is the "chemical pixel," (Fig. 1) a 4 × 2 array of concentric electrodes coated with a single chemical film. Half of the electrodes are permanently sealed from the environment, and serve as references. With the four sensing electrodes, we examine the origins of Mars' oxidizing potential by monitoring the resistivity of the films as a function of time. We use two kind of passive filters, one to exclude UV, and another to exclude dust. These two filters are deployed over the four sensing electrodes so that they exclude: (a) UV, (b) dust, (c) both, and (d) neither.

By monitoring differences in film reaction among the four electrodes, we will quantify the relative importance of soil-borne oxidants, UV photo-oxidation, and gaseous oxidants. Six identical chemical pixels are grouped into a "module". The total MAOS experiment consists of eight modules, each featuring a unique chemical film. The thin-film reactants include highly electropositive metals, semiconductors, and a set of organic functional groups. In an "experiment", we simultaneously expose 1 pixel from each module, and record the relative resistance of the eight chemicals, in four filter configurations, (total of 32 channels of data) as a function of time. Experiments differ in the time of day at which they are initiated, in the thermal profile we impose on the active pixels, and in the differences in ambient dust and UV fluxes. MAOS can conduct six experiments. The final interpretive identification of oxidants will be made, if possible, in terrestrial laboratories by matching the reactivity pattern of these reference reactants with a series of synthesized oxidants.

6.2 Scientific goals and objectives

6.2.1 The possibility of martian life, past or present

There is ample evidence that Mars was once much warmer and wetter than it is today (e.g. Carr, 1996). Although the martian surface has not yet been dated, warm wet conditions may date from the period of pre-biotic chemical evolution and abiotic development of life on Earth (3:85 Ga) (Schidlowski, 1988; Mojzsis et al., 1996). If martian life also arose in that early period, it is plausible that evidence persists at depth within the regolith (e.g. McKay, 1997). Recent discoveries have emphasized the urgency of the search. The controversy surrounding martian meteorite ALH84001 (McKay et al., 1996) has greatly

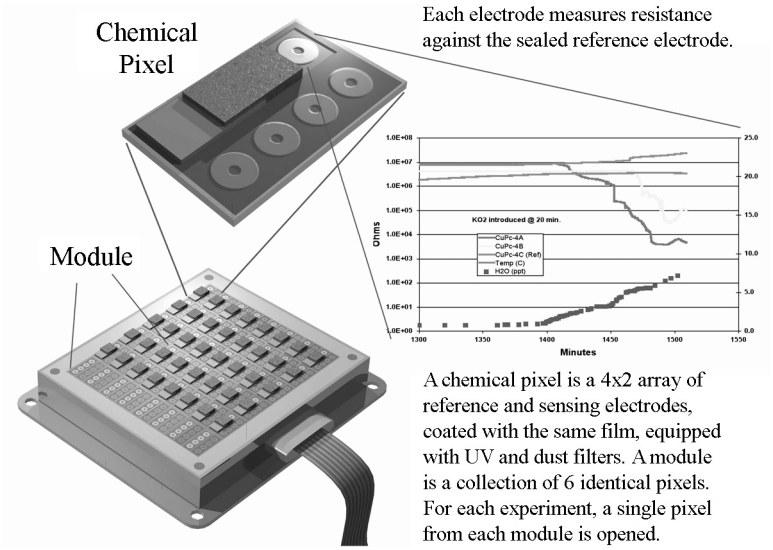

Figure 1. Illustration of the MAOS Concept

increased interest in martian life. Evidence of apparently recent water flow on the martian surface has further fueled speculation about geologically contemporary habitable environments (Malin and Edgett, 2000). Our understanding of the potential habitability of Mars has been broadened by discoveries of extraordinarily tenacious terrestrial life. Organisms have been found at depths of 2 km in the Columbia River basalt (Stevens and McKinley, 1995), evidently directly metabolizing the igneous rocks in which they live. Karl et al. (1999) recently recovered, from ice at 4 km depths, just above the surface of Lake Vostok, Antarctica, sample with viable bacterial cells, suggesting that Lake Vostok contains viable microorganisms. Anaerobic organisms recovered from a depth of 2:7 km beneath Virginia live at temperatures of 75°C. The microbes may have been trapped for 80 million years (Tseng et al., 1996). The limits of life do not rule out the persistence of life in sequestered habitats within the present-day martian regolith.

6.2.2 The Viking biology results

In response to telescopic observations through the 1950s suggesting that Mars could be the abode of life (e.g. Wyatt, 1964), the Viking mission was designed principally to search for such life. The Viking gas chromatograph mass spectrometer (GCMS) indicated no organic compounds containing more than two carbon atoms at concentrations greater than parts per billion. Nor did it find any one and two-carbon compounds at the parts per million level (Biemann et al., 1977; Biemann and Lavoie, 1979). This sensitivity level has recently been challenged (Benner et al., 2000; Glavin, et al., 2000). The absence, or in any event the depletion, of organics on Mars is a puzzle because, even in the absence of an in situ source, meteoritic infall will carry organics to Mars (e.g. Flynn and McKay, 1990).

These and other results led to the hypothesis that the martian surface material contains one or more oxidants that actively attack organic compounds (Klein, 1978, 1979). The Viking Biology experiments also provided evidence of soil components in a peculiar oxidation state. In the gas exchange experiment (GEx), exposure of soil of H_2O vapor led to rapid release of O_2, far in excess of the amount that could be produced by desorption (Oyama and Berdahl, 1977). In the labeled release (LR) experiment, incubation of radioactively labeled nutrient solution with martian soil led to release of radioactively labeled CO_2, presumably due to oxidation of the organics (Levin and Straat, 1977). However, because the LR activity was removed by heating, but the GEx activity was not, the oxidants responsible for them are believed to be different. It is generally held, but not demonstrably true, that the putative oxidant(s) responsible for the GEx and LR results are also responsible for actively destroying incoming organics at the martian surface. In addition, these oxidants may have destroyed relatively refractory reduced compounds relict of pre-biological chemical evolution. These hypotheses can only be tested by identifying the origin and nature of the martian oxidants. If oxidants render the near-surface martian regolith sterile, then martian life must be sought in special subsurface environments (e.g. Boston et al., 1992). Unfortunately, the depth of the organic-free, apparently oxidizing, soil is unknown. Theoretical considerations, however, suggest that the likely depth of the oxidized layer, assuming little aeolian mixing, is on the order of cm to a few m (Bullock et al., 1994; Zent, 1998).

6.2.3 Nature of the martian oxidants

A successful oxidant model must explain the release of O_2 in the Viking GEx, the decomposition of added nutrient in the LR, and the absence of organics in the GCMS. The concentration of oxidants in the soil sufficient to account for the GEx and LR results is shown in Table 1. Zent and McKay (1994) have argued that the amount of oxidant

Table 1
Comparison of GEx O_2 and LR^{14}C results (after Klein, 1978)

Sample	GEx O_2 (nmol/cm^3)	Possible oxidant (ppm; $KO_2 \rightarrow O_2$)	LR CO_2 (nmol/cm^3)	Possible oxidant (ppm; $H_2O_2 \rightarrow O$)
VL 1 surface	770	35	30	1
VL 2 surface	194	10	30	1

required would cover less than 1% of the surface area of grains that compose martian soil (Ballou et al., 1978). The soil concentration may be as low as a few ppm, which would not pose a serious hazard to humans or materials. The nature of the putative oxidant(s) has been discussed for over 20 years (Fig. 2). It has been argued by some that the oxidant must originate in the atmosphere, and hence may be able to diffuse through the regolith to unknown depths, wiping out the early chemical record as it goes (Hunten, 1974). Others maintain that the oxidant is strongly bound to dust surfaces, and hence potentially hostile to humans and their habitats (Nussinov et al., 1978; Yen et al., 2000). Oxidants do not intrinsically preclude the presence of organic material. SNC meteorites are also oxidizing (Gooding, 1992). There have, however, been reports of organic material in the SNCs (Wright et al., 1989), as well as in ALH84001 (McKay et al., 1996). It is also possible that the oxidizing species are virtually immobile, and could co-exist with organics (Zent, 2002).

Models of oxidant generation fall into several categories (Zent and McKay, 1994) which are described below. The exact oxidant cycle on Mars is not known and all or none of the proposed sources and sinks shown in Fig. 2 may exist, or be significant. The following sources, sinks, and cycles of oxidants have been proposed:

- Solar ultraviolet radiation may cause photolysis of atmospheric water vapor into "odd-H" (H, OH, HO_2, and H_2O_2) (e.g. Hunten, 1974; Barth et al., 1992). Subsequent recombination may produce oxidizing species that precipitate on to the surface. The total oxidant inferred from Viking results could have been produced in as little as 2–10 years by this mechanism (Kong and McElroy, 1977). Photochemical oxidant production ceases at sunset, and it has been hypothesized that some oxidants, such as hydrogen peroxide, which has roughly the same condensation properties as water, may precipitate at an accelerated rate just after sunset (Barth et al., 1992). Certainly, H_2O_2 is capable of degrading Mars analog organics (McDonald et al., 1998).

- Odd-H and odd-O groups produced by photolysis may subsequently complex with soils (e.g. Oro and Holzer, 1979). In particular, transition metals are capable of forming complexes with peroxy radicals that behave much as the Viking biology samples did (Quinn and Zent, 1999). If a significant portion of the oxidative power is bound to soil surfaces, we will note a lack of reactivity behind our dust-filtered electrodes.

- UV–silicate interactions may lead to generation of physically trapped oxygen (Nussinov et al., 1978) or radical species (Yen et al., 2000) directly in the silicate matrices. The non-bridging oxygen defects resulting from broken Si–O bonds are mobile, and could in principal migrate through silicate lattices. The soil and dust surfaces would be strongly oxidizing, but the atmosphere itself need not be oxidizing. Mineral and organic analog films exposed to UV will quantify these reaction mechanisms most acutely.

- Dust clouds and frictional generation for glow discharges have been invoked (Mills, 1977), which would argue that the regolith is organic free to whatever depth is scoured by wind.

- Other mechanisms require both UV and atmospheric oxidants. The dangling bonds from radiation damage are highly reactive, and could easily form semi-permanent complexes, such as perchlorates from photolyzed, complexed halide compounds (Zent and McKay, 1994).

- There may be bulk phase superoxidants of unknown origin (e.g. Ponnamperuma et al., 1997; Ballou et al., 1978; Tsapin et al., 2000).

- Banin and Rishpon (1979) and Banin and Margulies (1983) argued that the gas released in the LR experiment was due to intrinsically reactive clays, not oxidants. This hypothesis demands a separate mechanism to explain the lack of organics. Stoker and Bullock (1997) argue that the UV Aux at the martian surface is adequate to explain the lack of organics.

6.2.4 MAOS' scientific objectives

In order to explore the relative importance of these hypothetical mechanisms, MAOS will record, as a function of temperature, the differential DC resistivity of each element of an array of 192 active films relative to an identical sealed reference film. A subset of the films will be exposed to sunlight, a second to dust, a third to the combination of dust and sunlight, and a fourth only to the atmosphere.

MAOS operations are divided into six experiments, each of which involves exposure of eight types of chemical films to the martian environment. The experiments differ only in the environmental conditions and the applied temperature profiles. During any experiment, each of the eight films is deployed in four configurations (sharing a common heater) to separate the effects of air, dust, and ultraviolet illumination. Thus, for any experiment, the returned data consist of 32 resistance values relative to 32 sealed reference resistors, and eight temperature readings. Film resistivity is the dependent variable in the MAOS experiment. It is measured with respect to the independent variables of temperature, UV flux, and dust and soil loading. To control and record the temperature of each of

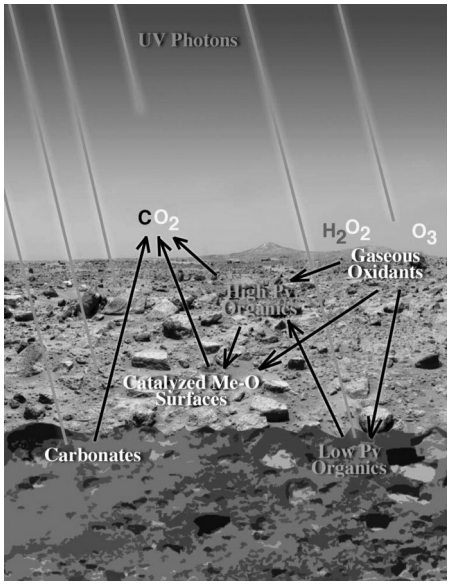

Figure 2. MAOS tests hypotheses of sources and sinks of martian oxidants.

the 4×2 pixels, a resistive ruthenium oxide heater is patterned on the substrate. The high thermal conductivity of the components will ensure uniform temperature across the pixel. Temperature is monitored with a small 12-bit digital serial thermometer on the sapphire surface. The experimental protocol calls for sampling the integrating films over an extended period (up to a martian year, approximately 2 Earth years).

In specific campaigns the temperature of the films can be raised to increase the chemical activity of adsorbed molecules, and thermal acceleration of very slow reactions. One film, comprised of thick Au, is relatively impervious to oxidizing species, but is reversibly sensitive to frost or thin water films. This film allows us to monitor the abundance of condensed H_2O as a function of time. The chemical and physical effects of thin H_2O films on martian surface materials can thus be constrained.

6.3 Hardware Implementation

6.3.1 Operating principles

In MAOS, the DC resistance of a thin solid-state film, deposited by evaporative deposition or solvent casting over a set of noble metal electrodes, is monitored. The electrode gap and spatial configuration are chosen to maximize the sensitivity of the thin film to oxidation. The resistance is an extremely sensitive function of the ambient gases. There are a variety of chemical mechanisms that can alter the conductivity of the films.

At the lower thickness, (10–20 nm) thin metal films consist of closely spaced clusters or islands with very large surface to volume ratios. At higher thickness, the films become continuous, but the surface contribution is still substantial. The measured resistivity of such thin films has a surface and a bulk component. With oxidation, a surface oxide is formed, severely changing carrier transport at the Fermi surface. Oxidation also results in conversion of some metal to non-conducting oxide, thereby reducing the cross-section for metallic conduction and increasing the effective resistivity of the film. In the limit, the film is completely oxidized, becoming an insulator. The extent of reaction is monitored by following the resistivity or impedance of the chemiresistor.

Semiconductor films, as a group, tend to be sensitive to reduction/oxidation reactions, because conductivity changes are related to changes in the carrier (hole) concentrations across their surfaces. In the case of an oxidizing environment such as Mars, a change in carrier concentration occurs when electrophilic gases abstract electrons from the conduction band, and become immobilized on the surface. The equilibrium conductivity varies with the type and abundance of oxidant because of differences in equilibrium adsorptive coverages and differences in the mobility of the sorbed ions (Gardener et al., 1982). The observed resistance is also affected by temperature, surface morphology, and the details of the contact of the thin film to the noble metal of the electrode array. Because of the relative precision and accuracy with which current and voltage can be determined, the chemiresistor is one of the best transducer configuration for high-sensitivity applications. A further advantage of this implementation is that chemiresistors can be actively probed or read during storage, as well as during transit.

6.3.2 Instrumentation

The MAOS experiment places an array of well characterized thin films in intimate contact with the martian atmosphere, exposing it to dust and UV (individually and in combination) while controlling the temperature of the contacting interface. MAOS is shown schematically in Fig. 3. This is not the configuration in which the data shown later are gathered, but a packaging drawing for flight. The reaction sensor arrays are made of a chemically inert substrate, filter sets for isolating the effects of UV and dust on chemical

reactivity, and silicon nitride hermetic seals for maintaining film integrity prior to deployment. MAOS detection sensitivity ranges from a few tenths of a monolayer to several monolayers of reaction product. The 60 × 70 × 20 mm^3 package has the sensor array on the front surface. The sensor array is directly mounted to the electronics support board that contains the measurement circuitry.

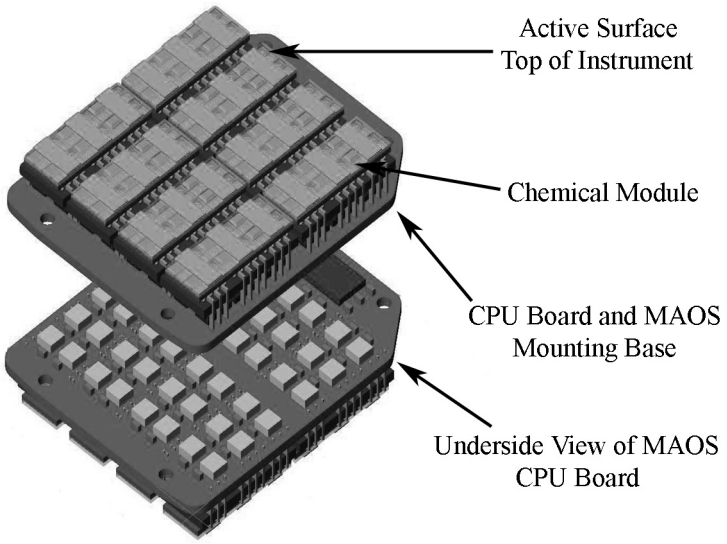

Figure 3. Isometric drawing of full MAOS instrument as packaged for flight with dimensions in mm. Total height from the top of the UV shade filter to the thickest component of the underside of the CPU board is 12:5 mm. The upper overlay shows the eight deferent chemical modules with filters and seals in place. All component boards are populated with active components on both sides. The lower underlay shows the bottom side of the MAOS instrument CPU board with the switch array and PIC controller (A/D not shown). The data in Fig. 4 (see below) were gathered with a prototype of this instrument.

6.3.2.1 Sensing films

MAOS chemiresistor transducers are thin films deposited on highly insulating substrates. The resistivity of each thin film is measured to determine the extent of film oxidation (Fig. 4). The active chemical sensing films are deposited through a contact shadow mask such that the deposited area covers the gold contacting electrodes with a generous margin. For deposition control, no less than 20 substrates are deposited simultaneously. The resistivity of several substrates is monitored during the deposition in order to keep the final thickness within acceptable margins. Eight film types and several backup choices were selected from a candidate list of 25, based upon their chemical specificity, ease of deposition, and chemical stability:

- Silver (15 nm): Extremely reactive to oxidants, particularly O• and O_3.

- Gold (10 nm): Relatively inactive with respect to oxidants, but (reversibly) sensitive to frost or thin water films.

- Iron (25 nm): A transition metal with complex oxidation chemistry. Several species can form, depending on the strength of the oxidant. This film models the response of the iron-rich soil to oxidants.

- Alkane thiol (1 monolayer) on gold (10 nm): Thiol molecules form a self-assembled monolayer on the Au base, strongly modifying the gold conductivity. Oxidation restores the gold conductivity to its original state. This fully aliphatic long chain thiol mimics meteoritic kerogen, the surface of cell walls, and chemical degradation products from biogenic processes.

- D-Cysteine or L-Cysteine (1 monolayer) on Au (10 nm): An amino acid similarly bonded to a thiol group, forming a self-assembled monolayer on the Au base. Cysteine/Au is sensitive to organic group oxidation, and therefore effectively monitors contaminants. C60(120 nm): A carbonaceous material, sensitive to combinations of UV and oxidants.

- Lead sulfide (100 nm): A semiconductor that is very reactive to oxidants and which exhibits a strong response to peroxide and oxide radicals. Semiconducting films show the strongest response to oxidation in our laboratory experiments because the fundamental charge transport mechanism within the film can change with oxidation.

- Copper phthalocyanine (250 nm): A well-characterized, traditional chemical sensor for oxidants, useful over a large dynamic range. (e.g. Wohltjen et al., 1985).

6.3.2.2 Seals

The only sensor deployment system used by MAOS is the electrically triggered rupturing of thin silicon nitride membrane seals, individually addressable on each chemical pixel. The effectiveness and reproducibility of the MAOS reference reactants depends on the extent to which they are delivered in pristine condition to their destination. To accomplish this, the films are encapsulated in a hermetically sealed enclosure. A micromachined top seal cover is bonded to the substrate immediately following sensor film deposition. The seal is strong enough to withstand more than 15 psi gauge differential across the membrane and has been tested to vibration loads of more than 500 G using the Proton launch vibration spectrum. (Manning et al., 1997). On computer command, a seal is deployed by rapidly heating. The sudden temperature increase thermally stresses the film, which decomposes into micron-sized particles, exposing the chemical pixel. These particles are chemically inert, and will have negligible impact on the experiment.

6.3.2.3 Filters

Captured within the silicon frame and suspended above the sensors are porous polymer dust filters, transparent to the ultraviolet and permeable to atmospheric gases. The dust filter will cover two of the four exposed sensors in each chemical pixel. External to the silicon nitride seal is an awning that blocks two of the sensors (one of which has a dust filter) from ultraviolet light.

6.3.3 Performance characteristics

MAOS sensors will respond to a variety of stimuli that will be distinguished using pattern recognition techniques. Figs. 4a through g display representative responses for many of the MAOS films. All of these data were taken at 9:3 mbar in a Mars-like atmosphere. Figs. 4a and b show the response of two self assembled monolayers (deposited on thin gold films) to a pulse of 40 ppm ozone. Both show a reduction in resistance, but the magnitude and rate of change are quite different for the amino acid (cysteine) and the simple hydrocarbon. The response of the CuPc chemiresistor (Fig. 4c) to 20 ppb of O3 shows a change of more than 10 MΩ. The signal is sufficiently strong that 10^9 cm^{-3} ozone molecules can readily be detected. Fig. 4d and e show the response of iron and fullerene thin films to 50 ppb of anhydrous hydrogen peroxide generated by decomposition of the peroxide–urea complex. The response of the iron sensor is moderate and integrating, while the C60 film changes drastically. On Mars, reactions in bulk soil may show different response during nighttime heating of the films, when adsorbed H_2O from the saturated boundary layer may activate the soil oxidants. In Fig. 4f, 200 ppm KO_2 has been mixed with Mauna Kea palagonite. The resistance of a 150 Å Ag sensing film is seen to be in-

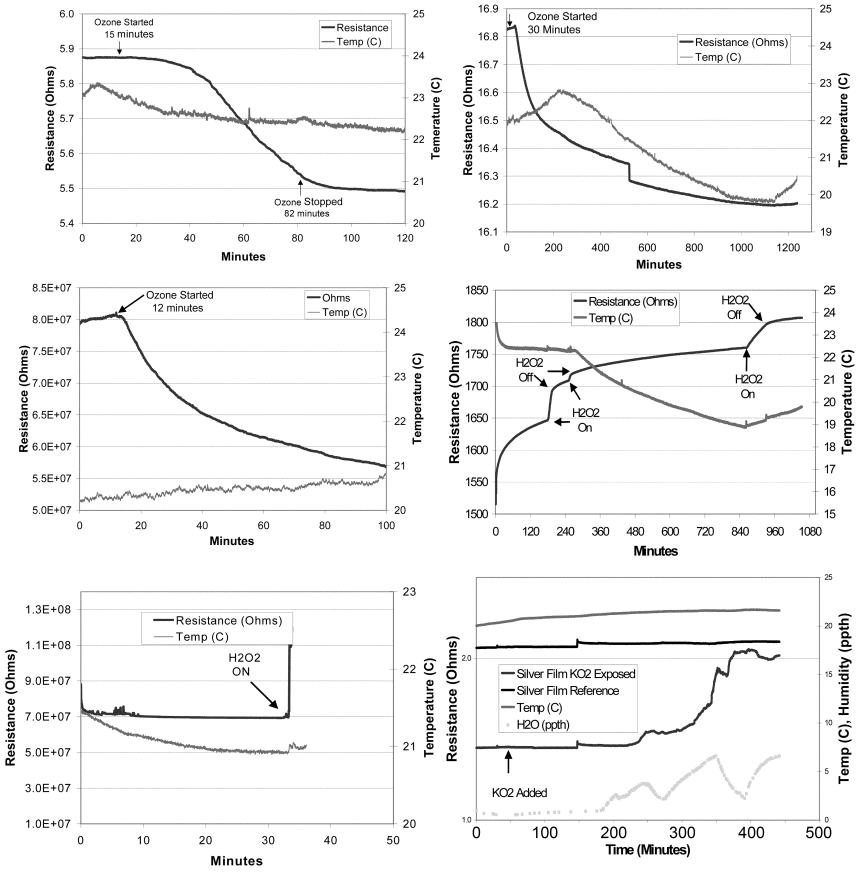

Figure 4. (a). Reaction of 1-heptanethiol self-assembled monolayer bonded to a 40 Å gold film with 40 ppb ozone. (b) Reaction of L-cysteine self-assembled monolayer bonded to a thin 40 Å gold film with 40 ppb ozone. (c) Reaction of 1000 Å thick copper phthalocyanine film with 20 ppb ozone. (d) Reaction of a 100 Å thick iron thin film with 50 ppb anhydrous hydrogen peroxide vapor. (e) Reaction of a 2000 Å C60 fullerene film with 50 ppb anhydrous hydrogen peroxide vapor. (f) Reaction of a 150 Å silver film with 200 ppm KO_2 in palagonite. Ag reference exposed to palagonite without KO_2. Gas phase oxidant exposure was done with a flowing carrier gas at 90 sccm. The gas composition was 0:13%O2, 27% N2; 97:17% CO_2 and the chamber pressure was maintained at 9 mbar to simulate Mars conditions. Thin semi-transparent films of gold, thin films of silver, iron, copper phthalocyanine and fullerene were deposited by vacuum evaporation. Self-assembled monolayers were deposited by immersing a 40 thin gold films on silica substrates in a water/alcohol solution.

sensitive to the presence of the dry, solid KO_2. No reaction takes place until the abundance of H_2O reaches approximately five parts per thousand in the laboratory air.

6.3.4 Analysis

Interpretation of the MAOS data requires careful characterization of the films and the contextual environment, both on Earth and on Mars. Pattern recognition techniques will enhance quantitative analysis. The primary MAOS objective, to measure the relative effect of air, dust, temperature, and ultraviolet light on reaction rates, will not require elaborate pattern recognition techniques. Nor will the second MAOS objective, to determine the oxidation potential and rate of oxidation. These rely on careful laboratory simulation and analysis. Beyond these objectives, however, the power of chemometric arrays lies in their combination with pattern recognition techniques. Chemical microsensors do not provide selective responses to specific molecules. Rather, selectivity is obtained through computational techniques that compare the response of the array to unknown analytes against a reference set of responses previously obtained from known analytes. Multivariate techniques are needed both in the array design phase and during array use in the field.

6.3.5 Calibration

MAOS sensors will be characterized with reference resistors on Mars, and against sophisticated analytical instruments on Earth. The calibration program begins with surface characterization at the time of sensor film deposition. X-ray photoelectron spectroscopy will be used to look at the quality of film and coverage, and to evaluate contamination from the deposition system. These same techniques will be employed on the deposition surfaces, before and after deposition, to verify the cleanliness of the surfaces. Ellipsometry will be employed to measure film thickness, and atomic force microscopy to assess morphology.

Laboratory models will be subject to extensive laboratory calibration of resistance as a function of oxidation, temperature, and illumination. Identical to the flight sensors, these test articles will be opened under Mars conditions. Resistivity will be monitored relative to a reference electrode in the presence of UV light, dust, and various gas phase and interfacial oxidants. Once on Mars, high-performance reference resistors will be used to calibrate the electronics, and to monitor possible degradation of films during storage launch, and cruise. Finally, witness sensors, identical to the flight units, will be maintained on Earth in environmental conditions similar in temperature and pressure to those experienced by the flight films. These units will be used to assess any long-term changes in sensor response.

6.3.6 Interferences

To ameliorate most interference, MAOS employs a four-fold passive filtering approach that separates the effects of dust and sunlight on oxidation. Possible interferences in the resistivity signal are due to environmental processes that foster additional charge separation. Solar illumination of the fully exposed films may produce transient carrier excitation, thereby changing bulk resistance. There may also by photoelectrons, photocurrents or photo voltages affecting measurements. Dust can acquire substantial surface charge in the low humidity environment, and may be responsible for charging film surfaces. Wind, if velocities are high enough, may result in triboelectric charging. To accomplish the required shielding from UV irradiation for one-half of all exposed sensors, an awning will be placed 2 mm above the surface of the sensors. In order to discriminate chemical effects caused by the presence of accumulated dust grains, half of the exposed sensors are covered with a gas-permeable membrane approximately 15 μm thick, with a pore size distribution centered at 1-2 μm in diameter. This filter is placed within the silicon-based hermetic seal assembly and bonded in place. With no strong gas flow, no blockage of the membrane is anticipated from particles down to 0.1 μm in diameter. The fluoropolymer has a UV cutoff near 200 nm, and will therefore transmit all but a minor portion of the UV illumination spectrum. System outgassing is viewed as the only potential source of actual chemical contamination of the system. Outgassing is more likely to be a problem during cruise, when MAOS is safely sealed, and degassing should be nearly complete by EDL.

6.4 Summary

In order to take definitive steps toward identifying the nature and origin of oxidants in the martian surface materials, to guide future astrobiological exploration of Mars, and to assist in design of equipment and procedures for future human exploration, we have developed the MAOS instrument. MAOS is a chemometric, chemiresistor-based sensor array that will measure the thin-film reaction rates of variety of materials as a function of dust abundance, UV Aux, and temperature. Analysis of MAOS data will allow us to quantify the in situ organic oxidation rate, as well as the overall oxidation potential. Utilized with sophisticated pattern recognition software, analysis of the MAOS data should allow us to determine the functional groups responsible for the oxidation potential of the martian dust and air.

References

Ballou, E.V., Wood, P.C., Wydeven, T., Lehwalt, M.E., Mack, R.E., 1978. Chemical interpretation of the Viking 1 life detection experiment. Nature 271, 644–645.

Banin, A., Margulies, L., 1983. Simulation of Viking biology experiments suggests smectites not palagonite as martian soil analogs. Nature 305, 523–526.

Banin, A., Rishpon, J., 1979. Smectite clays in Mars soil: evidence for their presence and role in Viking biology experimental results. J. Mol. Evol. 14, 133–152.

Barth, C.A.A., Stewart, I.F., Bougher, S.W., Hunten, D.M., Bauer, S.J., Nagy, A.F., 1992. Aeronomy of the current martian atmosphere, In: Kieffer, H.H., Jakosky, B.M., Snyder, C.W., Matthews, M.S. (Eds.), Mars, University of Arizona Press, Tucson, pp. 1054–1089.

Benner, S.A., Devine, K.G., Matveeva, L.N., Powell, D.H., 2000. The missing organic molecules on Mars. Proc. Natl. Acad. Sci. USA 97, 2425–2430.

Biemann, K., Lavoie, J.M., 1979. Some final conclusions and supporting experiments related to the search for organic compounds on the surface on Mars. J. Geophys. Res 84, 8383-8390.

Biemann, K., Oro, J., Toulmin III, P., Orgel, L.E., Nier, A.O., Anderson, D.M., Simmonds, P.G., Flory, D., Diaz, A.V., Ruchneck, D.R., Biller, J.E., LaFleur, A.L., 1977. The search for organic substances and inorganic volatile compounds in the surface of Mars. J. Geophys. Res. 82, 4641–4658.

Boston, P.J., Ivanov, M.V., McKay, C.P., 1992. On the possibility of chemosynthetic ecosytems in subsurface habitats on Mars. Icarus 95, 300–308.

Bullock, M.A., Stoker, C.R., McKay, C.P., Zent, A.P., 1994. A coupled soil-atmosphere model of H_2O_2 on Mars. Icarus 107, 142–154.

Carr, M.H., 1996. Water on Mars. Oxford University Press, Oxford.

Flynn, G.J., McKay, D.S., 1990. An assessment of the meteoritic contribution to the martian dust. J. Geophys. Res. 95, 14 497–14 509.

Gardener, J.W., Iskandrarani, M.Z., Bott, B., 1982. Effect of electrode geometry on gas senstivity of lead phthalocyanine films. Sensors Actuators, B Chem. 9, 133–142.

Glavin, D.P., Schubert, M., Botta, O., Kminek, G., Bada, J.L., 2000. Detecting pyrolysis products from bacteria on Mars. Earth Planet. Sci. Lett. 185, 1–5.

Gooding, J.L., 1992. Soil mineralogy and chemistry on Mars: possible clues form salts and clays in SNC meteorites. Icarus 99, 28–41.

Hunten, D.M., 1974. Aeronomy of the lower atmosphere of Mars. Rev. Geophys. Space Phys. 12, 529–535.

Karl, D.M., Bird, D.F., BjVorkman, K., Houlihan, T., Shackelford, R., Tupas, L., 1999. Microorganisms in the accreted ice of Lake Vostok, Antarctica. Science 286, 2144–2147.

Klein, H.P., 1978. The Viking biological experiments on Mars. Icarus 34, 666–674.

Klein, H.P., 1979. The Viking Mission and the search for life on Mars. Rev. Geophys. Space Phys. 17, 1655–1662.

Kong, T.Y., McElroy, M.B., 1977. Photochemistry of the martian atmosphere. Icarus 32, 168–189.

Levin, G.V., Straat, P.A., 1977. Recent results from the Viking labeled release experiment on Mars. J. Geophys. Res. 82, 4663–4668.

Malin, M.C., Edgett, K.S., 2000. Evidence for recent groundwater seepage and surface runoff on Mars. Science 288, 2330–2335.

Manning, C.M., Lamb, J.L., Williams, R., Pool, F., 1997. Mars Oxidant Experiment (MOx) Instrument Fabrication Overview and Films Report.

McDonald, G.D., deVanssay, E., Buckley, J.R., 1998. Oxidation of organic macromolecules by hydrogen peroxide: Implications for stability of biomarkers on Mars. Icarus 132, 170–175.

McKay, C.P., 1997. The search for life on Mars. Origins Life Evol. Biosph. 27, 263–289.

McKay, D.S., Gibson, E.K., Thomas-Keprta, K.L., Vali, H., Romanek, C.S., Clemett, S.J., Chillier, X.D.F., Maechling, C.R., Zare, R.N., 1996. Search for past life on Mars: possible relic biogenic activity in martian meteorite ALH84001. Science 273, 924–930.

Mills, A.A., 1977. Dust cloud and frictional generation of glow discharges on Mars. Nature 268, 614.

Mojzsis, S.J., Arrhenius, G., Mckeegan, K.D., Harrison, T.M., Nutman, A.P., Friend, C.R.L., 1996. Evidence for life on Earthbefore 3,800 million years ago. Nature 384, 55–59.

Nussinov, M.D., Chernyak, Y.B., Ettinger, J.L., 1978. Model of the fine-grained component of martian soil based on Viking lander data. Nature 274, 859–861.

Oro, J., Holzer, G., 1979. The photolytic degradation and oxidation of organic compounds under simulated martian conditions. J. Mol. Evol. 14, 153–160.

Oyama, V.I., Berdahl, B.J., 1977. The Viking gas exchange experiment results from Chryse and Utopia surface samples. J. Geophys. Res. 82, 4669–4676.

Ponnamperuma, C., Sahimoyama, A., Yamada, M., Hobo, T., Pal, R., 1997. Possible surface reactions on Mars.: implications for Viking Biology results. Science 197, 455–457.

Quinn, R.C., Zent, A.P., 1999. Peroxide-modified titanium dioxide: a chemical analog for putative martian soil oxidants. Origins Life Evol. Biosph. 29, 59–72.

Schidlowski, M., 1988. A 3,800-million-year isotropic record of life from carbon in sedimentary rocks. Nature 333, 313–318.

Stevens, T.O., McKinley, J.P., 1995. Lithoautotrophic microbial ecosystems in deep basalt aquifers. Science 270, 450–452.

Stoker, C.R., Bullock, M.A., 1997. Organic degradation under simulated martian conditions. J. Geophys. Res. 102, 10881–10888.

Tsapin, A.I., Goldfield, M.G., Mcdonald, G.D., Nealson, K.H., Moskovitz, B., Solheid, P., Kemner, K.M., Kelly, S.D., Orlandini, K.A., 2000. Iron (VI): hypothetical candidate for the martian oxidant. Icarus 147, 68–78.

Tseng, H.Y., Onstott, T.C., Person, M., 1996. A mesozoic age for the deep subsurface bacteria within the triassic Taylorsville Basin, Virginia. American Geophysical Union Meeting, San Francisco.

Wohltjen, H., Barger, W.R., Snow, A.W., Jarvis, N.L., 1985. A vapor sensitive chemiresistor with planar microelectrodes and a Langmuir-Blodgett organic semiconductor film. IEEE Trans. Electron. Dev. 32 1170–1174.

Wright, I.P., Grady, M.M., Pillinger, C.T., 1989. Organic materials in a martian meteorite. Nature 340, 220–222.

Wyatt, S.P., 1964. Principles of Astronomy. Allyn and Bacon, Boston.

Yen, A.S., Kim, S.S., Hecht, M.H., Frant, M.S., Murray, B., 2000. Evidence that the reactivity of the martian soil is due to superoxide ions. Science 289, 1909–1912.

Zent, A.P., 1998. On the thickness of the oxidized layer of the martian regolith. J. Geophys. Res. 103, 31491–31498.

Zent, A.P., 2002. Strategic reevaluation of the search for martian organics. Proc. SPIE 4495, 108–119.

Zent, A.P., McKay, C.P., 1994. The chemical reactivity of the martian soil and implications for future missions. Icarus 108, 146–457.

Chapter 7

Detection and characterization of oxidizing acids in the Atacama Desert using the Mars Oxidation Instrument

R.C. Quinn, A.P. Zent, F.J. Grunthaner, P. Ehrenfreund, C.L. Taylor, J.R.C. Garry

We have performed field experiments to further develop and validate the Mars Oxidation Instrument (MOI) as well as measurement strategies for the in situ characterization of oxidation mechanisms, kinetics, and carbon cycling on Mars. Using the Atacama Desert as a test site for the current dry conditions on Mars, we characterized the chemical reactivity of surface and near-surface atmosphere in the dry core of the Atacama. MOI is a chemiresistor-based sensor array that measures the reaction rates of chemical films that are sensitive to particular types of oxidants or that mimic chemical characteristics of prebiotic materials. With these sensors, the chemical reactivity of a planetary environment is characterized by monitoring the resistance of the film as a function of time. Our instrumental approach correlates reaction rates with dust abundance, UV flux, humidity, and temperature, allowing discrimination between competing hypotheses of oxidant formation and organic decomposition. The sensor responses in the Atacama are consistent with an oxidative attack by strong acids triggered by dust accumulation, followed by transient wetting due to an increase in relative humidity during the night. We conclude that in the Atacama Desert and on Mars, extremely low pH resulting from acid accumulation, combined with limited water availability and high oxidation potential, will result in oxidizing acid reactions on dust and soil surfaces during low-moisture transient wetting events (i.e. thin films of water). These soil acids are expected to play a significant role in the oxidizing nature of the soils, the formation of mineral surface coatings, and the chemical modification of organics in the surface material.

Chapter 7

7.1 Introduction

Nearly thirty years ago, the Viking Mars mission revealed that the surface materials at the landing sites were chemically but not biologically active under the conditions of the Viking biology experiments. The chemical reactivity observed in these experiments has been attributed to oxidants present in the soil (Klein, 1978, 1979). There are several plausible and competing hypotheses to explain oxidant formation on Mars and the roles of oxidants in both the Viking biology experiments and the decomposition of organics on the planet's surface. It is likely that, in fact, the processes described by a number of these hypotheses are occurring on Mars to some extent. There are undoubtedly many complex, photochemically-driven oxidative processes on Mars involving interrelated atmospheric, aerosol, dust, soil, and organic chemical interactions. To a large extent, the role of these photochemical processes in carbon chemistry on Mars is unknown. We propose that a key to understanding carbon chemistry on Mars and the ultimate fate of organics lies not only in identifying soil oxidants but, perhaps more importantly, in characterizing the dominant reaction mechanisms and kinetics of oxidative processes that are occurring on the planet. These processes may have decomposed or substantially modified any organic material that might have survived from an early biotic period. An understanding of these processes and are needed to determine how and where to look for unaltered organic material.

In this paper we present results from field experiments, using the Mars Oxidation Instrument (MOI), which were performed to further develop and validate instrumental methods and measurement strategies for the in situ characterization of oxidation mechanisms, kinetics, and carbon cycling on Mars. MOI has been selected as part of the European Space Agency ExoMars Pasteur payload, a landed Mars mission currently scheduled for 2011. Using the Atacama Desert as a test site for the current dry conditions on Mars, we have characterized the chemical reactivity of the near-surface atmosphere and surface soils. Our instrumental approach correlates soil and atmospheric reaction rates with dust abundance, UV flux, humidity, and temperature. The technique is designed to discriminate between, and evaluate the key features of competing hypotheses of oxidant formation and organic decomposition.

7.1.1 Oxidant formation on Mars

The primary objective of the Viking mission was to search for life on Mars. Today, more than two decades later, the results of the Viking experiments remain to be fully explained. These experiments revealed properties of the Martian surface material that were surprising in three respects: (1) the release of O_2 gas when soil samples were exposed to water vapor in the Gas Exchange Experiment (GEx) (Oyama and Berdahl, 1977); (2) the ability of the surface material to rapidly decompose aqueous organic material that was intended to culture microbial life in the Labeled Release Experiment (LR) (Levin and

Straat, 1977); and (3) the apparent absence of organics in samples analyzed by gas chromatography and mass spectroscopy (GCMS) (Biemann et al., 1977).

The most widely accepted explanation for the results of the GEx and LR experiments is the presence of oxidants in the Martian soil (Klein, 1978, 1979; Zent and McKay, 1994). Differences in stability of the active agents in the two experiments suggest that the GEx and LR oxidants are different species and that at least three different oxidizing species are needed to explain all of the experimental results (Klein, 1978). The absence of organics in samples tested by GCMS was also surprising; even in the absence of in situ production of organics, meteoritic infall would carry organics to Mars at a rate of 2.4 x 10^8 g yr^{-1}, or about 0.1 nm coverage per year (Flynn, 1996). The combined results of the Viking GEx, LR, and GCMS led to the hypothesis that the GEx and LR oxidants are evidence of the oxidative decomposition of organic compounds (Klein, 1978, 1979) in the martian environment.

There are currently several competing hypotheses to explain oxidant formation on Mars, and the roles of oxidants in both the Viking biology experiments and the decomposition of organics on the planet's surface. The majority of these hypotheses fall into two broad categories:

1) Oxidants are photochemically produced in the atmosphere. Solar ultraviolet radiation photolysis of the atmosphere (and for some species, subsequent recombination) can generate “odd-hydrogen” and "odd-oxygen" (e.g. H, OH, HO_2, H_2O_2, O, O_3). Some of these oxidizing species may adsorb onto the surface and hence may be able to diffuse through the regolith to unknown depths, decomposing organics as they proceed (e.g. Hunten, 1974, 1979; Barth et al., 1992; Bullock et al., 1994). The total oxidant load detected by Viking could have been produced in as little as 2-10 years by this mechanism (Kong and McElroy, 1977). Photochemical oxidant production ceases at sunset, and it has been hypothesized that some oxidants, such as hydrogen peroxide, may deposit on the surface at an accelerated rate just after sunset (Barth et al., 1992). H_2O_2, which has been identified in the martian atmosphere (Encrenaz et al., 2004), is capable of degrading Mars analog organics (McDonald et al., 1998; Benner, 2000). Some transition metal compounds are capable of complexing hydrogen peroxide, forming species that behave much as the Viking biology samples did (Quinn and Zent, 1999).

2) Oxidants are photochemically produced on soil surfaces. UV-surface interactions may lead to decomposition of organics due to superoxide radical formation on the surface of titanium oxides in the soil (Chun et al., 1978), or superoxide radicals may form directly in the soil silicate matrices (Yen et al., 2000), resulting in the generation of the Viking oxidants. The non-bridging oxygen defects resulting from broken Si-O bonds are mobile and can migrate through silicate lattices. The soil and dust surfaces would be strongly oxidizing, but the atmosphere itself need not be oxidizing. In this case, surface diffusion of superoxide radicals across grain boundaries, or regolith mixing combined with extremely

long oxidant lifetimes, are required to explain the detection by Viking of oxidants in soil shielded from UV light (e.g. beneath Notched Rock).

There are several other mechanisms that have been proposed to explain the formation of the Viking oxidants; in almost all cases UV light, atmospheric oxidants, or both are required (for a review see Zent and McKay, 1994). Each proposed mechanism for the degradation of organic compounds on Mars has a potentially different consequence for the ultimate fate of organics on the planet's surface. In case one, hydrogen peroxide would be expected to selectively oxidize organic compounds on Mars, resulting in the formation of species that may not have been detected by the Viking GCMS, such as mellitic acid salts (Benner et al., 2000). In case two, superoxide radicals, which are more strongly oxidizing than hydrogen peroxide, are generally responsible for "deep oxidation" of organics, resulting in more complete oxidation (Haber, 1996) and, possibly, the complete removal of organic material from the surface of Mars (Chun et al., 1978).

7.1.2 Field site description: why the Atacama?

Field experiments using the MOI technologies were performed in the Atacama Desert, which is located along the northern Chilean pacific coast from 30° S to 20° S latitude (Fig. 1). The part of this region between 22° S and 26° S is extremely arid; its total rainfall of only a few millimeters over decades (McKay et al., 2003) makes it one of the driest deserts in the world. These conditions have existed in the region for 10-15 Myrs (Ericksen, 1983), making this area of the desert one of the best analogs on Earth for the present dry conditions on Mars. The driest parts of the region appear to be depleted in, and in some cases essentially devoid of life, including hypolithic algae that are found in other arid deserts on Earth. Studies of the presence of culturable bacteria in the Atacama region from 24° S to 28° S indicate that the quantity and diversity of heterotrophic bacteria increase as a function of local water availability. In the driest regions (24° S) there are sites where no bacteria could be isolated (Navarro-Gonzalez et al., 2003). The driest regions also are extremely depleted of carbon in the soil. Soils collected from these regions were reported to be essentially free of organic matter based on a flash pyrolysis GCMS analysis protocol similar to the Viking GCMS experiment (Navarro-Gonzalez et al., 2003). Analyses of soils from this region using the Mars Organic Anaylzer (MOA), a microfabricated capillary electrophoresis instrument, detected the presence of amino acids at the 10 parts-per-billion level (Skelley et al. 2005). MOA is designed specifically for amine detection, therefore the possible presence of additional organic species in these soils could not be determined. The 10 ppb level of amino acids detected by MOA in the Yungay soils is significantly lower than the levels detected in soils from the southern regions of the desert, which is consistent with the trends observed by Narvarro-Gonzalez et al. (2003). The major mechanisms that have resulted in the lower levels of organics in Atacama soils collected from the Yungay region remain unknown; the same is true for Mars.

The MOI deployment site which is located at 24°4'10" S, 69°51'59" W (Fig. 1) is near an environmental monitoring station established by McKay et al. (2003) in 1994. The station, which is near the abandoned nitrate mine of Yungay, collected temperature, wind direction, relative humidity, and rainfall data over a four-year period. The region has a temperate climate with a mean temperature between 10°C and 30°C. During the four-year collection period, the only significant rain event resulted in only 2.3 mm of precipitation. Although dew occurs more frequently than rain, it is not a significant source of soil moisture. It is near the eastern limit of coast fog incursion as determined by Rech et. al. (2003), and therefore the soil formation may have been strongly influenced by marine deposition. Rech et al. (2003), using $\delta^{34}S$ and $^{87}Sr/^{86}Sr$ values, proposed that the marine influence is restricted to locations where marine fog can penetrate, i.e. where the altitude of the Coastal Cordillera is less than 1000 m. This excludes, in general, locations above 1300 m and more than 90 km inland.

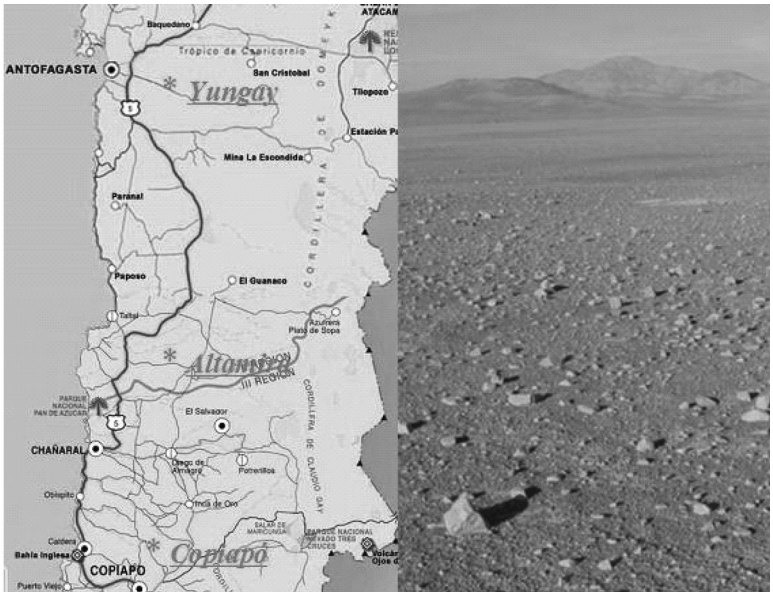

Figure 1. A map of the Chilean pacific coast showing the MOI deployment site which was located near Yungay (24°4'50" S) in the Atacama Desert. The photo shows the local geology at the field site in Yungay.

The Yungay site was chosen for this project because it has already been extensively characterized by Navarro-Gonzalez et al. (2003). Additionally, the cause of the depletion of organics in the region has not yet been established. The existence of organic- and mi-

crobial-depleted soil, is a remarkable Earth analog of the martian surface material. Another striking feature of the Atacama is the large nitrate deposits, probably of atmospheric origin (Bohlke et al., 1997), that have not been biologically decomposed. These salt deposits are also known to contain highly oxidizing species, including iodates (IO_3^-), chromates (CrO_4^{-2}), and the only known naturally occurring exploitable deposits of perchlorate (ClO_4^-) (Ericksen, 1981). There are significant differences between the chemical composition and mineralogy of the Atacama Desert and the surface of Mars. However, the oxidizing compounds found in Atacama soils are likely formed by photochemical reactions at soil/dust/atmosphere interfaces, analogous to the presumed photochemical origin of martian oxidants. Due to differences in water availability, solar flux, and soil composition, specific mechanisms and reaction products may differ, but similar chemical processes may well be occurring both in the Atacama and on Mars. The Atacama photochemical environment makes it an excellent site to test methodologies for the in situ characterization of oxidation mechanisms, kinetics, and carbon cycling.

7.2. Experimental

7.2.1 Mars Oxidant Instrument description

We have validated two instrumental approaches, the Mars Atmospheric Oxidant Sensor (MAOS) and the Mars Oxidant Instrument (MOI) (Zent et al., 1998; Zent et al., 2003). For simplicity, we will refer to our combined approach as MOI. The MAOS and MOI concepts are derived from the Mars Oxidant Experiment (Grunthaner et al., 1995; McKay et al., 1998), which was developed and delivered as part of the ill-fated Russian Mars ’96 mission. MOI uses the same measurement approach as MAOS, but is designed specifically for measurement of soil oxidants and has capability to add water to the soil/sensor system. MAOS, on the other hand, was designed to characterize the reactivity of the martian atmosphere and dust. Moreover, by controlling sensor exposure to dust and ultraviolet light, MAOS discriminates among mechanisms of oxidant production and organic decomposition. Both of these instruments are chemiresistor-based sensor arrays that measure the oxidation rates of chemical films that are sensitive to particular types of oxidants or that mimic some of the chemical characteristics of prebiotic and biotic materials. With these sensors, the chemical reactivity of the martian environment is characterized by monitoring the resistance of the film as a function of time.

The fundamental unit of the MOI configuration tested, shown in Fig. 2, is an array of chemical sensors. The sensors are custom, micromachined interdigitated electrodes fabricated on an alumina substrate (AG Communication Systems Corporation, Phoenix AZ). Each array contains four gold interdigitated electrodes each with 20 finger pairs and 25 μm finger spacing. The sensors were deployed in the field to discriminate the effects of UV and dust from soil reactions using bulk teflon test fixtures (Fig. 3). One set of five

sensors (referred to as UV/dust sensors) was exposed to dust, direct UV, and the atmosphere by mounting the sensors face-up six inches above the soil, pointing toward the sky. A second set of four sensors (referred to as atmosphere sensors) was mounted face-down six inches above the soil, with the sensors recessed in the teflon test fixture to shield the sensors from direct UV exposure and minimize dust deposition. The third set of five sensors (referred to as soil sensors) was de ployed face-down in the soil, blocking UV

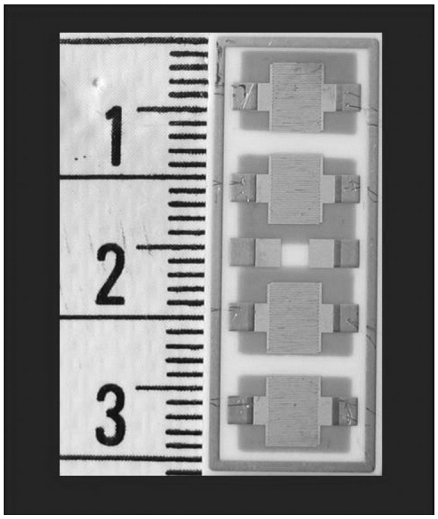

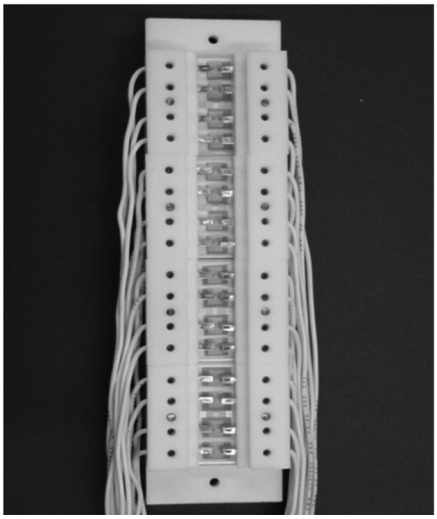

2 3

Figures 2 and 3. Four MOI sensors coated with 50 angstrom gold films (the grey areas). The sensors are fabricated on an alumina substrate. The sensor electrodes are interdigitated with 20 finger pairs and 25um finger spacing. The scale is in centimeters (2). MOI sensors in Teflon test fixtures. The sensors were deployed in the field to discriminate between the effects of UV, atmosphere, dust and soil. The UV/dust sensors were mounted pointing face up six inches above the soil. The atmosphere sensors were mounted face down six inches above the soil. The soil sensors were mounted face down in the soil (3).

radiation, dust accumulation, and direct atmospheric exposure. By monitoring differences in film reaction among the electrodes, this deployment mode measures the relative contribution of soil chemistry, UV photochemistry, and dust/aerosol chemistry to environmental oxidation processes.

7.2.2 MOI chemical sensing films

The choice of reactant films used to coat the electrodes is critical to the success and interpretability of the MOI experiment. The criteria for selection of chemical films for a Mars flight unit are more fully described by Grunthaner et al. (1995) and Zent et al. (2003). Contextual information on the chemistry of the Yungay region collected during earlier field campaigns allowed us to restrict our film set to thin (40 to 50 um) gold films deposited by thermal evaporation and monolayers of organic molecules self-assembled on these gold films. The surface layer at the deployment site is characterized by small quartz and plagioclase grains, derived from the surrounding terrain, which typically rest atop a gypsum-rich surface crust, approximately 5-6 mm thick. Measurements of soil pH and redox potential of this crust indicate that the surface material in the Yungay region is uniquely characterized by the dry-acid deposition and accumulation (Quinn et al., 2005). Since our goal was to validate the MOI measurement approach and demonstrate its ability to discriminate between the effects of UV, dust, soil, atmosphere, water, and temperature on chemical reactivity, we chose to deploy bare gold films and gold films chemically modified with self-assembled monolayers (SAMs) of organic chemicals in order to measure acid-oxidation processes at the Yungay field site. Organics with thiol functionality and disulfides can form a SAM on gold surfaces, modifying the conductivity of the gold film. Removal of the SAM through oxidation processes restores the gold conductivity to its original state. Four thiols and a disulfide with different functional groups to mimic some chemical characteristics of prebiotic and biotic materials were chosen for the MOI experiment. The organics used were: hexadecanethiol (a fully aliphatic long-chain hydrocarbon), L-cysteine, D-cysteine (the use separate of L- and D- amino acid films aids in discriminating between biotic and abiotic reaction mechanisms), naphthalenethiol (a polycyclic aromatic), and 4-aminophenyl disulfide. All organics used in the experiment were the highest purity available from Aldrich Chemical and used with out further purification. The SAMs were formed on the gold in ethanol solutions using mmolar concentrations of the organic compound.

7.2.3 Contextual environmental information at the field site

The MOI sensors were deployed in the field from February 23 to February 28, 2004. During this period, temperature and atmospheric humidity measurements were taken at the deployment site using an Onset Hobo® (Pro Series) relative humidity and temperature logger. Ogawa Passive Samplers were used to determine time-weighted averages of atmospheric NOx, SO_2, and O_3. The Ogawa samplers are diffusion sensors that are extensively used in environmental monitoring and use coated membranes to trap and stabilize the analyte of interest. The samplers were mounted two meters above the ground at the field site using Ogawa holders and housings. Post-exposure handling and transport con-

tainers designed for Ogawa sensors were used, and samples were analyzed by ion chromatography within days of completion of the field collection by Inter-Mountain Laboratories Air Science (Sheridan, WY). Ultraviolet radiation levels at the field site were obtained with an Ocean Optics USB2000 VIS/UV spectrometer optimized for solar flux measurements. These contextual measurements enable establishment of reaction-specific mechanisms for the MOI sensors through laboratory simulations.

7.2.4 Atacama laboratory simulations and laboratory analysis techniques

Interpretation and validation of MOI data requires careful characterization of film response and the contextual environment using laboratory simulations and analyses. Characterization of temperature and humidity coefficients for the MOI sensors were performed at the Leiden Institute of Chemistry and the European Space Research and Technology Centre (ESTEC) Mars simulation chamber, a European Space Agency (ESA) ground based facility (http://www.astrobiology.nl). Post-field laboratory simulations of MOI sensor responses were performed using a Thunder Scientific 2500 humidity chamber located at NASA Ames Research Center and MOI sensors that were identical to the field units. The humidity chamber was programmed to simulate Atacama-like diurinal fluctuations in temperature and humidity. Temperature, humidity, and the resistance of the sensors were measured at one-minute intervals throughout the duration of the simulations. A deuterium lamp was used in some of the simulations to investigate the effect of UV light on sensor response. Three types of experiments were carried out: no UV radiation, unfiltered UV radiation, and filtered UV radiation using a 350nm bandpass filter. Atacama soil and dust analogs used in the simulations were prepared from sodium chloride (Baker Analyzed® Reagent), calcium sulfate (Aldrich, reagent grade), potassium nitrate (Aldrich, 99.99%), and sodium bisulfate (LabPro, ACS grade). Information on the chemical modification of the gold surfaces during post-field experiment simulations was obtained using gold films (deposited on glass with a W and Ti underlayer) and examined with a Hewlett Packard 5950A x-ray photoelectron spectrometer (XPS). These gold substrates were exposed to the simulated Atacama conditions and dust/soil analogs in the same manner as the MOI sensors. After completing the simulation, the surface of the substrate was rinsed with ultra-pure water to remove salts from the surface and then air dried before performing XPS analysis.

7.3. Results and Discussion

7.3.1 MOI sensor responses in the Atacama Desert

Representative responses of the bare gold films for each of the three deployment configurations, overlaid with atmospheric temperature and relative humidity data, are shown in Fig. 4. Sensors were deployed for approximately four days. Over this four-day period, atmospheric temperatures ranged from nighttime lows of ~10ºC to daytime highs that reached ~34ºC. Relative humidity (RH) typically reached a low below 10% around 15:00 hours local time. Each day shortly after sunset, a rapid increase in RH occurred, rising several decades over a period of a few hours. At ~20:30 local time on day two, a very rapid increase of RH was observed, followed by a quick drop at ~22:00, followed by a rapid increase to ~90% RH, which is the upper limit of the relative humidity sensor. Although we were not at the sensor deployment site at the time of this event, based on previous experience, we interpret this signal as being the result of ocean-generated fog.

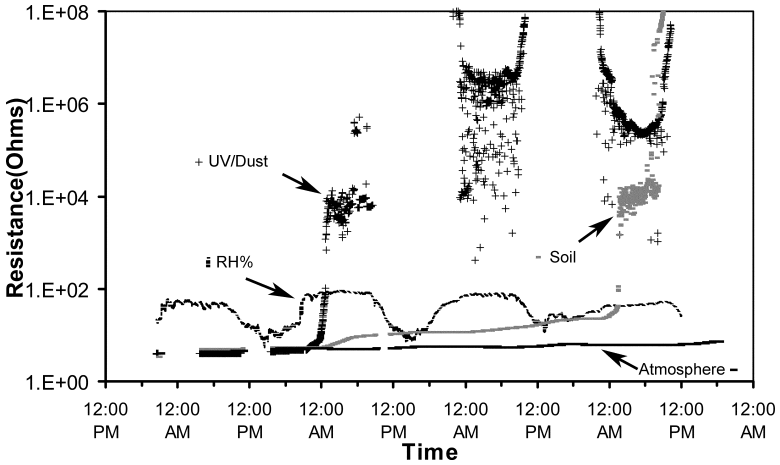

Figure 4. Representative responses for each of the three deployment configurations, overlaid with atmospheric temperature and relative humidity data. Distinct reaction patterns are observed for each of three different Au-film sensor deployment modes. Reactivity was highest and reaction kinetics were fastest for sensors exposed to atmospheric dust. For the UV/Dust sensors, reaction proceeded after a twenty four hour dust accumulation period followed by an increase in atmospheric humidity at night. The atmosphere and soil sensors exhibited a delay in onset of reaction or no response at all due to limited dust exposure (atmosphere sensors) or buffering of humidity by the soil (soil sensors).

The Yungay site is located ~50 km from the pacific coast and a rapid increase to high RH levels at night is not uncommon. During the night, strong winds from the west can carry moist air to the east, while during the day these winds are heated and desiccated as they descend the costal mountains, resulting in low daytime humidity levels (McKay et al., 2003). At other times, during the night, strong winds from the west can carry moist air to the east, while during the day the wind direction reverses due to dry downslope winds from the Andes in the east.

Despite two data drops due to memory-buffer overwrite during the first 24 hours, it can be clearly seen from Fig. 4, that during the first 24 hours of sensor deployment there was no significant change in sensor resistance levels. This is revealing in that the sensors are unaffected by short-term (one day) independent exposure to UV, high relative humidity, ambient atmosphere, or soil. The first chemical sensor response was observed in all five UV/dust sensors and occurred at night on the second day of deploy- immediately following the rapid increase in atmospheric relative humidity. None of the soil or atmospheric sensors reacted at this time. The UV/dust response was characterized by an increase in resistance, on average three orders of magnitude above the starting baseline for the sensors, which ranged from 1.7 to 3.9 ohms, over an ~4-hour period. The sensors remained in this resistance range, with a significantly higher noise level compared to the pre-reaction baseline, until a daytime drop in humidity occurred; then the resistance of the sensors increased above 100 MOhms, which was the upper limit of the instrument measuring range. On the third night of the experiment, the resistance of the UV sensors returned into the instrument measuring range with resistance values ~6 orders of magnitude above the pre-reaction baseline levels. This pattern of exceeding the high end of the resistance range during the day and returning into range at night, was repeated on day four. We attribute this response to changes in soil/dust conductivity at the sensor interface. Prior to chemical attack of the sensors, conduction occurs through the low resistance gold film, while after chemical attack, a continuous gold conduction path is no longer available, and the conduction path must include the high-resistance dust coating on the sensors. At night, higher moisture levels results in a decrease in sensor resistance as the water abundance at the dust/sensor interface increases.

The responses of the gold film atmospheric sensors and soil sensors were characterized by either a delay in the onset of the observed chemical response or by no response at all. Of the four atmospheric sensors, three did not react and for one, the onset of reaction was delayed until day three. One of the five soil sensors did not react, one reacted on day three, and the onset of reaction was delayed until day four for the other three. Organic self-assembled monolayers are sometimes used in electrochemical studies to passivate electrode surfaces. In the MOI field experiments, sensors with SAM covered gold films showed the same reaction patterns and kinetics as the uncoated gold films with the UV/dust sensors reacting preferentially over the atmospheric and soil sensors. In these field experiments, presence of an organic SAM on the electrode did not provide a barrier to the chemical reaction of the gold surface.

7.3.2 Interpretation of field data

The sensor responses shown in Fig. 4 are consistent with an oxidative attack of the gold films (and SAMs) by strong acids. In our deployment mode, oxidation occurred after a 24-hour period which allowed dust to accumulate on the UV/dust sensors during the day. The chemical response was then triggered during the night by high nighttime relative humidity, which caused the dust-deposited acids to solvate. The surface of the Atacama at the Yungay site is characterized by quartz and plagioclase grains mixed with high levels of salts (halide, sulfates, and nitrates). When the geochemical environment of the Yungay region is considered, oxidative acid reactions are the most plausible explanation for the observed sensor responses.

The MOI results indicate that the acid is carried in the atmosphere on the surface of dust grains and aerosols. In the Yungay environment, atmospheric sulfur dioxide and nitrogen oxides are oxidized through gas phase reactions into sulfuric acid and nitric acid, which then adsorb onto aerosols and deposit as dry particles (Quinn et al., 2005). Dry sulfuric acid formation can occur by reaction of SO_2 with OH radicals photochemically produced in the atmosphere:

$$O_3 + h\nu \rightarrow O(^1D) + O_2$$

$$O(^1D) + H_2O \rightarrow 2OH\cdot$$

$$SO_2 + OH\cdot + M \rightarrow HOSO_2 + M$$

$$HOSO_2 + O_2 \rightarrow HO_2 + SO_3$$

$$SO_3 + H_2O \rightarrow H_2SO_4$$

Nitric acid formation also occurs through a similar reaction with OH radicals:

$$OH\cdot + NO_2 + M \rightarrow HNO_3 + M$$

NO_2 may also react after sunset with O_3 (photochemically produced during daylight hours) to form nitric acid:

$$NO_2 + O_3 \rightarrow NO_3 + O_2$$

$$NO_3 + NO_2 \rightarrow N_2O_5$$

$$N_2O_5 + H_2O \rightarrow 2HNO_3$$

Although this is typically a minor formation mechanism, the presence of ground level ozone at the deployment site and the observed onset of the MOI sensor response after sundown indicates that this mechanism may play a role in oxidation processes in the Yungay environment. The time-weighted average levels of O_3, NO_x, and SO_2 present at the MOI site during sensor deployment are shown in Table 1.

Table 1
Time weighted Atmospheric Concentrations

Collection Period (hours)	NO_x ppb	SO_2 ppb	O_3 ppb
212.5	5.5 ± 0.5	3.3 ± .7	27.8 ± 0.4

The onset of gold oxidation during periods of high relative humidity indicate that the reaction is water mediated. For the soil and atmospheric sensors, reaction was delayed or absent due to the limited availability of water or acid. In the case of the atmospheric sensors, dust accumulation was limited by placing the sensors face down; however, filters were not used, so dust accumulation due to sticking or electrostatics was not prevented. This can explain why only one of the four atmospheric sensors reacted. The soil sensors were not in direct contact with the atmosphere, and availability of atmospheric water was buffered by the soil. This can explain the delay in the onset of reaction for these sensors. The at-night effective relative humidity in the soil was not at the ~90% atmospheric levels, but at some lower level due to diffusive and absorptive barriers. Although we measured atmospheric relative humidity and not soil humidity, the environmental measurements made by McKay et al. (2003) indicate that the relative humidity in the surface soil does typically not rise much above a baseline value of ~20% even when dew is present although levels as high as 40% were observed in some cases. For the observed MOI reactions to proceed at the soil/gold sensor interface, the adsorptive coverage of water must be sufficient to solvate the soil acids. The soil sensors were placed face down at the soil/atmosphere interface and the acid reactions would be expected to proceed during periods when multilayer coverage of adsorbed water occurs, which will result in dissolution of the soil acids.

Gold is not oxidized by concentrated sulfuric acid; it is, however, oxidized by concentrated nitric acid. The oxidized gold can then be stabilized by reaction with chloride ions. The increased resistance in the MOI sensors can be explained by the following reactions:

$$Au(s) + 3NO_3^- (aq) + 6H^+ \leftrightarrow Au^{3+}(aq) + 3NO_2(g) + 3H_2O(l)$$

$$Au^{3+}(aq) + 4Cl^-(aq) \leftrightarrow AuCl_4^-(aq)$$

Although the levels of acids in the dust and soil may be low, the effective pH of the soil is expected be highly acidic during periods of high relative humidity. This low pH is the result of the dissolution of acids during the formation of thin films of water on soil and dust surfaces resulting in a high ion concentrations at the soil/sensor interface. On silicate surfaces, although the thickness of a water film depends on hydroxylation state and the presences of surface ions, films greater than 20Å thick can form at relative humidity above 90% (Gee et al., 1990). At thicknesses above 20Å a multilayer water film is present which is sufficient to mobilize ions. As can be seen in the equations above, for gold oxidation to occur, solvation of nitrate ions in an acid system is required and this results in the oxidation of Au° to Au^{3+} by the nitrate. A second requirement is the availability of chloride ions which then stabilizes the oxidized gold as a tetrachloro-complex. Therefore, the observed sensor response which results from gold oxidation at the MOI deployment site does not require or preclude the formation of nitric and hydrochloric acid in the Yungay environment. The requirement for gold oxidation to occur is the presence of one or more strong acids and the availability of nitrate and chloride ions, which are abundant in the Yungay environment as soluble salts.

7.3.3 Laboratory simulations of MOI sensor responses

The hypothesis that the MOI sensor responses in the field were due to the oxidative attack triggered by the solvation of dry acid was validated through a series of laboratory simulations. In Fig. 5, the temperature and humidity profile used in the simulations is overlaid with the field data. Sodium bisulfate was used as a dry-acid stimulant and mixed in small quantities with a dust/soil analog made of equal parts sodium sulfate, sodium chloride, and potassium nitrate by weight. Chlorides, sulfates, and nitrates are all known to be components of aerosols, dusts, and soils in the Yungay region (Ericksen, 1981). Data on the relative ratios of these components in the dust present at the field site was not available; therefore an equal-part mixture was made to prevent any one component from becoming limiting. The sensors used in the simulations were identical to the field sensors.

The responses of reference sensors to the environmental simulation are shown in Figure 6. One set of four references was bare-thin films of gold exposed in the environmental chamber. These references exhibit minor reversible physical responses due to humidity and temperature changes; no chemical response was observed. The second set of reference sensors was covered with a thin layer (1-2 mm) of the un-acidified dust analog; the pH of this analog measured in a ratio of 1:2 (analog-to-water) by weight was 7. As was the case with the bare-gold sensors, the shift from low resistance to high resistance was not observed. A slow drift in resistance in these sensors was observed indicating some level of modification, however, this response is distinctly different from the field responses. The lack of response during simulations using UV radiation indicates that quantities of acid

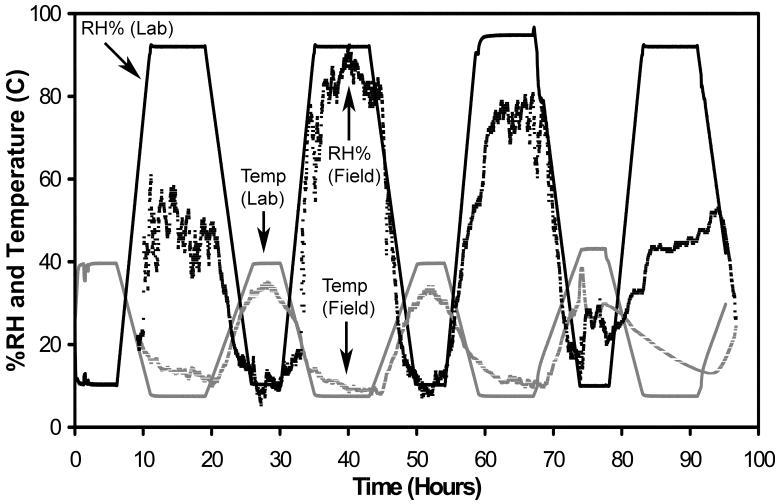

Figure 5. The temperature and humidity profile used in the simulations overlaid with the field data.

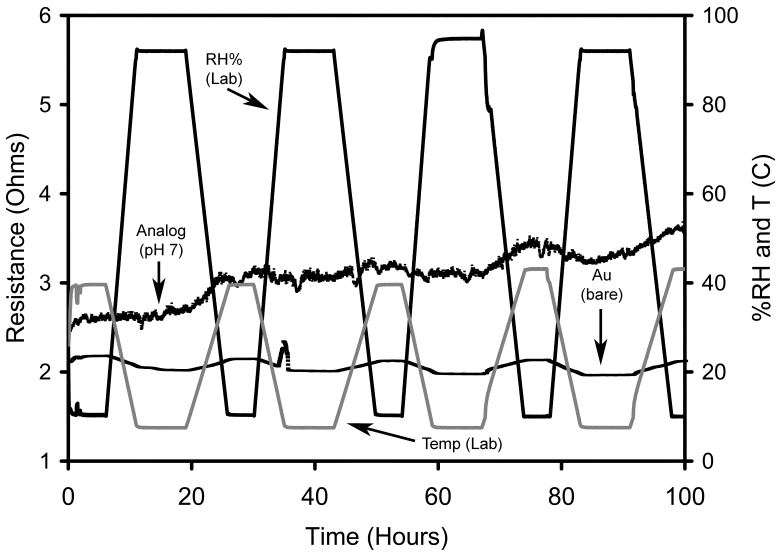

Figure 6. The response of reference sensors to the environmental simulation. The references used were bare-thin films of gold and thin films of gold covered with a thin layer of un-acidified dust/soil analog. The references exhibit minor reversible physical responses due to humidity and temperature changes.

sufficient to trigger an acid attack of the gold are not photochemically generated on the sensor surface under the simulation conditions.

The responses of MOI sensors exposed to sodium bisulfate-doped analog are shown in Fig. 7. This analog was doped with 25 mg of $NaHSO_4$ per gram of analog and the measured pH of the analog in solution was 2 (1:2 soil-to-water by weight). A chemical response was observed in these sensors during the second or third humidity cycle, mimicking the response seen in the field soil sensors. This response can be explained by com-

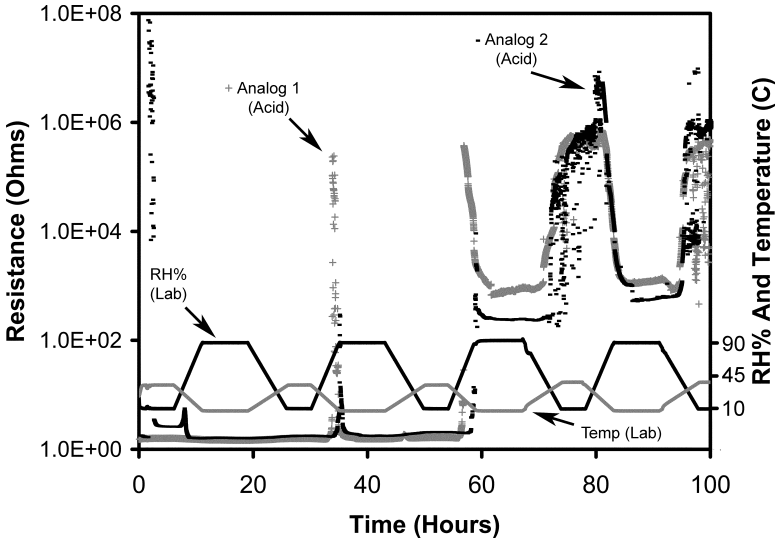

Figure 7. The response of MOI sensors exposed to sodium bisulfate doped desert analog (25 mg of $NaHSO_4$ per gram of analog). The measured pH of the analog in solution was 2 (1:2 soil-to-analog by wt.). The chemical response mimicked the response seen in the field soil sensors.

paring the relative amounts of dust coverage on the UV/dust sensors in the field with the analog coverage on the sensors in the simulation. In the field, a very fine layer of dust, with a thickness well under 1 mm, accumulated on the UV/dust sensor surfaces. In the simulation, the analog was applied to the sensor surface by hand, resulting in a layer ~1-2 mm thick. This likely resulted in a buffering effect by the analog (similar to that seen in the field soil samples) due to hydration of the sodium sulfate component, and resulted in a delay of the onset of the acid attack of the gold.

After the acid attack occurred, the sensor response in both the simulation and in the field was essentially the same (Fig. 8). The lower nighttime sensor resistance in the laboratory simulation is explained by differences in conductivity at the sensor interface in the

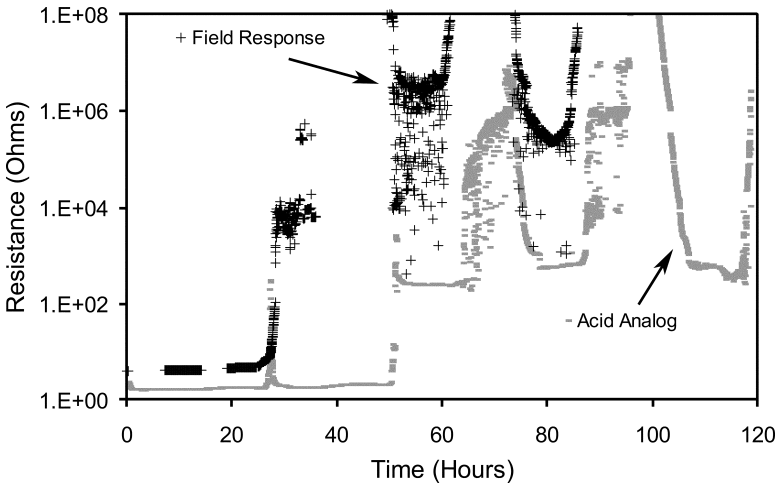

Figure 8. Comparison of the field responses and the laboratory simulation (acid analog). The laboratory data time is offset to synchronize the field and laboratory data. For both data sets, 0 hours is equivalent to the start time of the field experiment (20:22 hours). The field experiment ended at ~100 hours. The lower nighttime sensor resistance in the laboratory simulation is explained by differences in conductivity between the analog and the Atacama dust/soil.

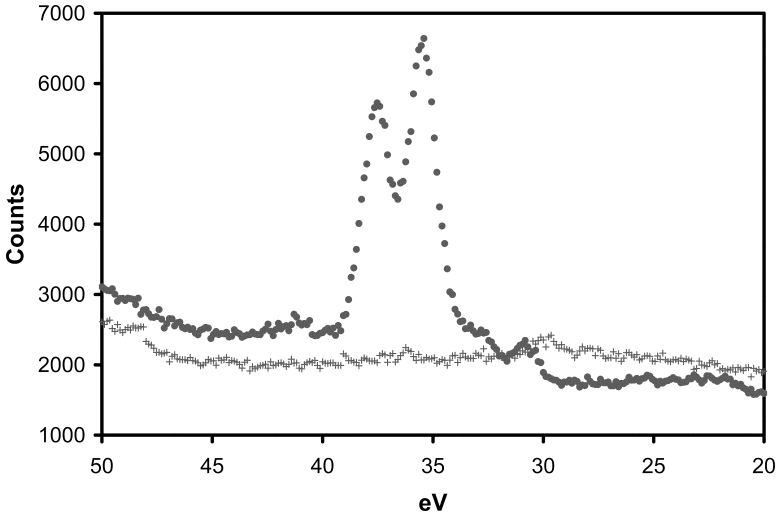

Figure 9. X-ray photoelectron spectra of gold films which under went the environmental simulation without exposure to the soil/dust analog and gold films that were exposed to acidified dust soil analog during the simulation. Exposure to the acidified analog resulted in removal of gold (+) from the surface of the electrode exposing the tungsten underlayer (dotted line). The figure shows the appearance of the tungsten underlayer in the acid exposed films with the W 4f7/2 peak at 35.5 eV, the W 4f5/2 at 37.6 eV, and the W 5p 3/2 at 40.9 eV.

simulation and in the field during periods of high relative humidity. The sensor conduction path changes from the gold film to the surface material (analog or dust/soil) as a result of the acid attack on the gold film. The analog used in the simulations is made entirely of soluble salts which results in a lower resistance when humidified than the Atacama surface material which is a mixture of salts and silicate materials. Comparison of the planer gold surfaces exposed to the neutral pH analog with those exposed to acidified analog, revealed that in the acid case gold was removed from the surface, exposing the tungsten underlayer on the electrode (Fig. 9).

7.3.4 Atacama surface environments and sensor response

Direct pH measurements have revealed that surface samples collected in the Yungay region of the Atacama contain soluble acids that are rapidly neutralized by soil components after dissolution (Quinn et al., 2005). During low moisture wetting events, the estimated Yungay soil pH was approximately 2. No evidence of these acid species was seen in surface samples collected from the wetter desert regions or from the subsurface in Yungay. In the wetter regions, either the conditions for acid formation are absent or the acid is neutralized as it precipitates to the surface. The absence of this acid component in the sub-surface samples in Yungay is consistent with a water transport mechanism for soil horizon formation. That is, the surface acids are neutralized during the episodic rain events that transport soluble salt and other materials forming soil horizons. As is the case with the MOI sensor response presented here, the pH response of surface soils collected at the Yungay site is consistent with the dry deposition and accumulation of acids on soil surfaces in Yungay. The MOI UV/dust sensor responses in the Atacama indicate that the soil acids are carried by the atmospheric dust and accumulate on surfaces. This acid accumulation continues until a sufficient amount of water is added to the system to cause dissolution. Once solvated, the acids act as strong oxidants and will react with soil components, including any organic material that might be present. These acids may also undergo neutralization through soil cation exchange processes. The fog event that occurred during the second night of the MOI deployment was a key to triggering the reaction of the soil acids with the gold films. Based on measurements of moisture levels in the Yungay region made by McKay et al. (2003) from 1994 through 1998, acid accumulation periods are expected to be variable. The McKay measurements indicate that moisture levels in the Yungay region are highly variable and although rain events are rare, dew is not uncommon. However, dew events showed significant year-to-year variability, with frequent occurrences in the last quarter of 1994 and the first part of 1995, but relatively infrequent occurrences during 1996. McKay et al. concluded that although dew and fog is not uncommon in the Yungay region, it is not a significant source of soil moisture. This conclusion is constituent with the observed MOI responses. The UV/dust sensors exhibited a greater level of reactivity compared to the soil sensors due to differences in water availability.

7.3.5 Acids in Mars surface materials

There is ample evidence that salts and acidic surface materials exist on Mars. Observations returned from the Mars Exploration Rover Opportunity have revealed the presence of sulfur-rich sedimentary rocks. Squyers et al. (2004) have concluded the that the sediments observed with the Opportunity payload at the Meridiani Planum site formed in shallow surface water followed by evaporation and desiccation. Sulfur salts appear to be abundant in the sedimentary outcrops and jarosite has been identified using Opportunity's Mössbauer spectrometer (Klingelhöfer et al. 2004). The detection of jarosite is significant since it forms in strongly acidic-sulfate rich aqueous environments.

Results from the Viking Mars missions also indicate the presence of acidic soil components. Viking did not measure pH directly, but examination of CO_2 partitioning between the headspace and aqueous phases in the biology experiments indicates the presence of soil acids. The CO_2 responses observed in the biology experiments include: the release of CO_2 from the soil prior to the wet mode in the GEx, an initial small CO_2 peak in the Pyrolytic Release Experiment (PR) (Horowitz et al., 1977), and the release of $^{14}CO_2$ from the heat-sterilized VL 1 cycle 2 sample (injection 1). These CO_2 responses have been attributed to an acidic soil component and the magnitude of CO_2 uptake by the aqueous solutions after the initial CO_2 release during the GEx and LR indicates that the acid component is neutralized upon wetting. Simulations of the GEx have indicated that after neutralization of the acidic components, the pH of the aqueous soil mixtures tested by Viking shifted overtime to a slightly basic pH (Quinn and Orenberg, 1993).

Comparisons of Viking soil pH responses, based on the LR experimental results, with direct measurements of Yungay surface soil pH measurements indicate both samples contain acid components that behave much in the same way when wetted (Quinn et al. 2005). These results, combined with data returned from MER indicate that the soils and dust examined in Yungay region are good analogs of sulfur-rich acidic Mars surface materials and that MOI is capable of characterizing acid activity and related oxidizing processes.

7.4 Conclusions

We have successfully performed the first field validation of the MOI measurement approach. By using multiple sensor deployment geometries we have characterized the relative importance of UV, atmosphere, soil, dust, temperature, and water abundance, to environmental chemical reactivity in the Atacama Desert. Our MOI measurements indicate that water abundance plays the key role in controlling reaction kinetics in the dry core of the desert. The sensor responses are consistent with an oxidative attack by strong acids triggered by dust accumulation, followed by transient wetting due to an increase in relative humidity during the night. The onset of reaction of the sensors with soil was de-

layed or inhibited by a lower level of water availability compared to the UV/dust sensors due to adsorptive buffering by the soil. During daylight hours, which are characterized by low atmospheric humidity levels, dry acids are produced photochemically in the atmosphere from SO_2 and NO_x precursors. These dry acids then adsorb onto dust and soil surfaces; oxidative acid soil reactions are then triggered at night during periods of high relative humidity. Soil pH is of interest in astrobiology because it plays a direct role in a number of processes that affect both soil organic chemistry and soil biological load. Soil parameters that are typically pH-dependant include the solubility of soil components (which determines the availability of plant nutrients and toxins); soil microorganism population diversity; and activity; and organic chemical degradation mechanisms. The MOI field results reveal that dust in the Yungay region is highly oxidizing. Additionally, coating the sensors with organics provided no passivating barrier against oxidation of the underlying gold films.

Evidence from the Viking biology experiments and the identification of jarosite at the MER field site on Mars indicate that the soils at these sites contain acid components. It has been shown that the pH response of the Viking and Atacama soils upon wetting are similar due to the presence of soil acids (Quinn et al., 2005). We conclude that in the Atacama Desert and on Mars, extremely low pH resulting from acid accumulation, combined with limited water availability and high oxidation potential, will result in acid-mediated reactions at the soil surface during low-moisture transient wetting events (i.e. thin films of water). This has important implications for the biopotential of both Mars and Atacama soils, in that the addition of small quantities of water greatly increase the oxidative activity of the soils. Oxidizing acid reactions on Mars and in the Atacama, combined with other possible photochemical oxidation mechanisms including Fenton and nitrate reactions, will play a significant role in the oxidizing nature of the soils, the formation of mineral surface coatings, and the chemical modification of organics in the surface material.

If deployed on Mars, the MOI responses seen in the Atacama tests might be similar to what would be observed on Mars. However, a MOI fight instrument would require a more comprehensive film set to allow a broad survey the chemical reactivity of the Mars surface environment. Using multiple film types, MOI can detect and characterize a broad range of reactants and reaction mechanisms. MOI analysis of the chemical reactivity of the martian surface environment coupled with a highly sensitive organic detection instrument such as MOA (Skelley et al. 2005), will provide detailed characterization of carbon chemistry on Mars.

Acknowledgements

This work was supported by the NASA Mars Fundamental Research program, the NASA Astrobiology Science and Technology for Exploring Planets program, and NASA Ames/SETI Institute cooperative agreement NCC2-1408. Pascale Ehrenfreund acknowledges grant NWO VI 016.023.003.

References

Barth, C.A.A., Stewart, I.F., Bougher, S.W., Hunten, D.M., Bauer, S.J., Nagy, A.F., 1992. Aeronomy of the current martian atmosphere. In: Kieffer, H.H., Jakosky, B.M., Snyder, C.W., Matthews, M.S. (Eds.), Mars, University of Arizona Press, Tucson, 1054-1089.

Benner, S.A., Devine, K.G., Matveeva, L.N., Powell, D.H., 2000. The missing organic molecules on Mars. Proc. Natl. Acad. Sci., USA 97, 2425-2430.

Biemann, K., Lavoie, J.M., 1979. Some final conclusions and supporting experiments related to the search for organic compounds on the surface on Mars. J. Geophys. Res. 84, 8383-8390.

Biemann, K., Oro, J., Toulmin III, P., Orgel, L.E., Nier, A.O., Anderson, D.M., Simmonds, P.G., Flory, D., Diaz, A.V., Ruchneck, D.R., Biller, J.E., LaFleur, A.L., 1977. The search for organic substances and inorganic volatile compounds in the surface of Mars. J. Geophys. Res. 82, 4641-4658.

Bohlke, J.K., Ericksen, G.E., Revesz, K., 1997. Stable isotopic evidence for an atmospheric origin of desert nitrate deposits in northern Chile and southern California, USA. Chemical Geology 136, 135-152.

Bullock, M.A., Stoker, C.R., McKay, C.P., Zent, A.P., 1994. A coupled soil-atmosphere model of H_2O_2 on Mars. Icarus 107, 142-154.

Chun, S.F., Pang, K.D., Cutts, J.A., Ajello, J.M., 1978. Photocatalytic oxidation of organic compounds on Mars. Nature 274, 875-876.

Encrenaz, Th., Bézard, B., Greathouse, T.K., Richter, M.J., Lacy, J.H., Atreya, S.K., Wong, A.S., Lebonnois, S., Lèfevreet, F., 2004. Hydrogen peroxide on Mars: evidence for spatial and seasonal variations. Icarus 170, 224-229.

Ericksen, G.E., 1981. Geology and origin of the Chilean nitrate deposits. US Geological Survey Professional Paper, 1188.

Ericksen, G.E., 1983. The Chilean nitrate deposits. American Scientist 71, 366-374.

Flynn, G.J., 1996. The delivery of organic matter from asteroids and comets to the early surface of Mars. Earth, Moon, and Planets 72, 469–474.

Gee, M.L., Healy, T.W., White, L.R., 1990. Hydrophobicity effects in the condensation of water films on quartz. J. Colloid and Interface Sci. 140, 450-465.

Grunthaner, F.J., Ricco A., Butler, M.A., Lane, A.L., McKay, C.P., Zent, A.P., Quinn, R.C., Murray, B., Klein, H.P., Levin, G.V., Terhune, R.W., Homer, M.L., Ksendzov, A., Niedermann, P., 1995. Investigating the surface chemistry of Mars. Analytical Chemistry 67, 605A-610A.

Haber, J., 1996. Selectivity in heterogeneous catalytic oxidation of hydrocarbons. In: Warren, B.K., Oyama, S.T., (Eds.), Heterogeneous Hydrocarbon Oxidation, ACS Symposium Series 638, 21-34.

Horowitz, N.H., Hobby, G.L., Hubard, J.S., 1977. Viking on Mars: the carbon assimilation experiment. J. Geophys. Res. 82, 4659-4667.

Hunten, D.M., 1974. Aeronomy of the lower atmosphere of Mars. Rev. Geophys. Space Phys. 12, 529-535.

Hunten, D.M., 1979. Possible oxidant sources in the atmosphere and surface of Mars. J. Mol. Evol., 14, 57-64.

Klein, H.P., 1978. The Viking biological experiments on Mars. Icarus 34, 666–674.

Klein, H.P., 1979. The Viking mission and the search for life on Mars. Rev. Geophys. Space Phys. 17, 1655-1662.

Klingelhöfer, G., Morris, R.V., Bernhart, B., Schroder, C., Rodionov, D.S, de Souza, P.A., Yen, A., Geller, R., Evlanov, E.N., Zubkov, B. Foh, J., Bonnes, U., Kankeleit, E., Gütlich, P., Ming, D.W., Renz, F., Wdowiak, T. Squyres, S.W., Arvidson, R.E., 2004. Jarosite and hematite at Meridiani Planum from Opportunity's mössbauer spectrometer. Science 304 1740-1745.

Levin, G.V., Straat, P.A., 1977. Recent results from the Viking labeled release experiment on Mars. J. Geophys. Res. 82, 4663-4668.

McDonald, G.D., deVanssay, E., Buckley, J.R., 1998. Oxidation of organic macromolecules by hydrogen peroxide: implications for stability of biomarkers on Mars. Icarus 132, 170-175.

McKay, C.P., Grunthaner, F.J., Lane, A.L., Herring, M., Bartmann, R.K., Ricco, A.J., Butler, M.A., Murray, B.C., Quinn, R.C., Zent, A.P., Klein, H.P., Levin, G.V., 1998. The Mars oxidant experiment (MOx) for Mars '96. Planetary and Space Science 46, 769-777.

McKay, C.P., Friedmann, E.I., Gomez-Silva, B., Cáceres-Villanueva, L., Andersen, D.T., Landheim, R., 2003. Temperature and mositure conditions for life in the extreme arid region of the Atacama Desert: four years of observations including the El Nino of 1997-1998. Astrobiology 3, 393-406.

Navarro-González, R., Rainey, F.A., Molina, P., Bagaley, D.R., Hollen, B.J., de la Rosa, J., Small, A.M., Quinn, R.C., Grunthaner, F.J., Caceres, L., Gomez-Silva, B., McKay, C.P., 2003. Mars-like soils in the Atacama Desert and the dry limit of microbial life. Science 302, 1018-1021.

Oyama, V.I., Berdahl, B.J., 1977. The Viking gas exchange experiment results from Chryse and Utopia surface samples. J. Geophys. Res. 82, 4669-4676.

Quinn, R.C., Orenberg, J., 1993. Simulations of the Viking gas exchange experiment using palagonite and Fe-rich montmorillonite as terrestrial analogs: implications for the surface composition of Mars. Geochim. Cosmochim. Acta 57, 4611-4618.

Quinn, R.C., Zent, A.P., 1999. Peroxide-modified titanium dioxide: a chemical analog to putative martian soil oxidants. Origins Life Evol. Biosph. 29, 59-72.

Quinn, R.C., Grunthaner, F.J., Taylor, C.L., Zent, A.P. 2005. Dry acid deposition and accumulation at the Viking lander sites and in the Atacama Desert, Chile. Icarus, in review.

Rech, J.A., Quade, J., Hart, W.S., 2003. Isotopic evidence for the source of Ca and S in soil gypsum, anhydrite and calcite in the Atacama Desert, Chile. Geochim. Cosmochim. Acta 67, 575-586.

Skelley, A.M., Scherer, J.R., Aubery, A.D., Grover, W.H., Ivester, R.H.C., Ehrenfreund, P., Grunthaner, F.J., Bada, J.L., Mathies, R.A., 2005. Development and evaluation of a microdevice for amino acid biomarker detection and analysis on Mars. Proc. Nat. Acad. Sci. in press.

Squyers, S.W., Grotzinger, J.P., Arvidsom, R.E., Bell, J.F., Calvin, W., Christensen, P.R., Clark, B.C., Crisp, J.A., Farrand, W.H., Herkenhoff, K.E., Johnson, J.R., Klingelhöfer, G., Knoll, A.H., McLennan, S.M., McSween, H.Y., Morris, R.V., Rice, J.W., Reider, R., Soderblom, L.A., 2004. Science 306, 1709-1714.

Yen, A.S., Kim, S.S., Hecht, M.H., Frant, M.S., Murray, B., 2000. Evidence that the reactivity of the martian soil is due to superoxide ions. Science 289, 1909-1912.

Zent, A.P., McKay, C.P., 1994. The chemical reactivity of the martian soil and implications for future missions. Icarus 108, 146–157.

Zent, A.P., Quinn, R.C., Grunthaner, F.J., Hecht, M.H., Buehler, M.G., McKay, C.P., 2003. Mars atmospheric oxidant sensor (MAOS): an in situ heterogeneous chemistry analysis. Planetary and Space Science 51, 167-17.

Chapter 8

An atmospheric oxidation monitor based on in situ thin-film deposition

R. C. Quinn, A. P. Zent, J. R. C. Garry, T. J. Ringrose, M. C. Towner, F. J. Grunthaner

We describe an atmospheric oxidation sensor developed and delivered as part of the European Space Agency Beagle 2 Mars Lander Environmental Sensor Suite. The sensor monitors atmospheric oxidation rates by measuring resistance changes in a thin-silver film deposited in situ onto a sapphire substrate while on the surface of Mars. Potential terrestrial applications of this sensing approach include long-term monitoring of oxidative contaminants in low-oxygen systems including process gases and environmental chambers. The sensor response to ppb levels of hydrogen peroxide vapor in carbon dioxide is demonstrated.

8.1 Introduction

We have developed a novel sensor to characterize, very broadly, the reactive nature of the martian atmosphere. The sensor monitors atmospheric oxidation rates by measuring resistance changes in a thin-metal film deposited in situ onto a sapphire substrate while on the surface of Mars. The novel use of in situ deposition avoids problems related to predeployment storage and sensor aging without using costly hermetic sealing technologies. Although the sensor is designed to monitor martian atmospheric oxidation, potential terrestrial applications of this sensing approach include long-term monitoring of oxidative contaminants in low-oxygen systems including process gases and environmental chambers.

The martian atmosphere is composed primarily of carbon dioxide (~95%); the absence of a martian ozone layer allows solar radiation of wavelengths greater than 190 nm (the CO_2 cutoff wavelength) to reach the surface of the planet. As a result of this low cutoff, photochemical models of the near-surface atmosphere of Mars predict the presence of low levels of reactive oxygen and hydrogen species including O_3, $O^{\cdot}$, H_2O_2, and $^{\cdot}OH$ Kong et al., 1977; Hunten et al., 1979). It is thought that reactions of these species, particularly H_2O_2, with the martian surface may be responsible for creating a chemically re-

active surface material on Mars containing multiple oxidizing species, as was discovered by the United States National Aeronautics and Space Agency (NASA) Viking Landers in 1976 (Klein, 1978). In this paper, we describe a sensor designed to investigate this theory.

The sensor, referred to as the Environmental Sensors Oxidation Sensor (ESOS), was developed and built for the European Space Agency (ESA) Beagle 2 (B2) Mars Lander and included on the payload as part of the lander's Environmental Sensor Suite (ESS). The B2 ESS was comprised of several components designed to return detailed chemical and physical characterizations of the spacecraft and martian environment during the course of the mission. In addition to the oxidation sensor, the package included a set of accelerometers for pre-descent, descent, and post-landing monitoring; atmospheric temperature and pressure measurement capability; an atmospheric dust impact sensor; an array of UV photodiodes for solar flux measurement; and wind speed and direction sensors (Towner et al. 2004). Unfortunately, a signal from the B2 lander was never received after successful release of the spacecraft by the ESA Mars Express orbiter in December 2003.

The sensor described in this paper is based on a series of chemical sensor array measurement strategies that have been developed for landed Mars missions to investigate the chemical reactivity of the martian surface material and near-surface atmosphere. After the Viking Mars mission in 1976, the first attempt to directly examine the chemical reactivity of the martian surface was planned as part of the Russian Mars '96 mission. The Mars Oxidant Experiment (MOx) was contributed to the mission by NASA and was unfortunately lost with the mission shortly after launch (Grunthaner et al., 1995; McKay et al. 1998). MOx used a fiber-optic array operating in a micro-mirror sensing mode to monitor chemical changes in chemical thin-film reactants. MOx was designed as a survey instrument to characterize the chemical nature of the soil by using an array of chemical-thin films with different reactivities. MOx used a chemometric approach in which the identity of unknowns is elucidated through the reaction pattern of the sample with reference compounds. Valuable lessons learned in the development of MOx have led to improved designs for both soil and atmospheric oxidant sensors. The Thermo-Acoustic Oxidant Sensor (TAOS) extended the use of thin-film sensors for Mars applications to chemiresistors and surface acoustic wave devices (Zent et al., 1998). Following TAOS, the Mars Oxidant Instrument (MOI) was developed to study soil oxidants using chemiresistor sensing. MOI added the capability of sealing the soil sample and heating and humidifying the sample headspace.

More recently, the Mars Atmospheric Oxidant Sensor (MAOS), which is based on MOx, TAOS, and MOI technologies, has been designed. MAOS is a chemometric sensor array that measures the oxidation rate of chemical thin-films that are sensitive to particular types of oxidants; these oxidants represent key elements in the martian soil or emulate prebiotic materials. The thin-film reactants include highly electropositive metals, semiconductors, and a set of organic functional groups. Half of the sensors are permanently sealed from the environment and serve as references. Two kinds of passive filters are used in combination with the non-reference sensors, one to exclude UV and one to exclude dust. These two filters are deployed over the sensors in combination to exclude UV, dust, both UV and dust, or neither. All sensors other than the sealed references are exposed to

the atmosphere. By monitoring differences in film reaction among the filter combinations, MAOS quantifies the relative contribution of soil-borne oxidants, UV photoxidation, and gaseous oxidants to the chemical reactivity of the Mars surface environment (Zent et al. 2003).

A major technical challenge associated with the deployment of these sensor arrays on Mars is the need to deliver unreacted and uncontaminated sensing films to the surface of the planet. Because the sensing films are highly reactive, exposure to air, water vapor, or other contaminants during instrument delivery, integration, or transport to Mars would seriously compromise experimental results. To ensure the delivery of pristine MAOS sensing films to Mars, they are encapsulated in a hermetically sealed enclosure using a micro-machined cover that is bonded to the sensor substrate immediately following film deposition. Fabricated using bulk Si micro-machining, the seal cover consists of a thick silicon frame with suspended films of silicon nitride. Once delivered to the planet's surface, on computer command the silicon nitride seals are ruptured, exposing the sensing thin-film to the martian environment. The micro-machined sealing system was fully designed, tested, and delivered as part of the MOx fight instrument; however, there is a high financial cost associated with the fabrication and integration of the sealing system. Additionally, there is a level of risk associated with the system since mechanical failure or leaking of the seals are potential instrument failure modes. Even in the absence of membrane failure or leakage, a low level of film oxidation is unavoidable during sensor fabrication. Since the MOx flight instrument, the combination of high fabrication costs and limited flight opportunities has prevented a second opportunity to land a chemical sensor array designed to measure environmental chemical reactivity on Mars.

The sensor described in this work was designed to characterize atmospheric oxidation rates on Mars and diurnal variations in these rates. By eliminating the need for hermetic sealing, the sensor also provides a proof-of-concept demonstration of in situ deposition of thin-film sensing materials on Mars as risk mitigation strategy and fabrication cost savings.

8.2 Sensor description and operating principle

8.2.1 Operating principle

The sensor's operating principle is based on the in situ thermal deposition on Mars of thin silver films onto a sapphire substrate and on monitoring changes in film resistance during both deposition and post-deposition oxidation by atmospheric gases. The evaporation source is placed in the center of an open-ended tube to provide a diffusion-controlled operating mechanism for the chemical sensor. Upon the initial flash heating of the source, evaporated metallic silver rapidly reacts with oxidizing gases in the tube. Unoxidized silver then deposits on the substrate subsequent to consumption of oxidizing gases in the vicinity of the source. The kinetics and extent of the chemical reaction between the depos-

ited film and the reactive gases diffusing into the tube are then measured by monitoring the changes in resistance of the film as a function of time. By depositing fresh films on the substrate at different times (e.g. sunrise, midday, sundown, midnight), diurnal variations in chemical activity can be mapped.

It is also possible that information on atmospheric H_2O levels can be derived from film deposition time and power requirements. Since the ends of the tube are open, atmospheric gases in the tube will cause a time delay as vapor phase silver reacts with the available oxygen and water; after the consumption of these gases in the tube, a silver film closes the chemiresistor circuit. Although not validated during the prototyping stage, in principle this operation mode provides a repeatable measure of the variable H_2O abundance, since O_2 levels are constant in the atmosphere, and the low levels of other oxidizing gases in the tube should not contribute significantly to the time delay. However, validation of the sensor's ability to measure H_2O was not performed since the B2 Lander was equipped with a Mass Spectrometer (MS) that would provide quantitative abundances of both atmospheric O_2 and H_2O. Quantification of O_2 and H_2O levels by the MS provides the ability to determine the relative contributions of these gases to overall post-film deposition oxidation rates.

8.2.2 Sensor description

Prototype specifications and performance of the sensor are described in this paper. There were some minor variations between the prototype specifications and the final flight unit (figure 1), which was fabricated at the Open University Planetary and Space Science Research Institute (Milton Keynes, UK); these are not addressed in this paper. The sensor consists of an open-ended 1 cm long sapphire tube with a 5 mm inner diameter. A 50 micron diameter tungsten filament with a centered silver point source is mounted coaxially in the tube. The inner surface of the sapphire tube is coated on each end with Cermet 8881B gold conductor (Electro-Science Laboratories, Inc.) to form 6 to 8 micrometer thick electrodes 4 millimeters in length, with an electrode gap of 2 millimeters. The silver source is centrally positioned in the tube and the electrode gap is centrally positioned on the inner surface of the tube.

The selection of the filament diameter, tube size, and electrode gap was based on performance compatibility and optimization with the B2 spacecraft circuitry. The ESOS flight sensor was packaged on an 8-pin dual-inline package (DIP) (figure 1) and mounted on an electronics board located on the spacecraft upper surface adjacent to the UV sensors. By placing the ESOS near the UV sensors, oxidation rates can be correlated with UV flux levels. The spacecraft battery used by the ESOS to evaporate the silver source was charged by the lander's solar panels and had an output voltage that was expected to fluctuate during the course of spacecraft operations. During the available time windows for sensor operation on Mars, the battery voltage was expected to be in the 20-to-26-volt

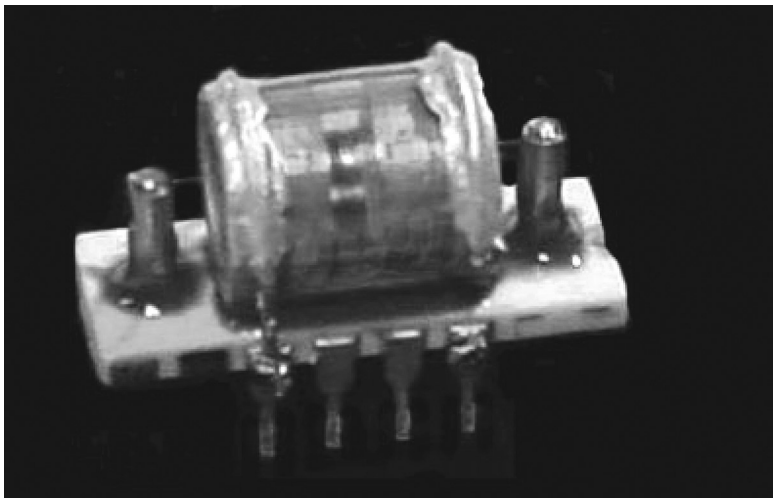

Figure 1. A Beagle 2 Environmental Sensors Oxidation Sensor. The sensor was developed and built for the European Space Agency (ESA) B2 Mars Lander and included on the payload as part of the lander's Environmental Sensor Suite. The open-ended sapphire tube is 1 cm long with a 5 mm inner diameter. The Au electrodes are 4 millimeters in length, with an electrode gap of 2 millimeters. A 50 micron diameter titanium filament with a centered silver point source is mounted coaxially in the tube.

range. This voltage is monitored as part of ESOS operation, and a particular voltage range could be used as a requirement for sensor activation, allowing a degree of reproducibility. The ESOS electronics printed circuit board was rated to 1.5A continuous and it was anticipated that short-duration current pulses of up to 4A could be used to heat the sensor filament if needed. A temperature sensor is also included within ESOS, to characterize temperature dependence in film resistance and deposition rates.

8.3 Experimental

Prior to use, the tungsten filament used in all prototypes was thermally annealed in dry N_2 for five minutes, and the silver source was then formed in dry N_2 by heating a 3 mm piece of 0.127 mm diameter silver wire (Aldrich Chemical, 99.99%) centered on the filament until a small bead formed. Film depositions were carried out in a test chamber at room temperature with a CO_2 atmosphere (99.99+%) at ambient Mars pressures (10 mbar). Optimization studies with tungsten filaments of different diameters demonstrated that given the battery operating range of 20 to 26 V, rapid evaporation of the silver source

could be achieved using a 50 μm diameter and a ~1 Amp current pulse. All current pulses referred to in the Results and Discussion section below are ~1 Amp.

Dry hydrogen peroxide vapor for sensor response testing was generated by passing the test gas over a urea-hydrogen peroxide addition compound (Aldrich Chemical). Hydrogen peroxide levels were calibrated using a Dräger Polytron 2. Because the Polytron operates only at atmospheric pressure and is temperature–sensitive, sensor response testing was carried out at a total pressure of 1 bar and at room temperature. The composition of the simulated Mars test gas used in this work was 0.13% O_2, 2.7% N_2, balance CO_2.

8.4 Results and Discussion

8.4.1 Primary film deposition

The magnitude and duration of a current needed to thermally deposit a film using 50 μm diameter tungsten filament with a silver source and a 24.2V power supply is shown in figure 2. It was determined that current pulses 600 msec or longer resulted in the deposition of unoxidized silver on the electrode. Pulses shorter than 500 msec resulted in a visible flashing of the filament/source, but no visible deposition or measurable resistance across the 2 mm gap electrodes. Pulses longer than 500 msec but shorter that 550 msec resulted in visible deposition of a film on the substrate, but still no measurable resistance across the electrodes. Figure 2 shows the formation of a film with a final resistance of ~10 Kohm after the second of two 550 msec pulses. This film resistance indicates the formation of either a discontinuous or a partially oxidized film; visual inspection and further testing (described below) suggest the latter is the case.

8.4.2 Secondary depositions

An example of secondary film deposition is shown in figure 3. In this case, a 1 Amp, 350 msec current pulse was used to deposit additional material on top of a primary film, resulting in an increase of film resistance. In all cases where current pulses between 250 and 350 msec were used, an increase in film resistance occurred, suggesting that for short current pulses (less than 550 msec), oxide formation occurs as the evaporated silver reacts with oxidizing gases in the electrode region. When a pulse of 550 msec or greater was used, deposition of unoxidized silver occurred after an initial period of oxide deposition during which the oxidizing gases in the region of the source were consumed. This effect is shown in figure 4. A 600 msec 1 Amp current pulse resulted in a rapid film resistance increase followed by a rapid decrease. Both the resistance increase and decrease were approximately one order of magnitude relative to the initial baseline film resistance.

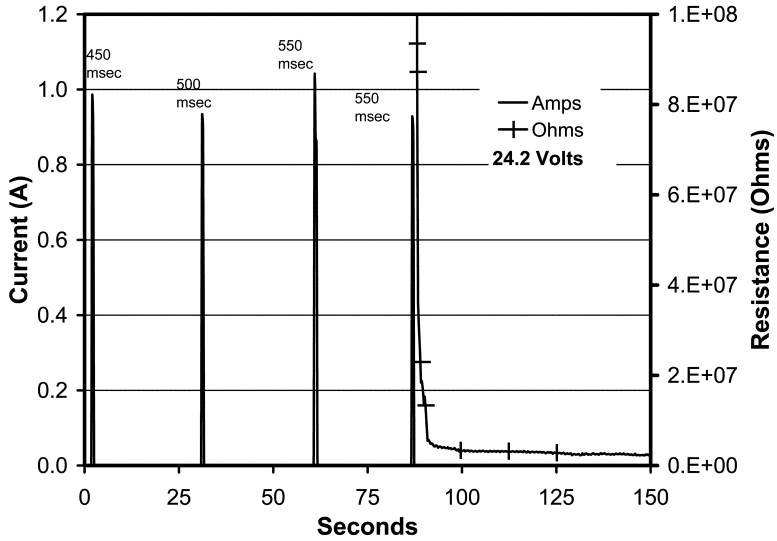

Figure 2. Thermal deposition of a film using 50 µm diameter titanium filament with a silver source in 10 mbar of CO_2. Visible film deposition occurred with a 500 msec pulse. A film with a measurable resistance deposited after the second 550 msec pulse.

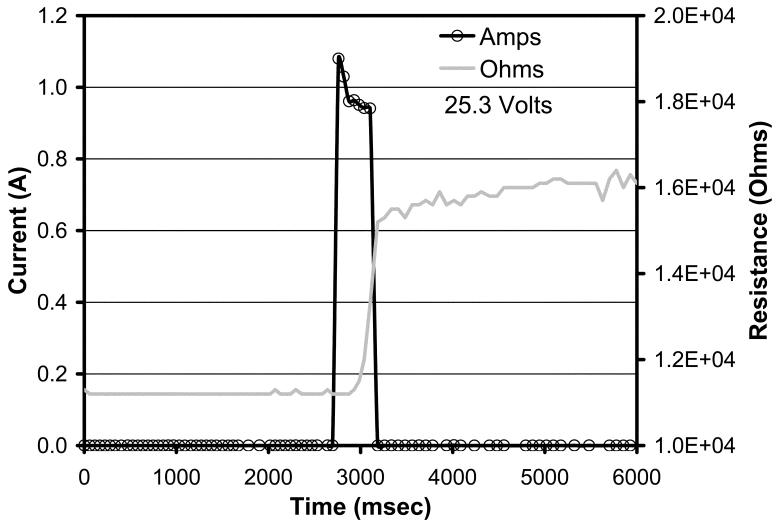

Figure 3. Secondary film deposition using a ~350 msec pulse. For short current pulses (less than 550 msec), oxide formation occurs as the evaporated silver reacts with oxidizing gases in the electrode region.

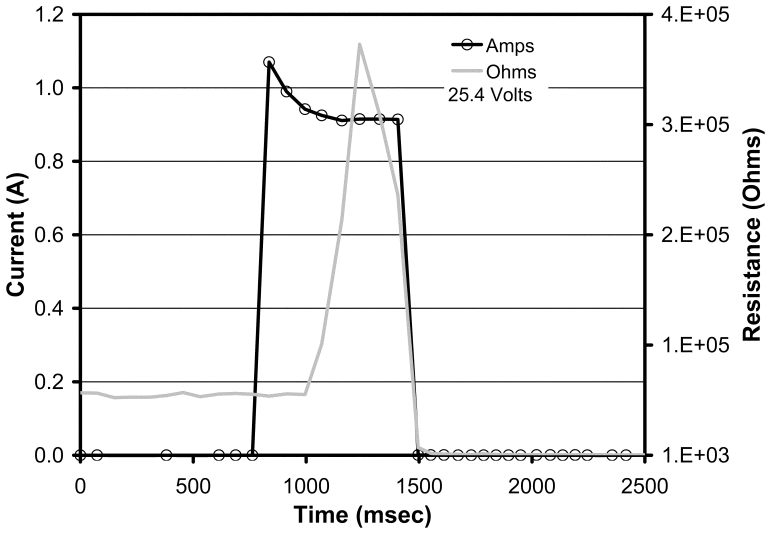

Figure 4. Secondary film deposition using a ~600 msec pulse. When a pulse 550 msec or greater was used, deposition of unoxidized silver occurred after an initial period of oxide deposition (resistance increase) as the oxidizing gases in the region of the source were consumed.

8.4.3 Sensor model

In order to better understand the behavior of the sensor, explore its utility for H_2O measurement, predict its behavior in a natural environment, and identify possible failure modes, we developed a numerical model of the laboratory experiment, and applied it to likely Mars conditions. The model predicts the behavior of the electrical circuit, the current flow, the voltage drop across each component of the circuit, the resistance temperature dependence for each component, and the resultant Joule heating. The model calculates separately the heating in the silver (Ag) bead, and the tungsten (W) filament that supports it. Within the W filament-Ag bead system, the model balances the Joule heating against radiation, sensible heat loss to ambient CO_2 and, latent heat loss from sublimating Ag atoms to calculate the temperature of the bead. Based upon the bead temperature, the model partitions the Ag among the solid, liquid and vapor phases. The latent heat of fusion is accounted for when the Ag bead reaches its melting temperature (1234K). The surface area of each component is tracked to allow calculation of the radiative and sensible heat exchange. Although the bead is allowed to melt, wetting of the W filament is not explicitly accounted for.

The flux of Ag atoms from the Ag bead is tracked continuously. In the gas phase, the number density of Ag and H_2O is calculated, along with their reaction rates on collision. Based on the high temperature of the silver atoms during deposition, it is assumed that there is no activation barrier associated with gas phase reactions, and that oxidation of Ag is complete upon collision. The Ag is assumed to be oxidized after a single collision, and is tracked as AgO. Subsequent collisions or alteration on the tube walls may result in substantial occurrence of other oxides, but for our purposes, all oxidized Ag is considered a poor conductor. The mass of unoxidized Ag, as well as Ag-oxide deposited on the walls of the tube is tracked as a function of time. The ambient air temperature, and the number density of H_2O and O_2 are assumed fixed and invariant, and are specified as boundary conditions. The tube is modeled as a symmetrical domain, with 6 finite elements from the center to the end. Each element has a length of 0.909 mm, allowing 11 elements along a 1 cm tube. Abundances of gas phase and surface deposits are tracked in each of the elements from 0 (center) to 5 (end).

The predicted current is shown in Figure 5, with the laboratory data overlaid. The relay opens the connection to the battery at t= 0.762 s. The subsequent drop in current is due to the rise in resistance of the circuit components with temperature. The current levels out at 0.92A because temperature rise in the Ag-W system is truncated when the Ag reaches its boiling temperature (1800 K at 100 mbar). In the simulation here, the mass of the Ag bead decreases to about 1% of it's original value. However, in the laboratory tests visual inspection of the Ag bead indicated that it was not fully exhausted before the end of the laboratory experiments. The abundance of Ag and H_2O in elements 0-2 (figure 6) suggests that Ag substantially depletes H_2O only near the center of the bead. In this simulation, it was assumed that the H_2O is buffered at the vapor pressure of ice at 230K. With substantially more H_2O, the finite rate of Ag supply to the gas phase means the H_2O abundance is less affected. Above some background H_2O abundance, oxidized Ag is deposited in every element in excess of metallic Ag.

The sensitivity of the system to H_2O is shown in Figure 7. The model supports the hypothesis that the onset of high conductivity between the Au electrodes is a function of the H_2O abundance in the ambient gas, but only to a limit. Because the flux of Ag atoms to the tube gas phase is limited by the Joule heating available, there is an upper limit to the effective range of H_2O sensitivity. In the present case, when H_2O abundances are buffered at 250K, unoxidized Ag never deposits in excess of silver oxide. However, for Mars conditions, unoxidized silver will deposit and the time delay for the deposition increases with H_2O abundance.

The potential behavior of the system for predicted Mars-like conditions is shown in Figure 8. The differences between the laboratory and Mars simulations are: 1) lower initial T (210 K); 2) Somewhat lower pressure (7 mbar); 3) An ambient H_2O abundance buffered at the vapor pressure of water at 210 K. In this Mars simulation, with a 650 msec pulse, all of the Ag is vaporized, allowing the W filament to continue heating.

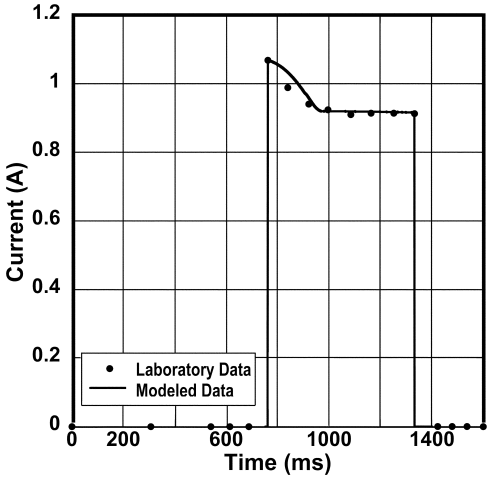

Figure 5. Comparison of the laboratory test data and the modeled sensor behavior. The model correctly predicts the current flow through the circuit. Since heating = I^2R, the heating rate must likewise be accurate.

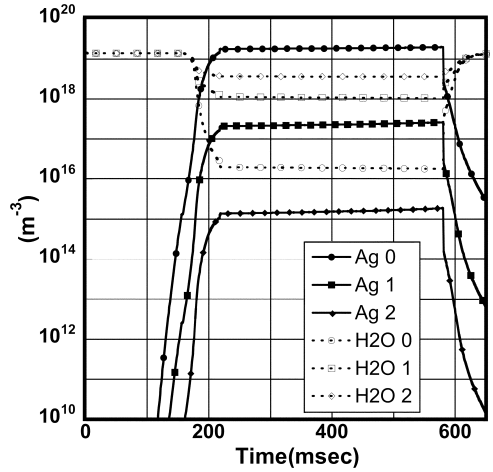

Figure 6. The modeled number density (m^{-3}) of metallic Ag (solid lines) and H_2O (dashed lines) in finite elements from 0 (center of tube including Ag bead – circles), through 2 – (diamonds). Although the end of the tube is element 5, we plot only to element 2 because elements 0 and 1 bridge the ends of the Au electrodes. Metallic Ag exceeds H_2O only near the source.

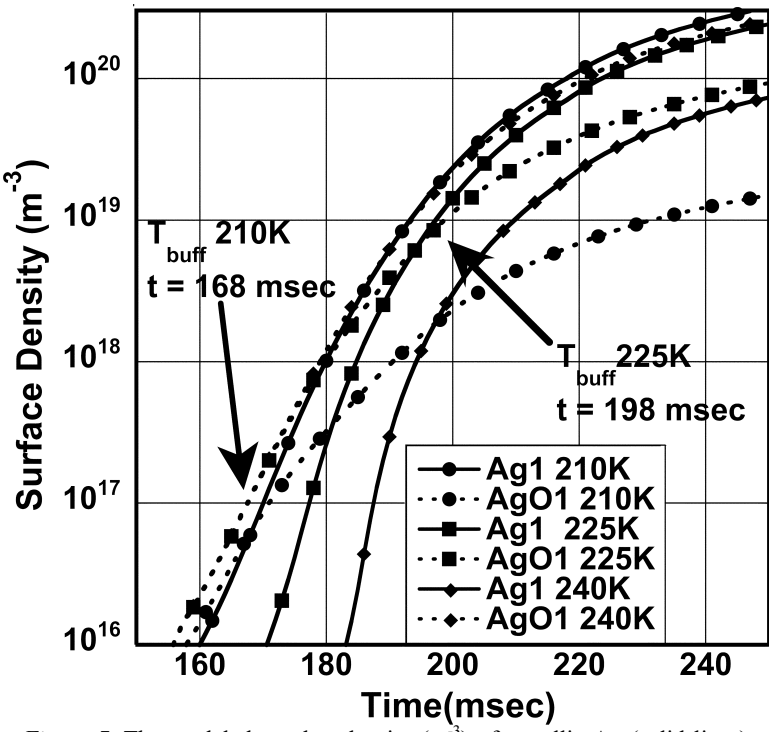

Figure 7. The modeled number density (m^{-3}) of metallic Ag (solid lines) and H_2O (dashed lines) in finite elements from 0 (center of tube including Ag bead – circles), through 2 – (diamonds). Although the end of the tube is element 5, we plot only to element 2 because elements 0 and 1 bridge the ends of the Au electrodes. Metallic Ag exceeds H_2O only near the source.

The modeled filament temperature prior to the end of the pulse was 3400K. Given the results of our model, to prevent melting of the filament, on Mars the current pulse would be sequentially increased from a value less than 650 msec until unoxidized silver deposits. The signature of complete Ag vaporization is a significant drop in the current prior to cut-off, a consequence of the increased resistivity of W at temperatures above 1800K. As a consequence mostly of the lower starting temperature, metallic Ag exceeds AgO deposition somewhat later than in the laboratory case. However, since the Ag bead has less sensible heat loss to the atmosphere (7 mbar assumed for Mars – 10 mbar in the laboratory), more heat is lost through Ag vaporization.

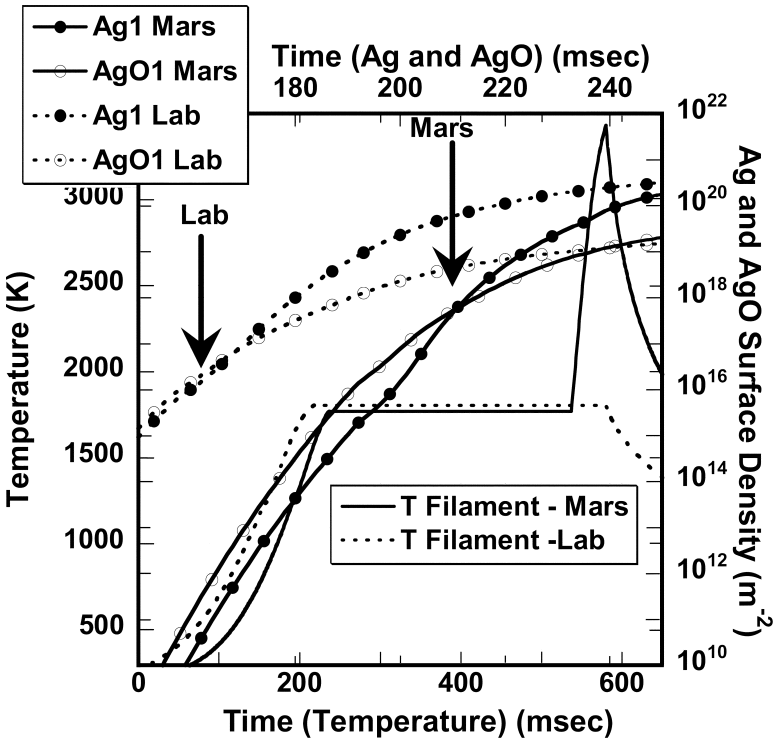

Figure 8. A comparison of the model using the laboratory test conditions with the model using predicted Mars conditions. Both cases, we have adjusted the ambient H_2O pressure to 0.71Pa, the pressure in equilibrium with ice at 210 K. In all cases, the solid lines represent Mars simulations, the dotted lines represent the laboratory simulations. The filled circles represent the number density of metallic Ag (m^{-2}), deposited on the walls of the tube in finite element *i=1*, which corresponds to the inboard edge of the Au electrode. The open circles represent the number density of AgO. Number densities are labeled on the right hand ordinate, and the upper abscissa. The arrows labeled "Lab" and "Mars" indicate the time at which metallic Ag begins to be deposited in excess of AgO in element *i=1*. On the left hand ordinate, and the lower abscissa, the thermal history of the metal filament is plotted for the laboratory and Mars experiments.

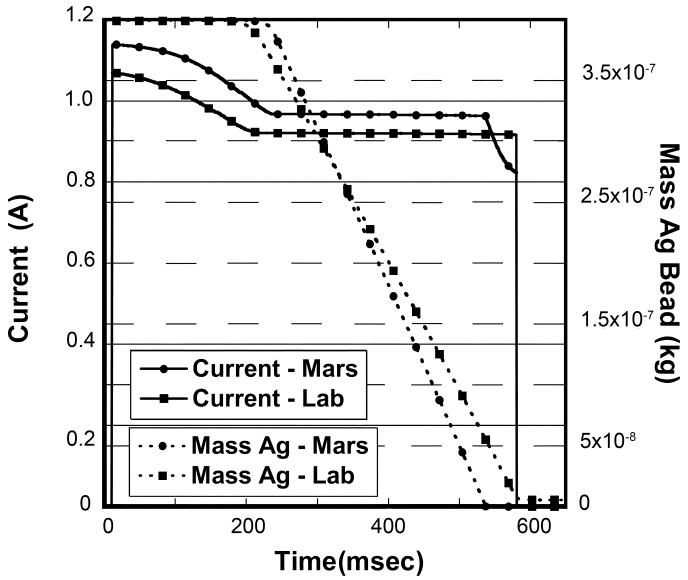

Figure 9. The predicted current for operations on Mars (solid) in the laboratory (dotted). The drop in I near the end of the current pulse is due to increased resistivity of the W filament after Ag is exhausted. The mass of the Ag bead is shown for comparison in the two simulations.

8.4.4 Gas sensing properties

The sensitivity of freshly deposited films to hydrogen peroxide vapor in carbon dioxide is shown in figure 10. The detection limit of the Polytron unit is 100 ppb, and the uncertainty in the measurements is ±50 ppb. This limitation prevents sensor testing at levels below 100 ppb. Although 100 ppb is significantly higher than the hydrogen peroxide concentrations expected in the martian atmosphere, the sensor response for this peroxide level indicates that sensor detection limits should be several orders of magnitude lower. Additionally, since the oxidation of the silver film is dosimetric, extremely low rates of oxidation can be measured by continual monitoring during long-duration atmospheric exposures. Figure 10 also shows the response of a freshly deposited film to pure CO_2. In the absence of oxidizing gases, the resistance of freshly deposited films slowly decreased over a period of several hours as the film annealed. The response of a freshly deposited The response of a freshly deposited film to a simulated, peroxide-free, martian atmosphere (0.13% O_2; 2.7% N_2; balance CO_2) shows a low sensitivity of the film to O_2 relative to H_2O_2.

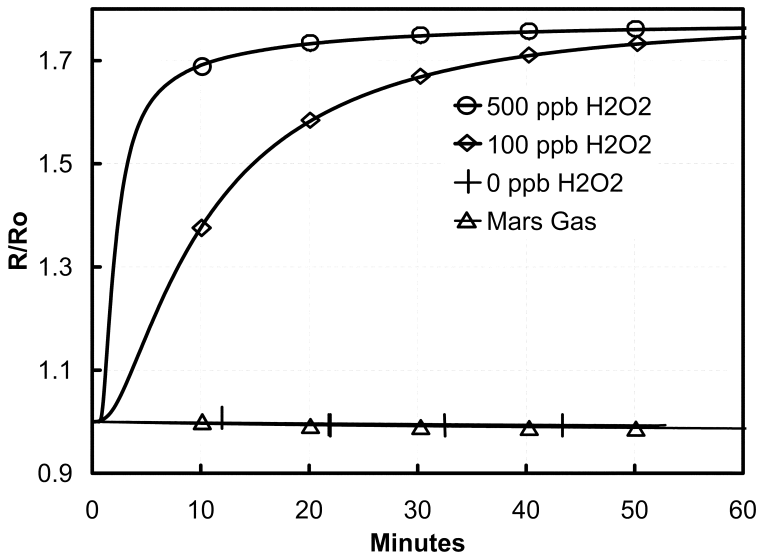

Figure 10.. The sensitivity of freshly deposited films to hydrogen peroxide vapor in carbon dioxide and response of a freshly deposited film to a simulated, peroxide free, martian at-morpheme (0.13% O_2; 2.7% N_2; balance CO_2).

8.5 Conclusions

The use of in situ deposition techniques can provide an inexpensive and practical means of overcoming thin-film chemical sensor limitations due to pre-deployment contamination and aging. We have demonstrated the use of this technique using a silver sensing layer thermally deposited in situ under Mars-like conditions. These films have a high sensitivity to H_2O_2 vapor and a comparatively low sensitivity to O_2, which is present at a level of approximately 0.13% in the martian atmosphere. The high sensitivity of the sensor to peroxide, along with the dosimetric nature of the thin-film oxidation, will enable low rates of atmospheric oxidation to be monitored on the surface of Mars. Simultaneous determination of H_2O and O_2 levels by the MS will allow the contributions of these gases to the sensor response to be removed during data analysis. By removing from the data the contribution of O_2 and H_2O to the sensor response, oxidation rates due to the presence of H_2O_2 and other photochemically produced atmospheric oxidants can be determined. The ability to deposit sensing films in situ allows the surface of the sensing film to be re-

freshed with unoxidized silver. By redepositing fresh film surfaces at different times of the day, diurnal variations in atmospheric oxidation rates can be determined. The diffusion-tube sensor configuration described in this paper has a number of potential terrestrial applications, including long-term monitoring of oxidative contaminants, process gases, and environmental chambers. The measurement capabilities of the in situ deposition technique can be expanded by though the use of metals with different electrochemical potentials and with arrays tailored to the chemical environment of interest.

Acknowledgements

Work performed at NASA Ames (R.C. Quinn, A.P. Zent) was funded by the NASA Ames Director's Discretionary Fund. Beagle 2 activities (M.C. Towner, J.C. Garry, T.R. Ringrose) were funded in part by the UK Particle Physics and Astronomy Research Council.

Chapter 8

References

Kong, T.Y., McElroy, M.B., 1977. Photochemistry of the martian atmosphere. Icarus 32, 168-189.

Hunten, D.M., 1979. Possible oxidant sources in the atmosphere and surface of Mars, J. Mol. Evol. 14, 57-64.

Klein, H.P., 1978. The Viking biological experiments on Mars. Icarus 34, 666-674.

Towner, M.C., Patel, M.R., Ringrose, T.J., Zarnecki, J.C., Pullen, D., Sims, M.R., Haapanala, S., Harri, A.-M., Polko, J., Wilson, C.F., Zent, A.P., Quinn, R.C., Grunthaner, F.J., Hecht, M.H., Garry, J.R.C., 2004. The Beagle 2 environmental sensors: science goals and instrument description, Planetary and Space Sci. 52, 1141-1156.

Grunthaner, F.J., Ricco, A., Butler, M.A., Lane, A.L., McKay, C.P., Zent, A.P., Quinn, R.C., Murray, B., Klein, H.P., Levin, G.V., Terhune, R.W., Homer, M.L., Ksendzov, A., Niedermann, P., 1995. Investigating the surface chemistry of Mars. Analytical Chemistry 67, 605A-610A.

McKay, C.P., Grunthaner, F.J., Lane, A.L., Herring, M., Bartmann, R.K., Ricco, A.J., Butler, M.A., Murray, B.C., Quinn, R.C., Zent, A.P., Klein, H.P., Levin, G.V., 1998. The Mars oxidant experiment (MOx) for Mars '96. Planetary and Space Science 46, 769-777.

Zent, A.P., Quinn, R.C., Madou, M., 1998. A thermo-acoustic gas sensor array for photochemically critical species in the martian atmosphere, Planetary and Space Science 46, 795-803.

Zent, A.P., Quinn, R.C., Grunthaner, F.J., Hecht, M.H., Buehler, M.G., McKay, C.P., 2003. Mars atmospheric oxidant sensor (MAOS): an in situ heterogeneous chemistry analysis, Planetary and Space Science 51, 167-175.

Nederlandse samenvatting

De vraag of er op dit moment leven is op Mars en of er ooit leven is geweest in het verleden, is interessant voor zowel planeetwetenschappers als het grote publiek. Studies naar leven onder extreme omstandigheden op aarde laten zien dat er op het oppervlak van Mars gebieden bestaan waar leven zou kunnen voorkomen. Strategieën voor onderzoek op Mars hebben zich tot nu toe vooral gericht op de leefbaarheid van de planeet, en dan voornamelijk op de zoektocht naar twee belangrijke voorwaarden voor het bestaan van leven zoals wij het kennen: het voorkomen van vloeibaar water en de aanwezigheid van complexe organische moleculen.

In 1976 voerden de Viking landers een uitgebreid onderzoek uit op het oppervlak van Mars, op zoek naar zowel leven als organisch materiaal. Missies na Viking, waaronder Mars Pathfinder in 1997 en de Mars Exploration Rovers in 2004, onderzochten de eigenschappen van het oppervlak van Mars, maar zochten niet specifiek naar organisch materiaal. De Viking experimenten lieten zien dat het materiaal op het oppervlak van Mars niet biologisch actief was, maar chemisch reactief en vrij van organische verbindingen. De algemene conclusie, gebaseerd op deze resultaten, is dat het materiaal op het oppervlak van Mars een verscheidenheid aan oxiderende stoffen bevat. Verschillende concurrerende hypothesen proberen te verklaren welke oxidanten dit zijn, hoe ze gevormd worden en wat hun rol is in zowel de biologische experimenten op de Viking landers als in de afbraak van organisch materiaal op het oppervlak van de planeet. Waarschijnlijk spelen de meeste processen, beschreven door deze hypothesen, op de een of andere manier een rol. Op Mars komen ongetwijfeld een groot aantal complexe, fotochemisch gedreven, oxiderende processen voor, waarin chemische interacties tussen atmosfeer, aerosolen, stof, grond en organisch materiaal een rol spelen. Wat de rol is van deze fotochemische processen in de koolstofcyclus op Mars is vrijwel niet bekend.

Het doel van dit proefschrift is het karakteriseren van reactieve chemische processen die zich voordoen op het oppervlak van Mars en het beschrijven van hun relatie tot de planetaire koolstofchemie en de mogelijkheid van het bestaan van gebieden waar leven voor zou kunnen komen. De sleutel tot het begrijpen van de koolstofcyclus op Mars en het uiteindelijke lot van organisch materiaal ligt niet alleen in het identificeren van oxidanten in de grond, maar ook, en wellicht belangrijker, in het karakteriseren van de dominante reactiemechanismen en -kinetiek van zowel de reactiviteit van de grond als de afbraak van organisch materiaal. Deze processen zouden het organisch materiaal kunnen hebben

veranderd of afgebroken, dat eventueel uit een vroeger biotisch tijdperk zou kunnen zijn overgebleven. Om te kunnen bepalen hoe en waar te zoeken naar onaangetast organisch materiaal, is het noodzakelijk om deze processen en hun rol in de koolstofcyslus te begrijpen. Dit proefschrift beschrijft verschillende manieren om de reactieve chemische processen die zich in de Mars-regolith voordoen, te karakteriseren. De volgende manieren worden beschreven:

- modellering en simulatie van de chemie op het oppervlak van Mars, door middel van in het laboratorium uitgevoerde experimenten en gebruik makend van gegevens van eerdere Mars missies,
- vergelijkende studies van extreme omgevingen op aarde en op Mars, om een beter begrip te krijgen van de vormingsmechanismen en de eigenschappen van oxidanten en hun rol in de planetaire koolstofcycli in deze omgevingen, en

- het ontwerp, de ontwikkeling en het veldtesten van instrumenten en meettechnieken voor het in situ karakteriseren van oxidatiemechanismen, oxidatiekinetiek en de koolstofkringloop op Mars.

In **hoofdstuk 2** laten we zien dat sommige overgangsmetaalcomplexen in staat zijn om waterstofperoxide-vormende stoffen aan zich te binden, die zich chemisch gezien hetzelfde gedragen als de Viking grondmonsters. Titaniumdioxide (anatase) blootgesteld aan waterstofperoxide reproduceert de resultaten van de biologische experimenten op de Viking landers. We concluderen hieruit dat de chemische activiteit het gevolg is van de vorming van verschillende soorten gechemisorbeerde stoffen op het titaniumdioxide. De vorming van complexen vindt plaats op Ti^{4+} locaties en verwacht wordt dat de vorming van gelijksoortige complexen ook optreedt op andere mineralen die titanium bevatten, zoals rutiel, ilmeniet en spheen.

In **hoofdstuk 3** beschrijven we experimenteel onderzoek naar het effect van UV straling op de stabiliteit van calciumcarbonaat in een nagebootste marsatmosfeer. We zien geen bewijs van afbraak en concluderen dat de totale hoeveelheid carbonaat op Mars onaangetast is door UV-fotochemische processen.

In **hoofdstuk 4** onderzoeken we de afbraak van organische verbindingen in aanwezigheid van waterhoudende bodems. Van sommige organische verbindingen is bekend dat ze afbreken wanneer ze in een waterige oplossing worden toegevoegd aan oppervlaktemateriaal van Mars. Hetzelfde geldt voor sommige grondmonsters uit de Chileense Atacama woestijn. De totale chemische reactiviteit van grondmonsters uit de Atacama is groter en de reactiekinetiek verschilt van wat er is waargenomen in Mars grondmonsters. Echter, zowel de Atacama als de Mars grondmonsters laten bewijs zien van oxidatieve oppervlaktekatalyse in aanwezigheid van water (H_2O). Dit wijst erop dat

organisch materiaal kan afbreken gedurende tijdelijke natte periodes op het oppervlak van Mars.

In **hoofdstuk 5** wordt de zuur-base evenwichtskinetiek van grondmonsters verzameld in de Atacama woestijn vergeleken met informatie over de zuur-base chemie van monsters van het oppervlak van Mars, afkomstig van de Viking experimenten. We concluderen dat, zowel in de Atacama als op Mars, een extreem lage pH, voortvloeiend uit ophoping van zuur in combinatie met een lage vochtigheidsgraad en een hoge oxidatiepotentiaal, resulteert in zuur-gedreven reacties op het grondoppervlak wanneer kleine hoeveelheden vloeibaar water aanwezig zijn.

De Mars Atmospheric Oxidant Sensor (MAOS) wordt beschreven in **hoofdstuk 6**. MAOS is een serie van chemometrische sensoren, die de oxidatiesnelheid meet van chemisch dunne lagen, die gevoelig zijn voor bepaalde types oxidanten of die bepaalde eigenschappen van prebiotisch en biotisch materiaal nabootsen.

MAOS is ontworpen om de temperatuur van de dunne-laag-sensoren en hun blootstelling aan stof en UV straling te regelen, wat het instrument in staat stelt onderscheid te maken tussen de belangrijkste hypothesen voor de productie van oxidanten. Door het bekijken van verschillen in reacties van de dunne lagen bij verschillende filtercombinaties, kan MAOS de relatieve bijdrage van oxidanten in de grond, gasvormige oxidanten en UV-fotoöxidatie aan de chemische reactiviteit van het oppervlak op Mars kwantificeren.

Veldexperimenten die gebruik maken van de MAOS technologieën, uitgevoerd in de Atacama woestijn, zijn beschreven in **hoofdstuk 7**. De testresultaten wijzen op duidelijk verschillende reactiepatronen voor elk van de verschillende gebruiksmogelijkheden van de sensoren. De reactiviteit is het hoogst en de reactiekinetiek het snelst voor sensoren blootgesteld aan atmosferisch stof. Deze resultaten geven de eerste praktijkvalidatie van de MAOS technologie weer.

Hoofdstuk 8 geeft de beschrijving van een oxidatiesensor die gebruik maakt van in situ depositie van sensormateriaal in dunne lagen. Het gebruik van in situ depositie van chemische dunne lagen voor oxidatiesensoren is een nieuwe benadering om de gevoeligheid en de levensduur van sensoren te verlengen, waarbij de risico's voor het instrument en de kosten worden geminimaliseerd. De sensor is ontworpen om atmosferische oxidatiesnelheden op Mars en de dagelijkse variaties in deze snelheden te karakteriseren.

Tot slot is de mogelijkheid dat er leven was op Mars ergens in het verleden, een van de belangrijkste onopgeloste vraagstukken over Mars. Er vindt echter zeker een groot aantal complexe, fotochemisch gedreven, oxiderende processen op Mars plaats, waarbij

chemische interacties tussen atmosfeer, aerosolen, stof, bodem en organisch materiaal een rol spelen. Astrobiologen moeten deze processen, evenals hun rol in de koolstofcyclus van de planeet, begrijpen om uitspraken te kunnen doen over leefbaarheid en “biopotentieel”. Het onderzoek van de unieke chemie die plaats vindt in de atmosfeer vlak boven het oppervlak van de Atacama woestijn, heeft geleid tot een verbeterd begrip van processen die wellicht kunnen voorkomen op Mars. Uitgebreide veldtesten van het MAOS-instrument in de Atacama hebben geleid tot nieuwe strategieën voor de in situ karakterisatie van oxiderende processen en de koolstofcyclus op Mars. Interpretatie van deze gegevens uit het veld over de geochemische geschiedenis van de Atacama, heeft nieuw licht geworpen op vroegere en huidige geochemische processen op Mars.

Curriculum Vitae

After being born and raised in New York, I moved to Washington D.C. and received my Bachelor of Science degree in chemistry from the George Washington University. Following my undergraduate studies, I worked for two years at the National Science Foundation (USA) in the science education division. I then continued my education at San Francisco State University where I received a Master of Science degree in chemistry. My thesis research at San Francisco State University was focused on the chemical and spectroscopic properties of the martian surface. My PhD research focuses on the experimental simulation of chemical processes occurring on the surface of Mars and on the development of instrument technologies for in situ characterization of these processes. I have served as a Co-investigator or Principal Investigator on numerous NASA funded projects including: the Mars '96 Mars Oxidant Experiment, the Mars Oxidant Instrument, the Mars Atmospheric Oxidant Sensor, and the Europa Ice Analyzer. I have participated as a science and instrument team member on several space missions including: the NASA Phoenix Mars Mission, the NASA Mars Polar Lander, and the Mars '96 mission. Upon completion of my PhD at Leiden University, I plan to continue with my research at the SETI Institute and NASA Ames Research Center in Mountain View California, USA.

Additional Publications

Refereed Papers

Khare, B.N., Wilhite, P., R.C. Quinn, B. Chen, R.H. Schingler, B. Tran, H. Imanaka, C.R. So, C.W. Bauschlicher, M. Meyyappan. Functionalization of carbon nanotubes by ammonia glow-discharge: Experiments and modeling. *J. Phys. Chem. B*, 108, 8166-8172, 2004.

M.C. Towner, M.R. Patel, T.J. Ringrose, J.C. Zarnecki, D. Pullen, M.R. Sims, S. Haapanala, A.-M. Harri, J. Polko, C.F. Wilson, A.P. Zent, R.C. Quinn, F.J. Grunthaner, M.H. Hecht, and J.R.C. Garry. The Beagle 2 environmental sensors: science goals and instrument description. Planetary and Space Sci. 52, 1141-1156, 2004.

Navarro-Gonzalez, R., F.A. Rainey, P. Molina, D.R. Bagaley, B.J. Hollen, J. de al Rosa, A.M. Small, R.C. Quinn, F.J. Grunthaner, L. Caceres, B. Gomez-Silva, C.P. McKay. Mars-like soils in the Atacama Desert, Chile. *Science* 302, 1018-1021, 2003.

Nguyen, P. H.T. Ng, J. Kong, A.M. Cassell, R.C. Quinn, J. Li, M. McNeil, M. Meyyappan. Epitaxial directional growth of indium-doped tin oxide nanowire arrays. *Nano Letters*, 3, 925-928, 2003.

Zent, A. P., J. Howard, R. C. Quinn. H_2O adsorption on smectites: Application to diurnal variation of H_2O in the martian atmosphere. *J. Geophys. Res.*, 106, 14667-14674, 2001.

Haberle, R. M., C. P. McKay, N. Cabrol, E. Grin, J. Schaeffer, A. P. Zent, R. C. Quinn. On the possibility of liquid water on present day Mars. *J. Geophys. Res*., 106, 23317-23321, 2001.

Boyton, W.V., S.H. Bailey, D.K. Hamara, M.S. Williams, R.C. Bode, M.R. Fitzgibbon, W.J. Ko, M. G. Ward, K.R. Sridhar, J.A. Blanchard, R.D. Lorenz, R.D. May, D.P. Paige, A.V. Pathare, D.A. Kring, L.A. Leshin, D.W. Ming, A.P. Zent, D.C. Golden, K.E. Kerry, H.V. Luer, R.C. Quinn. Thermal and evolved gas analyzer: Part of the Mars volatile and climate surveyor integrated payload. *J. Geophys. Res.*, 106, 17,686-17,698, 2001.

Zent, A. P., R. C. Quinn, and M. Madou. A thermo-acoustic gas sensor array for photochemically critical species in the martian atmosphere. *Planetary and Space Science*, 46 , 795-803, 1998.

McKay, C. P., F. J. Grunthaner, A. L. Lane, M. Herring, R. K. Bartmann, A. J. Ricco, M. A. Butler, B. C. Murray, R. C. Quinn, A. P. Zent, H. P. Klein, G. V. Levin. The Mars Oxidant experiment (MOx) for Mars '96. *Planetary and Space Science,* 46, 769-777, 1998.

Zent, A. P., R. C. Quinn. Measurement of H2O Adsorption at Mars-like conditions: Effects of adsorbent heterogeneity. *J. Geophys. Res.*, 102, 9085-9096, 1997.

Grunthaner, F. J., A. J. Ricco, M. A. Butler, A. L. Lane, C. P. McKay, A. P. Zent, R. C. Quinn, B. R. Murry, H. P. Klein, G. V. Levin, R. W. Terhune, M. L. Homer, A. Ksendzov, and P. Niedermann. Investigating the surface chemistry of Mars. *Analytical Chemistry*, 67, 605A-610A, 1995.

Zent, A. P., R. C. Quinn. Simultaneous adsorption of CO_2 and H_2O under Mars-like conditions and application to the evolution of the martian climate. *J. of Geophys. Res*., 100, 5341 - 5350, 1995.

Zent, A.P. and R.C. Quinn, and B.M. Jakosky. Fractionation of nitrogen isotopes on Mars: The role of the regolith as a buffer, *Icarus*, 112, 537-540, 1994.

Quinn, R.C. and J. Orenberg. Simulations of the Viking gas exchange experiment using palagonite and Fe-rich montmorillonite as terrestrial analogs: Implications for the surface composition of Mars, *Geochim. Cosmochim. Acta*, 57, 4611-4618, 1993.

Conference Proceedings

Quinn, R. C., Zent, A. P., Ehrenfreund, P., Taylor, C. L., McKay, C. P., Garry, J. R. C., Grunthaner, F. J., Dry acid deposition and accumulation on the surface of Mars and in the Atacama Desert, Chile. *36th Annual Lunar and Planetary Science Conference*, abstract no. 2282, 2005.

Dalton, J. B., Jamieson, C. S., Quinn, R. C., Prieto-Ballesteros, O., Kargel, J. S., Cryogenic reflectance spectroscopy of highly hydrated sulfur-bearing salts. 36th *Annual Lunar and Planetary Science Conference*, abstract no. 2280, 2005.

Moore, J. M., Bullock, M. A., Sharp, T. G., Quinn, R. C., 2005. Mars-analog evaporite experiment: Initial results. *36th Annual Lunar and Planetary Science Conference,* abstract no. 2246, 2005.

Quinn, R. C., Grunthaner, F. J., Taylor, C. L., Zent, A. P., McKay, C. P., Gomez-Silva, B., 2004. Electrochemical studies of Atacama desert soils: an analog of Martian surface chemistry. *Proceedings of the Third European Workshop on Exo-Astrobiology*, ESA SP-545, Noordwijk, Netherlands, 2004.

Dalton, J. B., Jamieson, C. S., Quinn, R. C.; Prieto-Ballesteros, O., Kargel, J., Highly hydrated sulfate salts as spectral analogs to disrupted terrains on Europa. *Workshop on Europa's Icy Shell: Past, Present, and Future*, abstract no. 7049, 2004.

Bada, J. L., Zent, A. P., Grunthaner, F. J., Quinn, R. C., Navarro-Gonzalez, R., Gomez-Silva, B., McKay, C. P., AstroBioLab: A mobile biotic and soil analysis laboratory. *Sixth International Conference on Mars*, July 20-25 2003, Pasadena, California, abstract no. 3175, 2003.

Quinn, R. C., Grunthaner, F. J., Taylor, C. L., Zent, A. P.; McKay, C. P.; Gomez-Silva, B.; Bada, J. L., Organic chemical decomposition in the Atacama Desert and on the surface of Mars: A comparison of potential reaction mechanisms. *American Astronomical Society, DPS meeting* 35, 09.09, 2003.

Quinn, R. C., Grunthaner, F. J., Taylor, C. L., Zent, A. P., Mars Redox Chemistry: Atacama Desert soils as a terrestrial analog. *34th Annual Lunar and Planetary Science Conference*, abstract no. 1951, 2003.

Sutter, B., Sriwatanapongse, W., Quinn, R., Klug, C., Zent, A., Physisorbed water on silica at Mars temperatures. *33rd Annual Lunar and Planetary Science Conference*, abstract no.1682, 2002.

Zent, A. P., Quinn, R. C., Grunthaner, F. J., Hecht, M. H., Buehler, M. G., McKay, C. P., Ricco, A. J., Mars atmospheric oxidant sensor (MAOS): An in-situ heterogeneous chemistry analysis. *33rd Annual Lunar and Planetary Science Conference*, abstract no. 1423, 2002.

Quinn, R. C.; Zent, A. P., Limits on UV photodecomposition of martian carbonates. American Astronomical Society, DPS Meeting 33, 48.03; *Bulletin of the American Astronomical Society*, Vol. 33, p.1126, 2001.

Quinn, R. C., Zent, A. P., McKay, C. P., Photodecomposition of carbonates on Mars. *32nd Annual Lunar and Planetary Science Conference*, abstract no.1463, 2001.

Quinn, R. C., Zent, A. P., McKay, C. P., Haberle, R. M., The stability of liquid-water films on the surface of Mars. American Astronomical Society, DPS Meeting 32, 62.08, *Bulletin of the American Astronomical Society*, Vol. 32, p.1119, 2000.

Boynton, W. V., Bailey, S. H., Hamara, D. K., Williams, M. S., Bode, R. C., Fitzgibbon, M. R., Ko, W. J., Ward, M. G., Sridhar, K. R., Blanchard, J. A., Lorenz, R. D., May, R. D., Paige, D. A., Pathare, A. V., Kring, D. A., Leshin, L. A., Ming, D. W., Zent, A. P., Golden, D. C., Kerry, K. E., Vern Lauer, H., Jr., Quinn, R. C., Applicability of the Mars polar lander TEGA instrument to future Mars missions. *Workshop on Concepts and Approaches for Mars Exploration*, abstract no. 6206, 2000.

Zent, A. P., Quinn, R. C., Grunthaner, F. J., Beuhler, M., Mars oxidant instrument (MOI): An in situ heterogeneous chemistry analysis. *31st Annual Lunar and Planetary Science Conference*, abstract no. 1886, 2000.

Zent, A. P., Howard, J., Quinn, R. C., H_2O Adsorption kinetics on smectites. *31st Annual Lunar and Planetary Science Conference*, abstract no. 1882, 2000.

Zent, A. P., Howard, J., Quinn, R. C., Adsorptive kinetics in smectite clays: Role in the martian boundary layer. *American Astronomical Society, DPS meeting*, 31, 43.09, 1999.

Quinn, R. C., Zent, A. P., The role of electrophilic oxygen in the Viking biology results and in the in situ destruction of organics on Mars. *American Astronomical Society, DPS meeting*, 31, 43.07, 1999.

Quinn, R. C., Zent, A. P., Heterogeneous catalysis of hydrogen peroxide vapor by martain soil analogs: Implications for regolith penetration depths of photochemically produced oxidants on Mars. *29th Annual Lunar and Planetary Science Conference*, abstract no. 1896, 1998.

Quinn, R. C., M. Madou, A. J. Ricco, A. P. Zent, B. J. Chen, and R. White. A performance-optimized gas sensing array through instrument hybridization. *Chemical and Biological Sensors and Analytical Electrochemical Methods; Proceedings of the Electrochemical Society and The International Society of Electrochemistry*, 19, 126-133, 1997.

Quinn, R. C.; Zent, A. P., Diffusion of photochemically produced hydrogen peroxide in the martian regolith and estimates of the depth of oxidized strata on the surface of Mars. American Astronomical Society, DPS meeting 29, 06.07, *Bulletin of the American Astronomical Society*, V29, 968, 1997.

Zent, A. P., Quinn, R. C., Measurement of H_2O adsorption at Mars-like conditions: revision of estimates. American Astronomical Society, DPS Meeting, 27, 15.01, *Bulletin of the American Astronomical Society*, V27, 1097, 1997.

Zent, A. P.; Quinn, R. C.; Jakosky, B. M., Fractionation of Nitrogen Isotopes on Mars: The role of the regolith as a buffer. American Astronomical Society, DPS Meeting 26, 14.03, *Bulletin of the American Astronomical Society*, V26, 1112, 1994.

Zent, A.P., Quinn, R.C., Simultaneous adsorption of CO_2 and H_2O under Mars-like conditions and application to the evolution of the Martian climate. *Twenty-Fifth Lunar and Planetary Science Conference*. Part 3: 1543-1544, 1994.

Zent, A. P., Quinn, R., Simultaneous laboratory measurements of CO_2 and H_2O adsorption on palagonite: Implications for the martian climate and volatile reservoir. Lunar and Planetary Inst., *Mars: Past, Present, and Future. Results from the MSATT Program*, Part 1 p 57-58, 1993.

Orenberg, J. B.; Handy, J.; Quinn, R., Reflectance spectroscopy and GEX simulation of palagonite and iron-rich montmorillonite clay mixtures: Implications for the surface composition of Mars. Lunar and Planetary Inst., *MSATT Workshop on Chemical Weathering on Mars*, 29-30, 1992.

Nawoord

Over the course of this research I have received the help and support from a large number of co-investigators and collaborators. In particular, I would like to acknowledge Dr. Aaron Zent, Dr. Frank Grunthaner, and Dr. Christopher McKay for their support. Additionally, Cindy Taylor of the SETI Institute contributed to many of the field and laboratory experiments that are part of this thesis. I would like to recognize the thoughtful reviews and comments provided by the referent of this thesis, Dr. Christopher Chyba, as well as the members of my committee, including Prof. Dr. Richard Mathies and Dr. Oliver Botta. I am also grateful to the members of the Astrobiology Group in Leiden including: Inge L. ten Kate, Dr. Richard Ruiterkamp, Dr. James Garry, and Zan Peeters, for their help and assistance. Finally, it would not have been possible to complete this thesis without the support of my family and friends.